Cell Line Development for and Characterization of Mono- and Bivalent Antibody Derivatives

Von der Fakultät Energie-, Verfahrens- und Biotechnik der Universität Stuttgart zur Erlangung der Würde eines Doktors der Naturwissenschaften (Dr. rer. nat.) genehmigte Abhandlung

Vorgelegt von

Verena Berger

aus Dresden

Hauptberichter: **Prof. Dr. Roland Kontermann**
Mitberichter: **Prof. Dr. Klaus Pfizenmaier**

Tag der mündlichen Prüfung: **12. Juli 2013**

Institut für Zellbiologie und Immunologie der Universität Stuttgart 2013

I hereby declare that I performed the present thesis independently without further help or other material than stated.

Verena Berger

Jülich, May 13, 2013

TABLE OF CONTENTS

ABBREVIATIONS

(HP-) SEC	High pressure size exclusion chromatography
(m) Ab	(monoclonal) Antibody
(R) WCB	(Research) working cell bank
ADA	Anti drug antibody
ADCC	Antibody dependent cytotoxicity
AUC	Area under the curve
BCA	Bicinchoninic acid assay
BGH	Bovine growth hormone
bp	Base pairs
BSA	Bovine serum albumin
CCK-8	Cell Counting Kit 8
CDC	Complement dependent cytotoxicity
CDR	Complementarity determining region
CDS	Coding sequence
CEX	Cation exchange chromatography
CH	Constant heavy chain
CHO	Chinese hamster ovary
CL	Constant light chain
CMV	Cytomeglalovirus
CRD	Cystein rich domain
CSP	Cell specific productivity
CV	Column volume
CV/AV	Celonic Vector / Order Vector
d	day
DHFR	Dihydrofolate reductase
DMSO	Dimethyl sulfoxide
DNA	Deoxyribonucleic acid
dNTP	Deoxyribonucleotide
dO	Dissolved oxygen
DTT	Dithiothreitol
EC_{50}	Half maximal effective concentration
EDTA	Ethylenediaminetetraacetate
ELISA	Enzyme-linked immuno-sorbent assay
Fab	Fragment antigen binding
Fc	Fragment crystallizable
FcRn	Neonatal Fc-Receptor
FCS/FBS	Fetal calf serum Fetal bovine serum
FDA	Food and Drug Administration
FPLC	Fast protein liquid chromatography
G418	Geneticin
GMP	Good Manufacturing Practice
GOI	Gene of interest
GS	Glutamin synthetase
h	hour
hu	human
H_2SO_4	Sulfuric acid
HACA	Human anti chimeric antibodies
HAHA	Human anti human antibodies
HAMA	Human anti mouse antibodies
HCl	Hydrogen hhloride
HCP	Host cell protein
hEF1	Human elongation factor 1
HES	Hydroxyethyl starch
HPLC	High pressure liquid chromatography
HRP	Horse raddish peroxidase
HSA	Human serum albumin
IBD	Inflammatory Bowel Disease
IC_{50}	Half maximal inhibitory concentration
Ig	Immunoglobuline

IL	Interleukin
IMAC	Immobilized metal ion affinity chromatography
IMDM	Immune mediated inflammatory disease
IPTG	Isopropyl β-D-1-thiogalactopyranoside
I-SceI	Meganuclease
IVCD	Integrated viable cell density
kcps	kilocycle per second (kilohertz)
K_D	Dissociation constant
LB	Luria broth
LD	Limiting dilution
LD_{90}	90 % Lethal dosis
LPS	Lipopolysaccharide
MCS	Multiple cloning site
MEF	Mouse embryonic fibroblasts
$MgSO_4$	Magnesium sulfate
MHC	Major histocompatibility complex
min	Minutes
MS	Multiple sclerosis
MTX	Methotrexate
MW	Molecular weight
NaOH	Sodium hydroxide
$NaPO_4$	Sodium phosphate
NEPHGE	Nonequilibrium pH gel electrophoresis
NF	Nucleofection
OD	Optical density
pA	Polyadenylation signal
PBS	Phosphate buffered saline
PDT	Population doubling time
PEG	Polyethylenglycol
PK	Pharmacokinetics
PLAD	Pre-ligand assembly domain
POD	Peroxidase
PSB	Primary seed bank
QCM	Quartz crystal microbalance
r	Recombinant
RA	Rheumatoid arthritis
RCME	Recombinase mediated cassette exchange
rpm	Rounds per minute
RT	Room temperature
scFv	Single chain fragment variable
SDS-PAGE	Sodium dodecyl sulfate polyacrylamide gel Electrophoresis
SOC/SOB	Superoptimal broth
TBE	Tris borate EDTA buffer
TBS	Tris buffered saline
TCA	Trichloroacetic acid
tcd	Total cell density
TE	Tris EDTA buffer
TLR	Toll-like receptor
TMB	3,3',5,5'-Tetramethyl-benzidine
TNF	Tumor necrosis factor
TNFR	Tumor necrosis factor receptor
TRAPS	TNF receptor associated periodic syndrome
UF/DF	Ultrafiltration / Diafiltration
UV	Ultraviolet light
vcd	Viable cell density
VH	Variable heavy chain
VL	Variable light chain

SUMMARY

Immune mediated inflammatory diseases (IMDM) can affect a variety of tissues and organs causing a broad spectrum of symptoms. Yet, rheumatoid arthritis, multiple sclerosis, psoriasis or inflammatory bowel disease share mechanistic similarities. A major factor in the development is the imbalance of tumor necrosis factor (TNF) regulation. With a prevalence of 5-7 % in the western society, a great interest exists in the development of an effective therapy. Current treatment involves primarily corticosteroids and non-biologic disease-modifying antirheumatic drugs (DMARDs) like methotrexate (MTX). The fast progression made in the development of biopharmaceutics, especially of antibody based therapeutics allowed for a more specific treatment. TNF-related diseases are tried to tackle by intervention in the TNF signaling. To date, five such therapeutics are approved by the US Food and Drug Administration (FDA). They are aiming at the neutralization of TNF or lymphotoxin alpha (LTα), thereby reducing exaggerated TNF signaling and curtailing inflammation. However, neutralization of TNF facilitates opportunistic infections and several warnings have been issued by the FDA. In 1990, an antibody directed specifically against TNFR1 was discovered, when mice were immunized with human TNFR1. A humanized variant was generated in 2008, paving the way for the use of this antibody as a therapeutic in humans.

The present study describes the development of chinese hamster ovary (CHO) cell lines expressing three different variants of the humanized TNFR1 specific antibody IZI06.1, a full length antibody and two human serum albumin fusion proteins (scFv-HSA and Fab-HSA). Cell lines were generated by site directed integration of the GOI into the CHO host genome in order to investigate the influence of the individual construct on growth performance and producibility. Cell lines expressing the IgG1 and the scFv-HSA perfomed similarly, showing productivities of 5-10 pg/c/d. Both proteins assembled properly and could be purified to satisfactory purity. These constructs were found to be applicable for the generation of a regulatory compliant cell line. The Fab-HSA revealed multiple issues in terms of productivity and purification and was therefore excluded from further investigation.

The monovalent fusion protein scFv-HSA and full length antibody (termed ATROSAB) were investigated in more detail to determine the impact of variables like composition, size and valency on their biochemical and functional properties. Reduced size of the fusion protein

translated into a reduced plasma half-life compared to the antibody. But although being also more susceptible to thermal degradation, comparison with the respective scFv showed that the scFv-HSA clearly benefits from fusion to HSA in terms of stability. It could be further demonstrated that both proteins specifically bind TNFR1, but not TNFR2 and that both proteins are generally able to inhibit TNFα-induced TNFR1 signaling. However, potency of the fusion protein was demonstrated to be significantly reduced, most probably due to its monovalency. Without further improvement of the scFv-HSA, the full length IgG remains first choice for the development of a prospective, highly specific therapeutic with indication for TNF mediated inflammatory diseases.

These results are in accordance with bio-functional data generated earlier for the three constructs that also indicated a better affinity of the full length IgG to hTNFR1 compared to the scFv-HSA and upon which it was decided to generate a full regulatory compliant cell line in CHO for the IgG1 (ATROSAB). A set of cell lines could be developed, that meet all requirements for a prospective use in an industrial, GMP regulated environment. This includes next to a high productivity and favorable growth characteristics the absence of adventitious agents. The cell lines were generated by Limiting Dilution, clonality was verified by microscopy. More than 400 clones were screened from which high producers were identified and cell-banked. The most promising clone K20-3 achieved a productivity of 10 pg/c/d. In order to further enhance productivity without employing destabilizing gene amplification, this clone was re-transfected with the slightly modified expression vector for the IgG1. A more than 3 fold increase in productivity could be achieved with clone K35-1. However, quality analysis of ATROSAB produced by the re-transfected clone revealed a greater heterogeneity and also bio-functionality was affected negatively. Therefore it was decided for the time being to proceed with original, not re-transfected clone in order to set up a GMP production process. Yet, further analysis of the re-transfected clones may be worthwhile regarding their increased productivity. Adapted process and handling protocols probably can overcome the encountered limitations in product quality.

ZUSAMMENFASSUNG

Chronisch entzündliche Erkrankungen betreffen eine Vielzahl von Geweben und können sich in einem breiten Spektrum von Symptomen manifestieren. Bestimmte molekulare Mechanismen haben sie jedoch gemein. So spielen im Verlauf der Krankheit zumeist eine fehlgeleitete, gegen körpereigene Epitope gerichtete Immunantwort sowie ein Ungleichgewicht in der Regulation pro-inflammatorischer Zytokine wie TNFα eine entscheidende Rolle. Entzündliche Erkrankungen der Gelenke (Rheumatoide Arthritis) oder chronisch-entzündliche Darmerkrankungen (Morbus Crohn, Colitis ulcerosa) haben eine hohe Prävalenz in der Bevölkerung (geschätzte 5-7 % in der westlichen Gesellschaft). Es besteht daher ein hohes Interesse an der Entwicklung effektiver Therapien. Bisherige Therapieansätze sehen den Einsatz von Kortikosteroiden oder nicht-biologischen, sogenannten „disease-modifying antirheumatic drugs (DMARDs)“ wie Methotrexat (MTX) vor. Der in den letzten Jahren erzielte Fortschritt im Bereich der Biotherapeutika, insbesondere von pathogen-spezifischen Antikörpern, ermöglicht heutzutage eine gezieltere Behandlung. Für den Einsatz gegen TNFα-vermittelte entzündliche Erkrankungen sind zurzeit fünf Antikörper-basierte Therapeutika für den Markt zugelassen, die alle TNF im Blut neutralisieren. Dieser Wirkmechanismus begünstigt jedoch opportunistische Infektionen, weswegen bereits mehrere Warnungen durch die Food and Drug Administration (FDA) ausgegeben wurden. 1990 wurde ein Antikörper entdeckt, der für den humanen TNFR1 spezifisch ist. Die Entwicklung einer humanisierten Variante im Jahr 2008 ebnete den Weg für die Weiterentwicklung zu einem potentiellen Therapeutikum für den Einsatz im Menschen.

Die vorliegende Arbeit beschreibt zunächst die Entwicklung von CHO basierten Zelllinien für die Expression von drei Antikörperderivaten des humanisierten hTNFR1 spezifischen Antikörpers, einem IgG1, einem scFv-HSA und einem Fab-HSA Fusionsprotein. Alle Zelllinien wurden durch Locus spezifische Genintegration erzeugt, um eine höhere Vergleichbarkeit in Bezug auf Wachstumsverhalten und Produzierbarkeit zu erzielen. Die Zelllinien für den Antikörper und das scFv-HSA Fusionsprotein zeigten ein günstiges Wachstums- und Produktionsverhalten mit Produktivitäten von 5-10 pg/c/d. Beide Proteine wurden korrekt exprimiert und konnten mit vergleichbar geringem Aufwand bis zu einer zufriedenstellenden Reinheit aufgearbeitet werden. Im Gegensatz dazu bereiteten sowohl die

Produktion wie auch die Aufreinigung des Fab-HSA Probleme. Um den Einfluss von Größe, Aufbau und Valenz auf die biochemischen und -funktionalen Eigenschaften des TNFR1 Blockers zu untersuchen, wurden das monovalente scFv-HSA und der bivalente IgG1 (ATROSAB) miteinander verglichen. Die geringere Größe des Fusionsproteins bedingte eine verringerte Plasmahalbwertszeit. Eine ebenfalls beobachtete geringere thermische Stabilität wurde jedoch im Vergleich zu dem einfachen scFv Fragment durch die Fusion mit HSA deutlich verbessert, wenngleich die Stabilität des Antikörpers nicht erreicht wurde. Die Bindungsspezifität beider Moleküle für den humanen TNFR1 blieb von ihrem unterschiedlichen Aufbau unbeeinflusst. Die Affinität war jedoch deutlich verringert für das Fusionsprotein, was zum größten Teil auf seine Monovalenz zurückzuführen ist. Entsprechend konnte für beide Proteine die Fähigkeit nachgewiesen werden, eine TNFα-vermittelte Ausschüttung von pro-inflammatorischen Zytokinen zu verhindern, wobei sich der Antikörper als deutlich effektiver herausstellte. Ohne weitere Optimierung der Bindungsaffinität blieb daher der IgG1 der vielversprechendste Kandidat für eine Weiterentwicklung zum Therapeutikum.

Für das Antikörperformat wurde eine Auswahl regulationskonformer CHO Suspensionszelllinien generiert, die den Anforderungen für eine zukünftige Produktion in einem industriellen, GMP regulierten Umfeld gerecht werden. Das schließt ein günstiges Wachstumsverhalten und eine gute Basisproduktivität ein, den Verzicht auf Materialien, die potentielle Überträger von Infektionserregern sein könnten, sowie die vollständige Dokumentation aller benutzten Materialien. Die Zelllinien wurden durch Limiting Dilution erzeugt, wobei die Klonalität durch Mikroskopie überprüft wurde. Über 400 Klone wurden untersucht, von denen gute Produzenten identifiziert und kryokonserviert wurden. Der beste Klon (K20-3) erreichte eine Produktivität von 10 pg/c/d. Durch eine erneute Transfektion dieses Klons konnte ohne potentiell destabilisierende Genamplifikation eine mehr als dreifache Steigerung der Produktivität erreicht werden. Das Produkt zeigte jedoch eine deutlich größere Heterogenität als bei dem Ursprungsklon, was sich auch in einer verringerten Biofunktionalität wiederspiegelte. Für den Aufbau einer GMP Produktion wurde daher Klon K20-3 ausgewählt. Die weitere Untersuchung des retransfizierten Klons ist aber dennoch lohnenswert, denn ein abgestimmter Produktionsprozess bzw. genaue Vorschriften zur Handhabung des Produktes könnten diese Heterogenität vermindern.

1 INTRODUCTION

1.1 Therapeutic Monoclonal Antibodies

Today, monoclonal antibodies form an important class among biotherapeutics. Up to 37 mAb have been approved for clinical applications by the FDA [2] so far and approximately 300 undergo current development. They are employed as therapeutics in a variety of indications like the non-Hodgkin's Lymphoma, Multiple Sclerosis, Rheumatoid Arthritis, Psoriasis and different types of cancer [40, 145, 166, 187, 39, 4]. The major advantage of antibodies is the combination of highly specific targeting with a variety of effector functions mediating either destruction of targeted cells or interruption/propagation of certain biological pathways [137].

Monoclonal Antibodies came into focus when Köhler and Milstein succeeded in 1975 in producing monoclonal antibodies by hybridoma technique [119]. In 1986, the first monoclonal antibody was approved by the Food and Drug Administration (FDA). The antibody, OKT3, was derived from mouse hybridoma and intended for prevention of transplant rejection [166]. However, the non-human structure of the antibody induced a human anti-mouse antibody (HAMA) response in the patients [116]. This affected safety, efficacy and half-life of the antibody. The generation of human hybridomas in order to minimize immunogenicity, i.e. the use of human B-cells, was impossible due to ethical considerations. Since then, efforts have been made to reduce immunogenicity and further develop this new promising class of therapeutics. So, the next consequential step was to try to replace constant parts of the mouse antibody by their human equivalent, leaving the variable regions untouched [31, 154]. This was achieved by recombinant DNA technology, developed in the 1980s. These chimeric antibodies induced less human anti-chimeric antibodies (HACA), but adverse immune responses could not be fully abrogated [180]. In order to further minimize non human sequences in the antibody, a technique has been developed by Sir Gregory Winter in the late 1980s in which the complementary-determining regions (CDRs), that are mainly responsible for antigen recognition, were "grafted" onto a human immunoglobulin framework [98]. Detailed knowledge on the individual residues and their importance for antigen binding facilitated the development of this method which was further developed and is routinely used until today [61, 73, 86, 104]. Several humanized antibodies are approved for the market (Campath™, Herceptin™, Myelotarg™). In order to overcome the obstacle of only partly human sequences which bear the risk of provoking HAMA/HACA responses, two alternatives evolved. Transgenic mice with human immunoglobulin gene reservoir allowed for the generation of fully human antibodies by hybridoma technique [141].

The antibodies underwent affinity maturation and are therefore highly specific. However, highly conserved or toxic targets cannot be addressed. The other alternative is phage display. The initial method was established in 1985 [205], the use with antibodies demonstrated in 1990 [149]. This enabled the development of fully human antibodies *in vitro*, which allows for the generation of antibodies against virtually every possible target. A drawback is that the initial antibodies often require for further affinity maturation, which is done by mutation and multiple selection rounds.

1.1.1 Antibody Structure and Function

Antibodies are glycosylated members of the immunoglobulin superfamiliy that are produced by B-cells. They recognize and neutralize foreign organisms or antigens and thereby form an important tool of the adaptive immunity. Antibodies are bivalent and consist of heavy and light chains that assemble via intermolecular disulfide bonds. Heavy and light chains in turn comprise constant and variable domains from which the hypervariable regions in the latter form the antigen binding site (complementary determining regions, CDR) (Figure 1-1). Two types of light chains exist in mammals, lambda and kappa, from which kappa light chains are more frequent in humans. The type of heavy chain (μ, γ, ε, α and δ) groups antibodies into 5 classes with different effector functions like neutralization and opsonization, mediation of NK-cell attack, activation of the complement cascade as well as the sensitization of mast cells. Additionally, different sub classes exist for IgG (γ_1, γ_2, γ_3, γ_4) and IgA (α_1, α_2). These effector functions are mainly mediated by the interaction of the Fc domain (fragment, crystallizable) of the antibody with their respective Fc-receptors (e. g. FcγR, FcαR, FcεR). These receptors are expressed mainly by B lymphocytes, macrophages and natural killer cells (NK cells). Predominantly antibodies of class γ_1 and γ_3 mediate antibody dependent cellular cytotoxicity (ADCC) by interaction with Fcγ receptors on immune effector cells. They also trigger complement dependent cytotocxicity (CDC) by binding C1q resulting in the activation of the complement cascade with formation of the membrane attack complex and subsequent cell lysis. The specific amino acids responsible for Fc effector function have been identified [8]. But also the glycosylation site contributes to effector function [3]. Both are the source for Fc antibody engineering (see below). Depending on the desired therapeutic effect, the respective isotype is chosen. Regarding the variety of effector functions, the IgG is the isotype most commonly used for therapeutic applications [96, 191]. Immunoglobulins exhibit long serum half-lifes of 2-21 days, mostly due to their large size, which ranges above the threshold

for renal clearance (~65 kDa). It is known that for the IgG the interaction with the neonatal Fc receptor (FcRn) contributes to an extended half-life [131]. This membrane bound receptor is expressed on endothelial cells as well as on cells of the liver, kindney or intestine. The IgG is taken up by endocytosis and the resulting endosomes fuse with lysosomes, resulting in a decreased pH of 6.0-6.5, which facilitates the binding of the IgG to the FcRn. All none bound proteins are degraded while the bound IgG is transported to the cell surface and released from the FcRn at pH 7.4.

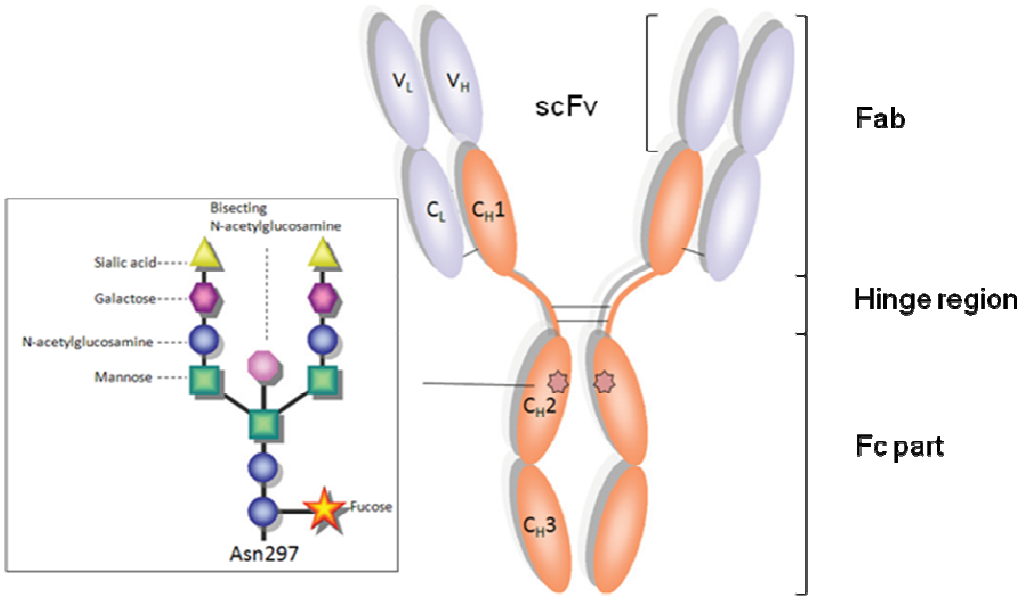

Figure 1-1 Antibody structure (γ subtype). V_L – light chain variable region, V_H – heavy chain variable region, C_L – light chain constant domain, C_H – heavy chain constant domain 1, C_H2 – heavy chain constant domain 2, C_H3 – heavy chain constant domain 3. Heavy chains are linked in the hinge region by two disulfide bridges, C_H1 and C_L also linked by disulfide bridges, resp. C_H2 comprises one glycosylation site at Asn297, resp. Figure adapted from Kubota et al., *Cancer Science* 2009

1.2 Antibody Engineering

In the last decade, efforts have been made in antibody engineering to meet specific demands, e.g. higher efficacy, reduced immunogenicity and prolonged half-life. Nowadays it is possible to design completely new, antibody based molecules for the generation of “tailor made” therapeutics.

1.2.1 Engineered Fc Function

The crystallizable fragment (Fc-) part of an antibody determines its effector functions. Interaction with FcγRIIIa (in humans) mediates ADCC via engagement of NK-cells, leading to the destruction of target cells by exocytosis of the cytolytic franule complex perforin/granzyme. Selection for variants with higher affinity for FcγRIIIa will lead to enhanced ADCC [200, 129, 89]. Capacity for ADCC is also dependent on the oligosaccharide structure of the Fc-domain (Asp297) [3]. So, presence or absence of the proximal fucose is critical for the interaction with FcγRIIIa and its elimination leads to a marked increase in ADCC [201, 102]. CHO production cell lines have been established that totally lack fucosylation due to knock out of α-1,6-fucosyltransferase (FUT8, Potelligent® technology, BioWa, Princeton, USA) [229]. Another approach is the overexpression of heterologous β-1,4-N-acetylglucosaminyltransferase III (GnTIII) in antibody-producing cells (GlycoMab® technology, Glycart Roche, Schlieren, Switzerland). Xencor´s XmAb® technology provides engineered Fc domains as building blocks for the development of antibodies with enhanced ADCC. Besides ADCC, the Fc-part also mediates complement dependent cytotoxicity (CDC). Improvement of Fc domain binding to C1q by amino acid modifications in the CH_2 domain and in the hinge region led to improved CDC activity [153]. Also an interchange of IgG1 sequences with those of IgG3 showed markedly improvements [163]. The Fc domain also facilitates binding of the antibody to the neonatal Fc receptor (FcRn) at a pH of 6.0 to 6.5 in endosomes. By that the molecule is recycled and exhibits a long half-life of about two weeks in serum. Mutants were found that exhibited an even longer half-life that had a higher affinity towards FcRn [55].

1.3 Therapeutic Antibody Fragments

Besides full length antibodies, the class of antibody fragments grows more and more important since they are generally of smaller size and therefore allow for a better access to the diseased tissue. As a consequence, the dose to be administered can be reduced in comparison to the high-dose administrations for antibodies (e. g. rituxan, [72]). This also reduces off-target actions and production costs. The class of antibody fragments comprises amongst others Fc fragments, Fab, single chain variable fragments (scFv) and even single domain antibodies (dAb) which consist only of a variable domain V_L or V_H. These small functional components can be used as building blocks which give rise to a great many of tailor made

therapeutics [178, 87] (Figure 1-2, Table 1-1). One of the first applications was the fusion of the Fc part to different effector proteins, thus enhancing their serum half-life or conferring secondary immune functions [95, 90]. Today, seven Fc-fusion proteins are approved for clinical use by the FDA, the most prominent being Enbrel®. Antibody fragments lacking the Fc domain are not capable of mediating effector functions like ADCC or CDC, but may redirect cytokines or drugs to specific tissues. Thus, fragments containing the variable regions can be used as antibody drug conjugates (ADC) to efficiently deliver drugs like chemotherapeutica or toxins with greatly reduced off-target effects (Mylotarg®, Zevalin®, Bexxar®). These fragments can also be used for the neutralization of biological pathways. Then they are either directed against soluble molecules like cytokines and growth factors or against receptors to block signaling pathways. To date, three such fusion proteins are approved for the clinic (ReoPro®, Lucentis®, Cimzia®). Recently, scFvs were used to address intracellular pathways by so-called intrabodies [121]. Intrabodies are tagged with intracellular trafficking signals, redirecting them to the desired cellular compartment.

Besides their obvious advances, antibody fragments exhibit a very short serum half-life due to their small size. Several approaches have been made towards half-life improvement [122]. One possibility is to couple the fragments to molecules of larger size, like polyethylene glycol (PEG) or human serum albumin (HSA) [159, 26]. Another would be the introduction of HSA binding sites to the molecule [88, 9]. Also multimerization of the fragments is under investigation, leading to molecules with higher avidity/valency and higher serum half-life [178]. Coupling to HSA provides additional benefit, because it does not mask small antibody fragments like PEG, it is recycled actively by interaction with FcRn and is also known to accumulate in tumors, thus enhancing the targeting effect of a, e. g. scFv-HSA, fusion protein [195, 215, 43].

Nevertheless, many issues remain to be addressed, like immunogenicity, manufacturing and downstream processing (purification/formulation), quality control, toxicology and pharmacology studies as well as regulatory considerations.

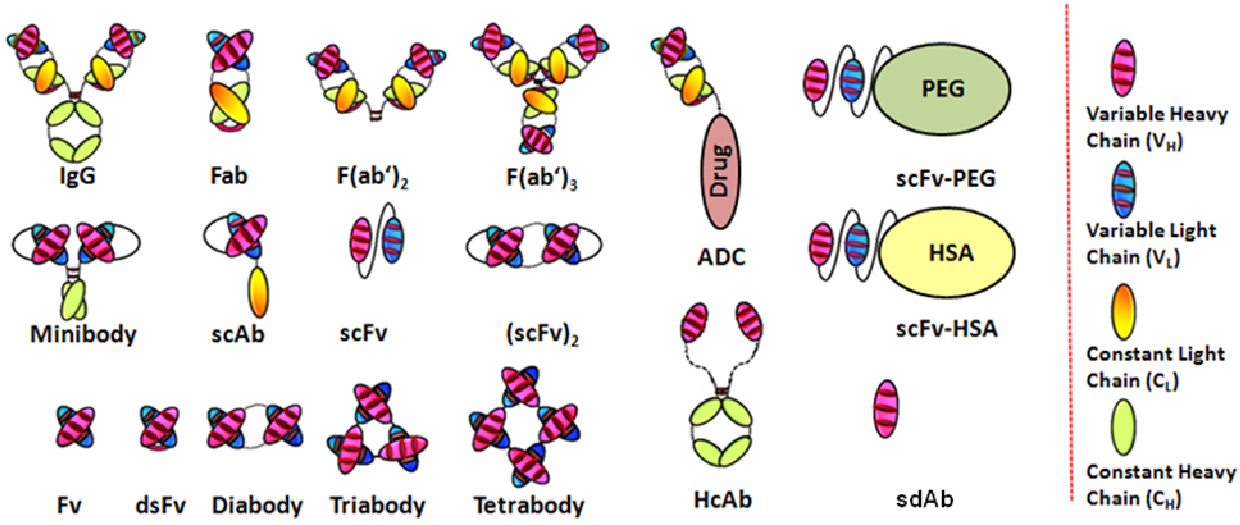

Figure 1-2 Variety of possible antibody formats. scAb – single chain antibody, scFv – single chain variable fragment, Fv – fragment variable, dsFv – disulfide variable fragment, ADC – antibody drug conjugate, HcAb – heavy chain antibody (found in camelids), sdAb – single domain antibody (derived from FcAb), PEG – polyethylene glycol, HSA – human serum albumin. Fragments are either linked by disulfide bonds (dsFv) and/or by linkers. Adapted from Vijayalakshmi Ayyar et. al, *Methods* 2012.

Generic name	Trade name	Composition	Antigen	Approved indication	FDA approval	Sponsor
Abciximab	ReoPro	Chimeric Fab´	αIIb-integrin (CD41)	Prevention of blood clotting	12/16/93	Centocor, Inc.
Nofetumomab	Verluma	Mouse Fab´	Glycoprotein carcinoma associated antigen	Diagnosis of small cell lung cancer	08/20/96	Boehringer Ingelheim
Etanercept	Enbrel	TNFR2:Fcγ1	TNFα	Rheumatoid Arthritis	11/02/98	Amgen/Pfizer
Arcitumomab	CEA-Scan	Mouse Fab´	Carcinoembryonic antigen (CEA)	Non-invasive imaging	06/28/98	Immunomedics
Alefacept	Amevive	LFA-3 domain I:Fcγ1	LFA-2 (CD2)	moderate to severe chronic plaque psoriasis	01/30/03	Biogen
Abatacept	Orencia	Extracellular domain CTLA-4: Fcγ1	B7 (CD80, CD86)	RA (with no response to DMARDs)	12/23/05	Bristol-Myers Squibb
Ranibizumab	Lucentis	Humanized Fab´	VEGF-A	(wet) age-related macular degeneration	06/30/06	Genentech
Rilonacept	Arcalyst	IL-1R/IL-1RAcP :Fcγ1	IL-1	Cryopyrin-associated periodic syndromes (CAPS)	02/27/08	Regeneron Pharmaceuticals, Inc.

Generic name	Trade name	Composition	Antigen	Approved indication	FDA approval	Sponsor
Certolizumab Pegol	Cimzia	Fab´:PEG2MAL40K	TNFα	Chron´s disease	04/22/08	UCB, Inc.
Belatacept	Nulojix	Extracellular domain CTLA-4: Fcγ1	B7 (CD80, CD86)	Kidney transplant rejection	06/15/11	Bristol-Myers Squibb
Aflibercept	Eylea	(VEGFR1 domian:VEGFR2 domain 3)$_2$: Fcγ1	VEGF	(wet) age-related macular degeneration	11/18/11	Sanofi-Aventis, Regeneron Pharmaceuticals, Inc.
ZIV-Alifercept	Zaltrap	(VEGFR1 domian:VEGFR2 domain 3)$_2$: Fcγ1	VEGF	Metatstatic colorectal cancer	08/03/12	Sanofi-Aventis

Table 1-1 Compilation of FDA approved therapeutics that are based on antibody fragments according to the actual data (November 2012) available online [2].

1.4 Human Serum Albumin

Albumin is a high abundant serum protein produced in the liver that occurs monomeric and has a molecular weight of about 67 kDa. The multi-domain protein is very stable, due to 17 disulfide bonds. Its functions comprise amongst others the maintenance of osmotic pressure, regulation of pH and the transport of a variety of ligands like fatty acids, hormones and metal ions. The latter makes HSA also important for detoxification [181, 186, 60]. HSA circulates from blood to interstitial compartments and is returned by the lymphatic system after about 16 hours. The overall half-life of human serum albumin is with approx. 19 days comparable to that of IgG. The long half-life results from binding of HSA to the neonatal Fc receptor (FcRn), a salvage mechanism known to also save IgGs from lysosomal degradation [43]. Human serum albumin is also a marker for a variety of diseases like rheumatoid arthritis, cancer and infectious diseases, since cells increase albumin uptake as a source of energy and amino acids when undergoing stress [211]. This contributes to an additional targeting effect in molecules fused to or associated with HSA. Receptor gp60 (albondin) mediates transcytosis of HSA through endothelial cells in underlying tissues [196] (Figure 1-3, A), whereas the protein SPARC (secreted protein, acidic and rich in cysteine) is believed to be important for the cellular uptake [57] (Figure 1-3, B), subsequent lysosomal degradation and delivery of building blocks to anabolism. Altogether, long half-life, natural abundance and targeting effects of HSA makes it an ideal drug carrier and fusion partner for a vast of molecules in different applications. Thus, accumulation of HSA in solid tumours and inflamed tissue can be exploited for the development of diagnostic tools (Nanocoll®, Vasovist®). Also several

albumin based drugs are already approved for the market, like Abraxane®, which uses albumin as a carrier for paclitaxel and is used for the treatment of breast cancer, or Levemir®, an albumin binding derivative of human insulin for the treatment of diabetes of type I and II. Combination of HSA with antibodies and derivatives thereof resulted in encouraging results for several molecules like an αHER2 directed Fab fragment with attached albumin binding sequence, AB.Fab4D5 (Genentech), or a bispecific scFv-HSA-scFv fusion protein targeting ErbB2 and ErbB3, MM-111 (Merrimack), both intended for the treatment of breast cancer. Actually tested in phase II is an αTNF-αHSA trivalent nanobody ATN-103 (Ablynx) for the treatment of rheumatoid arthritis.

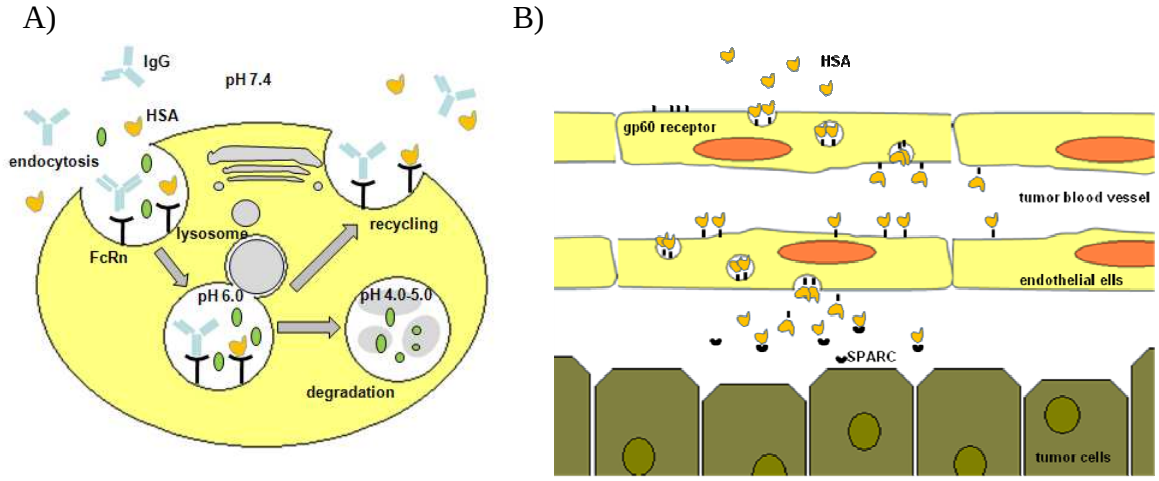

Figure 1-3 A) FcRn mediated recycling of IgG and HSA. Both molecules bind to the FcRn at a modest acidic pH of 6.0-6.5 and are thereby salvaged from lysosomal degradation. At a pH of 7.4, they are released from the receptor for prolonged circulation. B) Transcytosis of HSA mediated by the gp60 receptor to extravascular space and binding to SPARC (secreted protein, Acidic and rich in cysteine). Adapted from Elsadek, *Journal of Controlled Release* (2012).

1.5 Antibody-based therapeutics in TNF-related diseases

TNF, the most prominent member of the TNF cytokine family, is an important key mediator in immune defence with widespread and ambiguous effects [5, 23, 139]. Due to its global biological impact, TNF is implicated in many diseases and addressing TNF signaling may be the key to therapy [124, 33]. To date, five antibodies or antibody-based therapeutics for the treatment of TNF-related diseases are approved for the market. These are Infliximab (Remicade, chimeric IgG1κ), Adalimumab (Humira, human IgG1κ), Golimumab (Simponi, human IgG1κ), Etanercept (Enbrel, TNFR2:Fcγ1) and Certolizumab Pegol (Cimzia, humanized Fab-PEG). All these molecules capture and neutralize TNF, Etanercept also lymphotoxin alpha (LTα).

TNF is mostly produced by activated macrophages [146, 38] and T lymphocytes [126] and can be displayed either as a membrane associated form (mTNF, 26kDa) or, after cleavage by matrix metalloproteinases, be released as a soluble protein (sTNF, 17kDa) [25]. TNF acts as a trimer [206] with a molecular weight of 51 kDa and is recognized by two receptors, TNFR1 and TNFR2. Soluble TNF is predominantly recognized by TNFR1, the membrane associated form by both TNFR1 and TNFR2 [75, 76, 140]. Both receptors belong to the tumor necrosis receptor superfamily. Receptors of this family are characterized by one to six cysteine rich domains (CRD) and an intracellular interaction site for adapter proteins. The most membrane distinct CDR (CDR1) comprises a homophilic interaction site, the pre-ligand assembly domain (PLAD).

Most tissues co-express both receptors, with TNFR1 at constitutively higher levels than TNFR2. Expression of the latter is rather induced depending on cell activation. The number of TNFR1 available on the cell surface was found to be controlled by enzyme mediated receptor shedding [228]. This mechanism provides a negative feedback loop to keep TNFR1 signaling in balance and mutations in TNFR1 that inhibit receptor shedding are believed to be a reason for the TNFR associated syndrome (TRAPS) [17]. Intervention with this mechanism offers a possibility to prevent TNFR1 hyper-activation. TNF receptors occur pre-associated on the cell surface by interaction of the pre-ligand assembly domain (PLAD) [41] (Figure 1-4). Upon TNF binding, large ligand/receptor cluster assemble, likely facilitated by micro-compartmentalization [130, 160]. This brings the intracellular domains of the receptors into spatial proximity and allows recruitment of adaptor proteins in the cytoplasma that initiate the TNFα signaling pathway. The exact stoichiometry of receptor signaling is still a matter of discussion and recent data suggest a different stoichiometry for TNFR1 (two receptor dimer associated with two TNF molecules) and TNFR2 (one receptor dimer with one bound TNF molecule) [29]. Lewis et al. proposed a model for TNFR1 signalling where upon ligand binding and ligand-receptor network formation a sterical conflict arises between the receptor network and the cellular membrane. Receptors undergo conformational changes to alleviate this conflict that convert them at the same time into an active state. In contrast to the previous understanding, signaling is then achieved by separation rather then by spatial proximity of the intracellular death domains, revealing previously concealed binding sites for TNFR associated death domain (TRADD) [134].

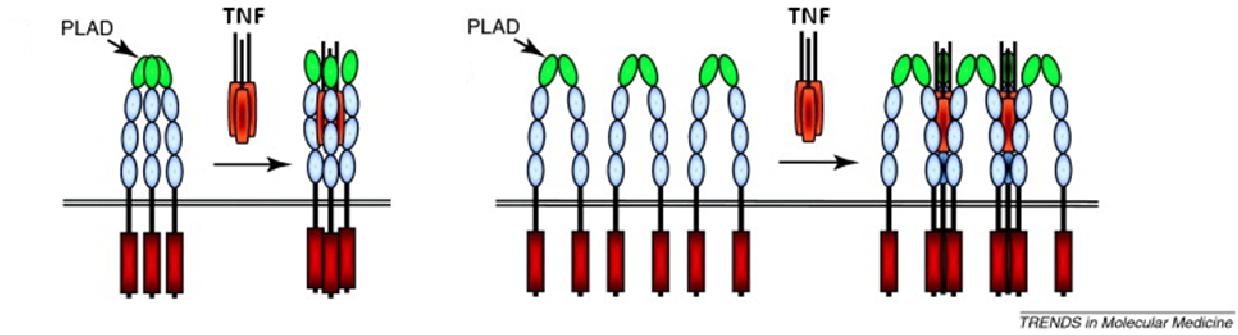

Figure 1-4 Preligand assembly via TNFR PLAD domain. The PLAD can be found in the most membrane distinct cystein rich domain (CRD) of the TNFR. Exact stoichiometry of receptor cluster formation remains to be determined. Tough, supermolecular clustering is necessary for effective signaling. Adapted from Lobito et al, *Trends in Molecular Medicine* 2011 [138].

Both receptors trigger different signaling cascades, resulting in as distinct biological outcomes as apoptosis or proliferation. Activation of TNFR1 initially causes formation of a transmembrane signaling complex (complex I) which controls the expression of anti-apoptotic proteins via activation of transcription factors AP-1 and NF-κB. Upon internalization though, conformational changes lead to formation of complex II which in turn controls apoptotic (via caspase 8 activation) or even necrotic (via RIP-1 and RIP-3 phosporylation) processes [194, 151]. TNFR1 is thus associated with pro-inflammatory responses and activation of apoptotic pathways. TNFR2 in contrast controls anti-apoptotic processes and mediates tissue repair, angiogenesis and proliferation [147, 68, 152]. For example it promotes oligodendrocyte proliferation and remyelination [12]. In neurodegenerative diseases associated with chronic inflammation like multiple sclerosis or Alzheimer´s disease, therapies targeting TNFR2 mediated signaling may be promising [64].

As a consequence to these oppositional effects, receptor expression and ratio is tightly balanced in response to ischaemic or inflammatory tissue injury and interference with TNF signaling is critical. Imbalanced TNF production in inflamed tissue is cause of many inflammatory and autoimmune diseases, like rheumatoid arthritis (RA), inflammatory bowel disease (Crohn´s disease, ulcerative colitis), psoriasis or multiple sclerosis [185, 117, 120].

Rheumatoid arthritis is a chronic inflammatory autoimmune disease with its exact origin not known. Genetic as well as environmental factors seem to contribute [222]. The interplay of T- and B-cells as well as of pro-inflammatory cytokines (mainly TNFα and IL-6, but also IL-1 and IL-17) result in the propagation of local inflammation and the formation of autoantibodies. This leads to synovitis, osteoporosis and subsequent joint damage [46]. TNF has major local as well as systemic effects in the pathobiology of RA. Locally, increased TNF

expression leads to an increased monocyte activation, priming of polymorphonuclear leukocytes, expression of endothelial cell adhesion molecules, release of cytokines and matix-metalloproteases (MMP), a decrease of synovial fibroblast proliferation and collagen synthesis. Additionally it induces apoptosis and oxidative burst of affected cells. Systemically, TNF overexpression results in the production of acute-phase proteins, progression of cardiovascular disease (CVD), fatigue and depression [47, 172].

Consequentially, blockade of excessive TNF signaling by neutralization of high serum levels of TNF is an obvious and, by now, also well proven therapeutic approach [124]. Nevertheless, a number of accompanying infections/malignancies are reported with the use of TNF blockers (e. g. granulomatous infections, leukemia or new-onset psoriasis) [71, 27, 182, 70]. Thus, other measures are under investigation to more specifically modulate TNF signaling. Possible working points are the interference with the ligand-receptor interaction and intracellular signaling pathways. Since intracellular signaling is a complex crosstalking network it will be hard to predict possible side effects and therefore offers no attractive alternative. A dominant negative TNF mutein has been developed, that is biologically inactive and incapable of binding to TNFR1 or 2 (XPro1595, Xencor) [231, 209]. This mutein forms heterotrimers with native soluble TNFα which fail to bind to TNFR1. In contrast, there is no formation of heterotrimers with mTNFα, leaving mTNF signaling intact. Another TNF mutein, R1antTNF, specifically binds to TNFR1, not TNFR2, thereby abrogating TNFR1 signaling [199, 198]. Similarly, TNFR1 specific antagonists inhibit selectively binding of native TNF to TNFR1, leaving signaling via TNFR2 intact (Dom0100, domain antibody, developed by Domantis; ATROSAB, humanized IgG, Celonic) [123, 214]. These approaches, which are all in preclinical development or early clinical testing, account much more for the complexity and importance of TNF signaling than the actual therapies that are based on a complete TNF blockade.

1.6 Antagonistic Anti TNFR1-specific Antibody (ATROSAB)

ATROSAB (anti tumor necrosis receptor one-specific antibody) is a very recent development being currently tested in phase I clinical studies. The antibody originates from a new molecular entity (NME) being discovered in 1990, when mice were immunized with the human TNF receptor 1 (TNFR1). A hybridoma was generated that expressed an antibody specifically binding to TNFR1 (mouse monoclonal IgG2a, termed H398) [214]. In 2008, a humanized variant, termed IZI-06.1, was developed by CDR grafting that retained the binding

specificity of H398 [123]. IZI-06.1, originally being a scFv fragment, was finally converted into a humanized IgG1 with silenced ADCC and CDC function in 2010 [233]. Therefore, residues of IgG2 (position 233-236) and IgG4 (positions 327, 330 and 331) were introduced into the original IgG1 Fc part of the allotype G1m17,1 [11]. The antibody, now termed ATROSAB, also retained binding specificity towards TNFR1 and exhibited a comparable binding affinity like H398. Furthermore, Zettlitz et al. elucidated the binding epitope of ATROSAB to be the N-terminal region including CDR1 and the A1 sub-domain of CDR2. Currently, attempts are made to further improve the affinity towards TNFR1 for an even better efficacy.

1.7 Immunogenicity

A permantent issue in the design of antibody based therapeutics is the possible provocation of adverse immune responses [180, 173, 192]. This is due to eventually new formed epitopes that may be recognized as non-self by the patient´s immune system. But also proteins of human origin that naturally occur in a low abundance may break immune tolerance [197]. The consequence is the formation of anti-drug antibodies (ADA), either via the T-cell-dependent or –independent pathway. ADA can alter the pharmacokinetic/pharmakodynamic properties of the therapeutic, possibly leading to its neutralization. More seriously, they can also cross-react with the endogenous analogon, shutting down important pathways. To immunogenicity contribute product-related, patient-related and treatment-related factors, which are highly interdependent. The genetic and disease status of the patient is of great influence but least accessible. For example some MHCII haplotypes may make a patient more susceptible for a disease and less respondent to treatment [16, 179]. Also important is the way of administration, i.e. dose concentration, route and frequency of administration [177]. Lower concentrations may break immune tolerance more readily than high concentrations [1, 190]; subcutaneous injections may be less tolerated than intravenous injection [183, 174]. Also short termed administration does not induce as sustained an immune response as prolonged or intermittent prolonged administration [93]. Nevertheless, no general rule can be derived from this but has to be determined anew for every new therapeutic. Product-related factors are more accessible. Immunogenicity is linked to the structure of the protein [82, 221], as well as to production/procession [53, 108], storage and handling conditions [32, 24, 217, 97]. Antigenic epitopes may be introduced by altered post translational modifications (PTM) [103], artificial molecule design (fusion proteins) [180, 15, 81] and chemical alteration of the molecule

(deimination, methylation, isomerization, deamidation etc.) [50]. This may result in heterogeneity of protein preparations with parts of truncated, misfolded, differently glycosylated or aggregated forms. The latter is regarded to have the strongest effect in inducing immune responses [99, 127]. Also production related impurities (HCP, DNA, endotoxins) do have an impact on the safety of biotherapeutics and need to be removed [208]. Production processes, DSP, storage/formulation and filling are therefore carefully monitored and controlled in order to avoid molecule alterations and ensure for highly pure preparations [144, 157, 20].

1.8 Manufacturing of recombinant biotherapeutics

Choice of the appropriate expression system is the first critical step in the production of recombinant proteins. A broad range of expression systems is available today which have specific benefits and also drawbacks, dependent on application. So the identity and physiological function of many proteins (glycoproteins, e. g. antibodies) is critically dependent on its correct glycosylation [13]. It also influences product yield, solubility and stability of the product. Some expression systems add no (bacteria) or non-human (yeast, insect or plant cells) glycosylation structures to the expressed proteins. These systems are applicable for aglycosylated proteins like hormones, enzymes and certain cytokines. They might also be suitable for monoclonal antibodies and fragments thereof without effector functions. Market approved examples are Certolizumab-Pegol (Cimzia®, UCB) and Ranibizumab (Lucentis®, Genentech Inc.). Since these expression systems are generally more cost effective than mammalian systems, efforts have been made in glycoengineering to make them applicable for the production of glycoproteins, too [167, 80]. However, other contaminants from the culture itself can be riskful, like endotoxins from bacterial cultivation. Even in mammalian expression systems there are two abundant epitopes that human proteins do not feature: the Galα-(1,3)-Gal modification and N-glycolylneuraminic acid (Neu5Gc) [170]. However, the glycosylation structure in mammalian systems come as close to the human equivalent as possible. Most of the approved antibody-based therapeutics are thus produced in mammalian cells and predominantly in Chinese Hamster Ovary cells (CHO). Despite a variety of mammalian cell lines like human embryonic kidney cells (HEK-293), human retina-derived Per.C6, baby hamster kidney cells (BHK) or mouse myeloma and hybridoma cell lines NS0 and SP2/0, respectively, CHO cells remain the working horse in the production of recombinant proteins [36, 227]. Seventy percent of all bio-therapeutics are

recently produced in CHO [94]. Human-like glycosylation of the product and consistent quality throughout production argue for that, but also the explicit experience that researchers as well as regulatory authorities do have with this expression system.

CHO cells were also subject of intensive engineering efforts mainly in order to increase the integral of viable cell concentration (IVCC) and/or specific productivity (*q*). Nowadays, a typical production cell line reaches peak viable cell densities of 5-30 x 10^6 cells/ml, specific productivities of 20-70 pg/c/d and product titer of up to 5 g/l (7-14d cultivation) [62]. A basic approach to achieve high productivity is to sub-clone transfected cells in order to obtain individual, single cell derived clones, which can be screened for robust cell growth and high specific productivity. To further enhance protein expression, gene amplification is often employed. In 1978, methotrexate driven gene amplification of dihydrofolate reductase was described for the first time (DHFR/MTX system). DHFR catalyzes the conversion of folate to tetrahydrofolate, which is an important precursor for the synthesis of purines, pyrimidines and glycin [7, 218]. Together with the development of DHFR negative CHO mutants in 1980 it was possible to develop an expression system for the efficient gene amplification and expression of recombinant proteins. DHFR negative cells are transfected with the gene of interest closely linked to the gene for DHFR. Positive clones are selected by cultivation in hypoxanthine and thymidine deprived medium. Gene amplification is achieved as an adaption to increasing levels of methotrexate, which is an analogue to folate and inhibits DHFR. Similar to the DHFR/MTX system is the glutamine synthetase – methionine sulfoxamine system (GS/MSX) [18]. An up to 50 fold increase in productivity compared to non-amplified cells was already reported in 1983 with the production of human interferon. To circumvent laborious clone selection and reliably gain high productivity, approaches for site-directed rather than random integration of the GOI were developed. Here, a DNA repair mechanism is capitalized for site directed integration. Simultaneously to the repair of artificially induced DNA double strand breaks, the GOI is integrated by homologous recombination (recombinase-mediated cassette exchange, RMCE, Figure 1-5) [216]. The most prominent examples are the Cre/*lox* [100, 112] and Flp/*FRT* systems [110], but also a variety of endonucleases (e. g. meganuclease) [202] are employed in combination with recognition sequences for homologous recombination. These systems have been further developed to generate host cell lines featuring artificial chromosomes with one or more specific integration sites (ACE system) [106, 169].

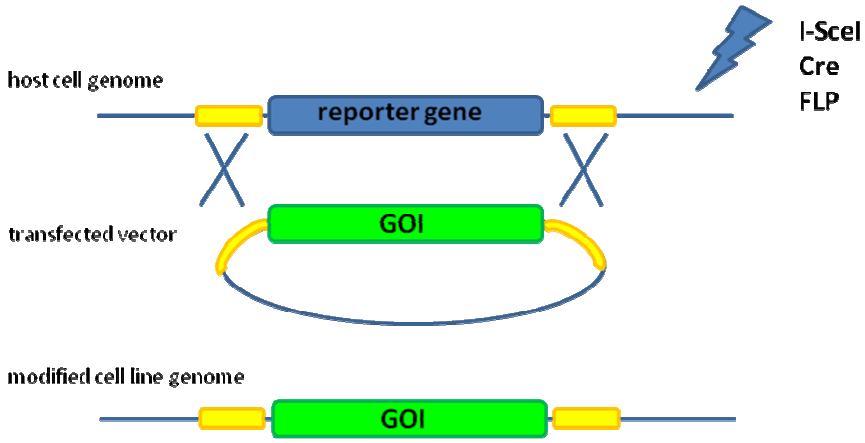

Figure 1-5 Basic principle of recombinase-mediated cassette exchange. I –SceI – meganuclease (homing endonuclease), Cre and FLP – recombinases.

But also several improvements are possible by plasmid vector design. Cytomegalovirus immediate early (CMV) promoter or elongation factor alpha (EF1α) promoter are strong inducers of protein expression and an integrated intron sequence enhances the transport of mRNA to the cytoplasm [189, 30]. Additionally, *cis*-acting elements (S/MAR, UCOEs) [22, 230, 74, 109]and *trans*-acting factors (transcription factors) [107] can be included to facilitate and enhance gene expression.

Despite merely increasing the number of transcripts, several approaches have been made to improve the overall protein expression, density and longevity of the culture [224]. Proteins involved in apoptosis were either suppressed (Bax-like and BH3-only proteins) [52] or enhanced (Bcl-2-like proteins) [44, 113, 115], resulting in a later onset of apoptosis and longer cultivation periods. Higher production rates could be demonstrated with cell cycle arrest [148, 213] and facilitation of post-translational modifications (PTM). In the latter, proteins of the unfolded protein response (UPR) like XBP-1 [19, 188] and transcription factor ATF4 [168] have been reported to be effective. The last step of successful protein expression is secretion. Factors that facilitate the transport of vesicles charged with protein to the cellular membrane and the fusion of both (CERT, SNAREs) showed also enhancement of specific productivity [67, 176, 175]. Recently, further efforts have been made to determine key regulatory factors on the level of the transcriptom, proteom and metabolism [45, 37, 158, 58]. Process optimization and medium development make up another field of further improvement in cell growth, specific productivity and product quality. By choice of appropriate culture medium, feed and culture strategies, negative events like nutrient starvation, oxygen

limitation, high osmolarity or accumulation of toxic by-products like lactate can be minimized [234, 156, 111, 101, 91]. This has to be developed anew for every cell line, since the metabolic profile differs considerably from clone to clone.

1.9 Aim of the thesis

All currently approved antibody based therapeutics for the treatment of TNF-related diseases disrupt the complete TNFR1 and TNFR2 signalling pathway by neutralization of TNF. Due to the prominent role of TNF in the homeostasis of pro- and anti-inflammatory responses of the immune system, side effects can be expected and are already reported. In 2008, an antibody has been developed, that specifically targets CDR1 of TNFR1 [123], while leaving TNFR2 and the associated anti-apoptotic signaling untouched. The present work presents cell line development and pilot-scale production of three structural variants of the humanized antibody H398 (IZI06.1). Taken the evolving skills in antibody engineering and the benefits of antibody fragments, two fusion proteins (scFv-HSA, Fab-HSA) were developed next to a conventional IgG. Impact of size, composition and valency on biochemical and biofunctional properties were investigated in detail by comparison of the scFv-HSA to the full length IgG.
Finally, a regulatory compliant cell line was established for the most promising structure variant. The IgG was chosen due to an overall better performance in terms of efficacy, affinity and bioavailability. The cell line is destined for the production of clinical material in an industrial, regulated environment

2 MATERIAL AND METHODS

2.1 Material

2.1.1 Equipment

Agarose Gel System	EX Cell Easy Cast [Owi Scientific, Asheville, USA]
	Ready Agarose Precast Gel Electrophoresis System [Biorad, Munich, Germany]
Autoclave	HST-4x5x6(8)-ES1073 [Zirbus, Bad Grund, Germany]
Balance	Feinwaage Basic [Sartorius AG, Göttingen, Germany]
	440-39N, 440-33N [Kern, Balingen, Germany]
	AG204 DeltaRange [Mettler Toledo, Gießen, Germany]
Benchtop Centrifuge	Biofuge fresco [Hereaus Kendro, Thermo Fisher scientific, Waltham, US]
	Eppendorf 5804R [Eppendorf, Hamburg, Germany]
Blotter	Trans-Blot SD Semi-dry transfer cell [Biorad, Munich, Germany]
Centrifuge	Z383K [Hermle, Wehingen, Germany]
	J2-MC, rotor JA14 [Beckman Coulter, Krefeld, Germany]
	CR422 [Jouan, Rennes, Frances]
	Multifuge 3S-R [Heraeus, Herrenberg, Germany]
Cleanbench	BDK-S1800 [BDK, Sonnenbühl-Genkingen, Germany]
	KR-130 BW [Kojair, Vilppula, Finland]
Digital Imaging System	FluorS [Biorad, Munich, Germany]
Flow Cytometer	Cytomics FC500 [Beckman Coulter, Krefeld, Germany]
FPLC	Äkta Explorer [GE Healthcare, Munich, Germany]
Heat Block	Thermomix Comfort [Eppendorf, Wesseling-Berzdorf, Germany]
	HBT-1-131 [Hlc-Haep Labor Consult, Bovenden, Germany]
HPLC	Waters HPLC System [Millipore, Billerica, USA]
	Gold HPLC System [Beckman&Coulter, Brea, CA USA]
Incubation Shaker, Temperature controlled	Ecotron [Infors HT, Basel, Switzerland]
Incubator, temperature controlled	Incucell [MMM, Munich, Germany]
Incubator,	HF160W [Shanghai Lishen, Shanghai, China]
temperature/CO_2controlled	Heracell [Thermo Fischer Scientific, Waltham, USA]
Microplate reader	Tecan infinite M200 [Tecan, Crailsheim, Germany]
	Spectramax 190 [Molecular Devices, Sunnyvale, CA US]
	Sector Imager 2400 (ECL) [MSD, Rockville, MA US]
Nucleofection device	Nucleofector [Lonza, Germany]
Pipettes	[Gilson, Middleton, WI US]
	[Eppendorf, Wesseling-Berzdorf, Germany]
Power Supply	E865 [Consort, Turnhout, Belgium]
QCM	Attana A100C-Fast System [Attana, Stockholm, Sweden]
Spectrophotometer	Ultrospec 100^E [GE, Munich, Germany]
	Nanodrop ND-1000 [peqlab Biotechnology, Erlangen, Germany]

Vortex	Vortex Genie 2 [Scientific Industries, Bohemia NY US]
Water Bath	Typ 1002 [GFL, Burgwedel, Germany]
Zetasizer	Zetasizer Nano ZS [Malvern Instruments, Herrenberg, Germany]
Cryo 1°C Freezing Container	Mr.Frosty [Thermo Fischer Scientific, Waltham, USA]
Gassing station	MX4/4 [DasGip, Jülich, Germany]
Microscope (inverse)	Eclipse TE200 [Nikon, Tokio, Japan]
WAVE station	System 20 SPS [Sartorius Stedim, Göttingen, Germany]
Photodocumentation System	Fluor-S [Bio-rad, Hercules, CA US]
Spinner incubator	Typ 3033 [GFL, Burgwedel, Germany]
Hot air sterilizer	SUT 6420 [Heraeus, Herrenberg, Germany]

2.1.2 Consumables

Filter Tips, 1000µl, 200µl, 100µl, 30µl, 10µ	Peqlab, Erlangen, Germany
Tips, 1000µl, 200µl, 10µl	Corning, Corning, NY USA
UV Cuvettes	Brand, Essex, CT USA
Centrifuge Tubes, 50ml	Corning, Corning, NY USA
Microtubes, 2ml, 1.5ml	Sarstedt, Nürnbrecht, Germany
Stripettes, 50ml, 25ml, 10ml, 5ml	Corning, Corning, NY USA
Petri Dishes, ∅10cm	Roth, Karlsruhe, Germany
Culture flasks, T25, T75, T150	TPP, Trasadingen, Switzerland
Culture plates, 24-well, 12-well, 6-well, ∅15cm	TPP, Trasadingen, Switzerland
ELISA plates	Microlon 96-well [Greiner Bio-one, Kremsmünster, Austria] NUNC Maxisorp [Thermo Fischer Scientific, Waltham, USA]
Dialysis chamber	Slide-A-Lyzer [Thermo Fischer Scientific, Waltham, USA]
Blotting Membrane	Nitrocellulose Protran BA85 [Whatman, Maidstone, Kent, UK]
Blotting filter paper	GB002 [Schleicher&Schuell, Dassel, Germany]
CultiBags 20l	#DBB020L [Sartorius Stedim, Göttingen, Germany]
Sterile filters	Bottle top #SCGPT01RE, SCGPT05RE [Millipore, Billerica, MA US] Syringe filter Acrodisc 0.2µm [Pall, Port Washington, NY USA]

2.1.3 Special Implements

SDS Gel	4-12% Bis-Tris NuPAGE #NP0322-BOX [Life technologies, Carlsbad, CA USA] IEF Gel pH 3-10 #LC5310 [Life technologies, Carlsbad, CA USA]
Carboxyl Sensor Chip	#3616-3103 [Attana, Stockholm, Sweden]
Prepacked chromatography columns	1ml HiTrap Blue HP #17-0412-01[GE Healthcare, Munich, Germany] 1ml MabSelect #11003493 [GE Healthcare, Munich, Germany]
Chromatography resin	His-Select Nickel Affinity Gel [Qiagen, Hilden, Germany]
Chromatography column SEC and CEX	BioSep-SEC-S2000 [Phenomenex, Aschaffenburg, Germany TSK gel G3000SWXG [Tosoh Bioscience, King of Prussia, PA USA] TSKgel CM-STAT 7µm, 4.6mm x 10cm [Tosoh Bioscience, King of Prussia, PA USA]

2.1.4 Chemicals

Bovine Serum Albumin Fr. V	#8076-3 [Roth, Karlsruhe, Germany]
Ethanol abs.	#12-052 [KMF, Lohmar, Germany]
Tween20	#9127.1 [Roth, Karlsruhe, Germany]
Geneticin	#11811 [GIBCO, Life technologies, Carlsbad, CA USA]
DMSO	#D2650 [SIGMA-Aldrich, Taufkirchen, Germany]
O-Phenylenediamine	#P-4664 [SIGMA Aldrich, Taufkirchen, Germany]
H_2O_2 30%	#8070.2 [Roth, Karlsruhe, Germany]
Milk powder	#T145.2 [Roth, Karlsruhe, Germany]
Triton-X100	#3051.2 [Roth, Karlsruhe, Germany]
Agarose low EEO	#A2114 [Applichem, Darmstadt, Germany]
Zeocin	#R250-01 [Invitrogen, Life technologies, Carlsbad, CA USA]
Ampicillin	#K029.1 [Roth, Karlsruhe, Germany]
Imidazol	#X998 [Roth, Karlsruhe, Germany]

All other used chemicals were purchased from SIGMA Aldrich [Taufkirchen, Germany], Roth [Karlsruhe, Germany]or Applichem [Darmstadt, Germany].

2.1.5 Reagents

Streptavidin Poly-HRP	#31334248 [Immunotools, , Friesoythe, Germany]
1-Step TMB Blotting	#34018 [Thermo Fischer Scientific, Waltham, USA]
4X LDS loading dye	#NP0007 [Invitrogen, Life technologies, Carlsbad, CA USA]
100XBSA	#B9001S [New England Biolabs, Ipswich, MA USA]
dNTP mix	#R0191 [Fermentas, Thermo Fischer Scientific, Waltham, USA]
Recombinant human TNFα	Soluble human scTNF, 0.5mg/ml, produced at the IZI, Stuttgart #PHC3015 [Invitrogen, Life technologies, Carlsbad, CA USA]
Coomassie protein assay reagent	#1856209 [formerly Pierce, now Thermo Fischer Scientific, Rockford, IL USA]
Coomassie dying solution	Simply Blue Stain [Invitrogen, Life technologies, Carlsbad, CA USA]
LAL H_2O	[Lonza, Cologne, Germany]
Trypsin-EDTA 10x	#15400-054 [Gibco, Life Technologies, Carlsbad, CA USA]

2.1.6 Buffers and solutions

PBS, 1x	D-PBS, powder [Biochrom, Berlin, Germany]
Blotting buffer	48mM Tris, 39mM glycine, 1,3mM SDS, 20% methanol
MOPS buffer, 20x	50mM MOPS, 50mM Tris, 3.5mM SDS, 1mM EDTA, ultra pure water, pH 7.7
MES buffer, 20x	50mM MES, 50mM Tris, 3.5mM SDS, 1mM EDTA, ultra pure water, pH 7.3
ProteinA binding buffer	20mM $NaPO_4$, pH 7.0
ProteinA elution buffer	0.1M glycine, pH 3.5
ProteinA neutralization buffer	1 M Tris-HCl, pH9.0
Blue Sepharose binding buffer	20mM $NaPO_4$, pH 7.0
Blue Sepharose elution buffer	20mM $NaPO_4$, 2M NaCl, pH 7.0
PBA	1XPBS, 2%fcs, 0.2% NaN_3
SDS running buffer, 10x	1.92M glycine, 0.25M Tris, 1% SDS, pH 8.3

TBS, 5x	495mM Tris, 749mM NaCl, in ultrapure water, pH 7.4
TBE, 5x	450mM Tris, 450mM boric acid, 10mM EDTA, pH 8.3
TMB substrate	50 parts TMB (100mg/ml stock), 1 part 30% H_2O_2, 5000 parts 0.1M Na-acetate buffer, pH 6 TMB One Step ELISA [Thermo Fischer Scientific, Waltham, USA] TMB One Step Blotting [Thermo Fischer Scientific, Waltham, USA]
Ligase buffer, 5x	#B0202S [New England Biolabs, Ipswich, MA US]
Antarctic Phosphatase buffer, 10x	#B0289S [New England Biolabs, Ipswich, MA US]
NEBuffer 1-4	B70001-4S[New England Biolabs, Ipswich, MA US]
Buffer Tango	#BY5 [Fermentas, Thermo Fischer Scientific, Waltham, USA]
React Buffer2,3,4	#Y92500, Y90004, Y900005 [Invitrogen, life technologies, Carlsbad, CA USA]
Periplasmatic preparation buffer (PPB)	30mM Tris-HCl, 1mM EDTA, 20% sucrose, in H_2O, pH 8.0
Erythrosin B staining solution	450 µM Erythrosin B, 1.4 mM NaCl, 441 µM KH_2PO_4

All buffers were prepared using MilliQ water or aqua dest.

2.1.7 Cell lines

14-CHO-S	CHO-K1 derived cell line, adapted to serum free cultivation by Celonic GmbH
23-CHO-S	CHO-K1 derived cell line, adapted to serum free cultivation by Celonic GmbH
HT1080	Human fibrosarcoma [ECACC85111505]
HeLa	Human cervix carcinoma [DSMZ ACC57]
MEF	Immortalized mouse embryonic fibroblasts from TNFR1 and TNFR2 double knock-out mice, stably transfected with TNFR1-Fas and TNFR2-Fas, resp. (Krippner-Heidenreich et al. 2002)

2.1.8 Vectors

pCV001	Celonic expression vector (pcDNA3.1 backbone)
pCV072	CEMAX shuttle vector (pcDNA3.1 backbone)

2.1.9 Bacteria strains

E. coli DH5α	F^- endA1 glnV44 thi-1 recA1 relA1 gyrA96 deoR nupG Φ80d*lacZ*ΔM15 Δ(*lacZYA-argF*)U169, hsdR17(r_K^- m_K^+), λ– #C2987H [New England Biolabs, Ipswich, MA US]
E. coli TG1	F' [*traD36 proAB*$^+$ *lacI*^{q} *lacZΔM15*]*supE thi-1 Δ(lac-proAB) Δ(mcrB-hsdSM)5, (*$r_K^-m_K^-$*)* [Stratagene, La Jolla, USA]

2.1.10 Kits, Markers

Nucleofection Kit V	#VCA-1003 [Lonza, Cologne, Germany]
Nucleobond Kit PC500 Endo-free	#740550 [Macherey&Nagel, Düren, Germany]
Human IL-6 ELISA Kit	#31670069 [Immunotools, Friesoythe, Germany]
Human IL-8 ELISA Kit	#31330089 [Immunotools, Friesoythe, Germany]
NuleoSpin Plasmid Kit	740550 [Macherey&Nagel, Düren, Germany]
NucleoSpin Extract II Kit	#740588 [Macherey&Nagel, Düren, Germany]
BCA Protein Assay Kit	#23227 [Thermo Fischer Scientific, Waltham, USA]
Cell Counting Kit	CCK-8 #96992 [SIGMA Aldrich, Taufkirchen, Germany]
DNA ladder	2-log DNA ladder, #N3200S [New England Biolabs, Ipswich, MA US]
Protein ladder	Precision Plus All Blue Marker, #161-0373 [Bio-rad, Hercules, CA US]
IEF Marker	Serva Liquid Mix #39212 [Life technologies, Carlsbad, CA USA]

Gel Filtration Standard	Gel Filtration Standard #151-1901 [Bio-Rad, Hercules, CA USA]

2.1.11 Antibodies

Goat α human IgG, POD conjg.	#109-036-098 [Jackson Immuno Research, West Grove, PA USA]
Rabbit α human IgG, unconjg.	#309-006-068 [Jackson Immuno Research, West Grove, PA USA]
hIgG from human serum	#I4506 [SIGMA Aldrich, Taufkirchen, Germany]
Rabbit α His, HRP conjg.	#3894.1, Roth, Karlsruhe, Germany
HisProbe H3, HRP conjg.	#sc-8036 [Santa Cruz Biotechnology, Santa Cruz, CA USA]
Goat α human Ig, Fab fragment specific, HRP conjg.	#A0293 [SIGMA Aldrich, Taufkirchen, Germany]
Human IgG from human serum	#I4506 [SIGMA-Aldrich, Taufkirchen, Germany]
Rabbit α human IgG whole molecule, HRP conjg.	#A8792 [SIGMA-Aldrich, Taufkirchen, Germany]
Goat α human kappa light chain	#2060-05 [Southern Biotech, Birmingham, Al US]

2.1.12 Enzymes

EcoRV	#15425-010 [Invitrogen life technologies, Carlsbad, CA USA]
XbaI	#15226-038 [Invitrogen life technologies, Carlsbad, CA USA]
NheI	#15444-011 [Invitrogen life technologies, Carlsbad, CA USA]
EheI	#ER0441 [Fermentas, Thermo Fischer Scientific, Waltham, USA]
BamHI	#15201-031 [Invitrogen life technologies, Carlsbad, CA USA]
NotI	#15441-017 [Invitrogen life technologies, Carlsbad, CA USA]
SacI	#R0156S [New England Biolabs, Ipswich, MA USA]
BglII	#15213-028 [Invitrogen life technologies, Carlsbad, CA USA]
HincII	#R0103S [New England Biolabs, Ipswich, MA USA]
SspI	#R0132S [New England Biolabs, Ipswich, MA USA]
NaeI	#R0190S [New England Biolabs, Ipswich, MA USA]
SmaI	#15228-018 [Invitrogen life technologies, Carlsbad, CA USA]
SmaI	#R0141S [New England Biolabs, Ipswich, MA USA]
MfeI	#R0589S [New England Biolabs, Ipswich, MA USA]
PvuI	#R0150S [New England Biolabs, Ipswich, MA USA]
EcoRI	#15202-021 [Invitrogen life technologies, Carlsbad, CA USA]
DraIII	#R0510S [New England Biolabs, Ipswich, MA USA]

T4 DNA Ligase	#M0202S [New England Biolabs, Ipswich, MA USA]
Antarctic Phosphatase	#M0289S [New England Biolabs, Ipswich, MA USA]
DNA Polymerase Large Fragment (Klenow-Fragment)	#M0210S [New England Biolabs, Ipswich, MA USA]

2.1.13 Media & Supplements

BD-Select	[Beckton Dickinson, Heidelberg, Germany]
CM1035	[HyClone, Thermo Fischer Scientific, Waltham, USA]
RPMI-1640	[SIGMA Aldrich, Taufkirchen, Germany]
F12K	[Invitrogen, Life Technologies, Carlsbad, CA USA]
L-glutamine	#25030 [GIBCO, Life technologies, Carlsbad, CA USA]
D(+)-glucose solution 45 %	#G8769 [SIGMA-Aldrich, Taufkirchen, Germany]
IS-CHO Feed-CD XP	#91122 [Irvine Scientific, Santa Ana, CA USA]
Fetal Bovine Serum	#12476-024 [GIBCO, Life technologies, Carlsbad, CA USA]

2.2 Methods

2.2.1 Cloning

2.2.1.1 Restriction digest

In general, procedures for plasmid DNA restriction have been performed according to procedures published earlier (Sambrook&Russel; 3rd Edition). For the individual enzymes, restrictions have been performed according to the manufacturer's protocol in terms of incubation conditions (buffer, time, temperature) and heat inactivation.

2.2.1.2 Isolation of DNA fragments

For the isolation of DNA fragments for cloning, preparative agarose gel electrophoresis has been performed. Gels were prepared in a way to avoid an overload of DNA per lane, so max.

1-2µg per lane and band were tolerated, otherwise slots were combined. For each electrophoresis, fresh running buffer (1XTBE) was used. DNA fragments were excised under UV light with λ = 366 nm. DNA fragments were isolated of from agarose gel pieces in the presence of chaotrophic salts and purified by binding to silica membranes (Nucleo Spin Extract II, Macherey&Nagel, Düren, Germany). When linearized DNA was prepared for transfection, fragments were not purified by gel electrophoresis but via precipitation in order to avoid contact of ethidium bromide with the DNA to be transfected. Therefore, DNA digest was treated directly with 15 mM EDTA, pH 8.0 before being heat inactivated. Preparations were pooled and DNA was precipitated by the addition of one-tenth of sodium-acetate and at least the double volume of ultrapure Ethanol. The DNA was allowed to precipitate for 15 min at - 20°C, before it was spun down for 10 min at maximum speed. The pellet was then washed twice in 70 % ethanol and resuspended in buffer TE.

2.2.1.3 Generation of blunt ends

To generate blunt ends for ligation after restriction digest of DNA with restriction enzymes that produce sticky ends, incubation of the restriction samples with the DNA Polymerase I Large Fragment (Klenow-Fragment) was performed according to the manufacturer's protocol. Approximately one unit of enzyme per µg digested DNA were added along with a dNTP mix and the appropriate reaction buffer. The sample was incubated 20 minutes at RT and column-purified according to the manufacturer's protocol (Nucleospin ExtractII, Macherey&Nagel, Düren, Germany).

2.2.1.4 Dephosphorylation

To avoid self ligation of blunt ended vector backbones, restriction samples were treated with Antarctic Phosphatase following the instructions of the manufacturer (NEB, Ipswich, MA USA). In brief, 5 units of enzyme were added per µg DNA and the mixture was then incubated for 15 minutes at 37°C and heat inactivated for 5 minutes at 65°C.

2.2.1.5 Ligation

Ligation of DNA fragments have been performed using T4 DNA-Ligase and buffer according to the supplier's recommendation. For ligation of blunt ends and for ligations of cohesive ends 1µl T4 DNA-ligase in a total volume of 20 µl have been used. Molar ratio of vector to insert

was 1:3, if not stated otherwise. Typically 100 ng of vector backbone was ligated with the respective amount of insert to reach the desired molar ratio. Incubation was performed for ~18h at 16°C.

2.2.1.6 Transformation

Chemically competent bacteria (DH5-alpha competent *E. coli*, NEB, Ipswich, MA USA) were thawed on ice and combined with DNA solutions. 50µl bacteria were mixed with 5µl of ligation-reactions or 25ng of supercoiled plasmid DNA. After incubation on ice for 30 minutes, bacteria were subjected to a heat-shock at 42°C for 30 seconds. After incubation on ice for 5 min, 900 µl SOC media (animal component free) without antibiotics were added. Bacteria were incubated for another hour at 37°C under rotation and plated on LB-agar-plates containing ampicillin.

2.2.1.7 Preparation of transfection grade plasmid DNA

From a miniculture of a clone positively tested for the respective vector, a pre-culture of approx. 3ml LB culture with the appropriate antibiotic was inoculated and cultivated throughout the day. From this culture, a 250ml LB culture was inoculated and cultivated over night at 37°C and 220rpm until the OD at λ=600nm reached values between 1.5-4. The culture was centrifuged 10 min at 4211g and the supernatant discarded. The bacterial pellets were processed according to the manufacturers' protocol (Nucleobond Kit PC500 Endo-free, Macherey&Nagel, Düren, Germany). The purified plasmid DNA was resuspended in LAL water under sterile conditions.

2.2.1.8 Cloning of ATROSAB

An expression vector for the use with the CEMAX system was cloned at the Institute of Cell Biology and Immunology, University of Stuttgart (AG Kontermann). Therefore IL-2 leader sequence and light chain (VHCL) of the antibody were cloned via *BamHI* and *NotI* into pCV072, a shuttle vector for the CEMAX System, generating transitional construct 1. The sequences for the heavy chain (VH-CH1CH2CH3) and the respective IL-2 leader sequence were cloned via *KasI* and *NheI* into pFUSE –hIgG1e3-Fc2 (Invitrogen, Life technologies, Carlsbad, CA USA), generating transitional construct 2. This vector features the hEF1 promoter and a mutated IgG1-Fc part with silenced ADCC and CDC function. From this

construct, the sequences for the heavy chain, the leader sequence, promoter hEF1 and the mutated Fc part were excised via *SwaI* and cloned into transitional construct 1 via *PsiI* 5' from the light chain sequences. The resulting vector (pAV036) was used for the generation of an initial cell line for research scale protein production.

Since this vector cannot be used for random integration, a second expression vector was cloned for the generation of a regulatory compliant cell line. Therefore, the CDS of the heavy chain including Kozak sequence and the kappa light chain signal sequence were excised from pAV036 by *EheI* and *NheI* restriction and cloned into Celonic expression vector pCV001 via *EcoRV* and *XbaI*, resulting in vector pCV105 with the heavy chain of the antibody put under control of an enhanced CMV promoter. In a second step, the IgG light chain including the kappa signal sequence was excised from pAV036 by restriction with *BamHI* and *NotI* and cloned into likewise digested pCV001, resulting in vector pCV006. Finally, the complete expression cassette of the heavy chain gene including promoter and polyadenylation signal were excised from pCV105 (*BamI*, *NotI*) and cloned into the *MfeI*-linearized pCV106 resulting in vector pCV107 in the third cloning step. PCV107 is the final, bicistronic expression vector in which light chain and heavy chain genes are under the control of an enhanced CMV promoter in separate expression cassettes. Endotoxin free plasmid DNA was generated for this plasmid and both CDSs were sequenced.

2.2.1.9 Cloning of scFv-HSA

The scFv-HSA expression vector for generation of a CEMAX cell line was again cloned at the Institute for Cell Biology and Immunology at the University of Stuttgart. The sequences of variable domains VLCL including the Ig kappa light chain leader and fused to HSA were cloned via *BamHI* and *NotI* into CEMAX shuttle vector pCV072.

2.2.1.10 Sequencing

Sequence confirmation of the final expression vectors was performed by GATC Biotech AG (Konstanz). The sequencing reactions were performed according to the didesoxy method. Results were analysed using the program OMIGA 2.0 (Gloucester, UK).

2.2.2 Cell culture

2.2.2.1 Cultivation cell lines 23-CHO-S and 14-CHO-S/CV063/25.004

For cell line generation, a new vial of cyropreserved cells was thawed according to a protocol adapted for the CHO cell line growing in suspension under serum free conditions. Cells were inoculated to an appropriate culture vessel with typically 0.2 to 0.3 x 10^6 cells/ml. Cells were then kept at 37 °C, 5 % CO_2, 21 % O_2. A serum-free, chemically defined medium supplemented with L-glutamine was used for cultivation. Cells were monitored routinely for cell density and viability every two to three days. At densities of approximately 1.5 to 2 x 10^6 c/ml, cells were diluted to a density of typically 0.3 x 10^6 c/ml. Well plates and T-flasks were cultivated in a standard incubator with defined atmosphere and spinner cultures were incubated at 37 °C and head space aeration using a gas mixing station.

2.2.2.2 Cultivation of cell lines HT1080, HeLa and MEF-TNFR1-Fas/MEF-TNFR2-Fas

A cryovial of the respective cell lines was thawed, cells resuspended in cold RPMI-1640 5% FCS and spun down 5 minutes at 209 g. The cell pellet was resuspended in prewarmed RPMI-1640 5% FCS and transferred to T75 flasks. Cultures were kept at 37 °C, 5 % CO_2, 21 % O_2 and sub cultivated every two to three days. Therefore cells were trypsinized and split 1:3 to 1:10.

2.2.3 Cell line development

2.2.3.1 Transfection

Transfections were performed by nucleofection. Nucleofection conditions were optimized for the suspension CHO host cell line. Cells were cultivated at least two passages before nucleofection and were used when growing in the exponential phase. For this cell line, cell densities between 1 and 2 x 10^6 cells/ml are typical for the exponential growth phase. The required cell culture volume was transferred to a 50 ml falcon and centrifuged at 209 g for 5 min at 20 °C. The supernatant was discarded and the pellet resuspended in a defined amount of nucleofection solution V (specific solution optimized for this cell line), so that a final cell density of 2 x 10^7 cells/ml was reached. For every approach, 110 µl of this cell suspension

was mixed with the appropriate DNA amount (2-7 µg) and subsequently 100 µl cells (2×10^6 cells) were transferred to a nucleofection cuvette, which then was positioned in the nucleofector device and pulsed with U-024 (specific pulse, optimized for this cell line). After nucleofection, cells were immediately resuspended in prewarmed (37 °C) medium and transferred into a 6-well plate, resulting in a cell density of 1×10^6 c/ml. The cells were incubated at 37 °C, 5 % CO_2, 21 % O_2, ≥ 80 % relative humidity.

2.2.3.2 Selection of high producer clones - SEFEX

The selection of positively transfected cells started 24 h after transfection by medium exchange against the culture medium containing the adequate antibiotic as selection pressure. During the following cultivation, every second to third day the medium was again exchanged by centrifugation of cells at 209 g for 5 minutes at room temperature. The supernatant was discarded and the cells resuspended in the same volume of fresh culture medium containing the respective antibiotic. In course of the selection, non transfected cells died and positively transfected cells replicated. Typically, around day 13 post transfection (specific for G418 selection), the overall viability of the nucleofection approach reached a minimum. When a slight increase of viability indicated an outgrowth of positively transfected cells, cells were conducted to single cell cloning. The remaining cells were further kept under selection pressure until they reached viabilities of 90-100 %. A first small cell bank was cryopreserved of the final clone pool.

Single cell cloning proceeded in two steps. In the first step cells were diluted to a final concentration of 3 cells/100 µl in cultivation medium and seeded in a 96-well plate, i.e. 100 µl and 3 cells per well. After one week, 100 µl cultivation medium was added to a final volume of 200 µl. Again one week later, a partial medium exchange was performed. These 96-well plates were analyzed two weeks after seeding for already grown clones. In the following days, growing clones were monitored for their confluence. Clones with a confluence ≥ 50 % were assayed at the same time for their protein titers in an ELISA which is specific for the expressed protein. Since some clones grew slower than others, this was done repeatedly. High producers were selected by comparison of product titers normalized against the confluence. By considering the overall expression levels, a cut off was determined from which then was decided, which clones to transfer to 12-wells for further cultivation. After all clones were analyzed, the best clones were chosen for the second single cloning step. The second cloning

step was essentially performed in the same way as the first, except that cells were seeded with a density of 10 cells/ml, i.e. 1 cell per well. Also, the 96-well plates were analyzed microscopically for real single cells within 24 h after seeding. These wells were recorded and only these wells were considered for further screening. Based on this procedure, the generated cell line was assumed to be a single cell derived cell line. High producers were again identified by the specific ELISA and the most promising clones were further cultivated.

2.2.3.3 Selection of high producers – CEMAX

For the initial lab-scale production of both derivatives, a small mini pool was generated by the use of the CEMAX System. Therefore the transfected cells were resuspended in medium containing 10 % FCS and cultivated in cell culture plates. From that timepoint, cells grew adherent. They were allowed to recover two days before selection power was applied by medium exchange. Cells were selected by geneticin and zeocin. After approx. two weeks, first growing clones were visible. Clones were transferred via cloning cylinders to 24-well plates and were expanded. High producer clones were identified by product specific ELISA.

2.2.3.4 Expansion of producer clones

After transfer to the 12-well plate, cells were checked microscopically after two days for growth and, if cell density was sufficient, were then transferred to a 6-well. During the 6-well cultivation, a cell specific productivity test was performed for the constriction of high producer cell clones. The cells were further expanded from 6-wells to T-25, T-75 and T-150 flasks. At that time point, a small research master cell bank of at least three cryovials was created.

2.2.3.5 Test for cell specific productivity

During clone expansion, a test for cell specific productivity was performed in order to further discriminate between high and low producers. A defined cell density (3×10^5 c/ml) was seeded into 6-well plates. A cell free sample was taken daily for three or four days, from which the product titer was determined via ELISA. From this titer and the cultivation time, a cell specific productivity was calculated.

2.2.3.6 Cryopreservation

1×10^7 cells/ml were cryopreserved in freezing medium containing 45% fresh and 45% conditioned medium (from current cultures) and 10 % DMSO. Therefore cells were transferred to 50 ml Falcon tubes and centrifuged at 209 g for 5 minutes at room temperature. The supernatant was collected in a new Falcon tube and once more centrifuged at 2630 g in order to obtain conditioned medium. 10% of DMSO was added to the medium. The cell pellet was resuspended in an appropriate amount of freezing medium to reach the cell density of 1×10^7 cells/ml. Homogeneously resuspended cells were aliquoted à 1 ml per vial and transferred into Nalgene croypreservation boxes (cooling rate 1°C/min). These boxes were stored at ≤ 65 °C for at least 24 hours before vials were transferred into the vapor phase of a liquid nitrogen tank.

2.2.4 Protein production

2.2.4.1 Purification of recombinant scFv from the periplasm

Bacterial strain *E. coli TG1* was transformed with a pAB1 expression vector containing the sequence of the scFv. From an 20 ml 2XTY 100 µg/ml ampicillin, 1% glucose overnight culture, a 1l culture was inoculated and grown at 37°C and 170 rpm until an OD at λ = 600 nm of 0.8 to 1.0 was reached. Protein expression was then induced by IPTG and incubated for further 3h at room temperature. Bacteria were harvested by centrifugation and resuspended in 50 ml periplasmatic preparation buffer. After addition of lysozyme (50 µg/ml), the suspension was incubated for 15 to 30 min on ice. Before the suspension was centrifuged again, $MgSO_4$ was added to stabilize the spheroplasts. The supernatant was then dialyzed against PBS over night and subjected to immobilized metal affinity chromatography (chapter 2.2.5.3). The concentration of the purified protein was determined photometrically at λ = 280 nm.

2.2.4.2 Research scale production of TNFR1 antagonists and hTNFR1

A cryo vial of a stably transfected, high producing clone was thawed and expanded. Research scale productions were performed in Bellco vessels with V_{max} = 800 ml, inoculated at a cell density of 0.3×10^6 cells/ml and cultivated in batch or fed batch mode until viability dropped

below 80 %. The culture was then harvested and the supernatant further processed by affinity chromatography.

2.2.5 Protein purification

2.2.5.1 Protein A chromatography

The affinity of the human IgG Fc part towards Protein A was utilized to purifiy the antibody from cell-free culture supernatant. Chromatography was performed on an Äkta Explorer FPLC system. The cell culture supernatant was adjusted to binding conditions. Before applying the sample, the column was equilibrated with 20 mM $NaPO_4$, pH 7.2 for at least 10 CV. After sample application, unbound protein was washed from the column until a stable baseline had established. Bound protein was eluted by pH shift from 7.2 to 2.5. Fractions were collected and tested in a Fast Bradford Assay for their protein content. Peak fractions were pooled and dialyzed against PBS at 4°C.

2.2.5.2 Purification by blue sepharose

Recombinant fusion protein scFv-HSA was purified from cell culture supernatant via the affinity of HSA towards Cibacron Blue 3G. The purification itself was performed essentially as described above for Protein A chromatography.

2.2.5.3 Immobilized metal affinity chromatography (IMAC)

Recombinant antibody fragment scFv was purified manually by covalent binding of its c-terminal histidin-tag to positively charged nickel ions. Protein from periplasmatic production was applied to approx. 1 ml Ni-NTA resin, equilibrated with ~10 ml IMAC binding buffer (20 mM $NaPO_4$, 0.5 mM NaCl, pH 7.4). Unbound protein was washed from the resin with IMAC binding buffer. Bound protein was eluted by increasing concentrations of imidazole (20 mM – 200 mM) in wash and elution buffer at which less tightly bound host cell proteins were removed in a washing step before the final elution.

2.2.6 Biochemical characterization

2.2.6.1 SDS-PAGE and Western Blot Analysis

SDS-PAGE of samples of supernatant or purified protein is performed according to Laemmli using ready-to-use 4-12% BisTris gradient gels (NuPAGE, Invitrogen) or 8% separation gels. 1 x MOPS running buffer was used. For Western Blot analysis, gels from SDS-PAGE were used for semi-dry blotting onto a nitrocellulose membrane. After blocking free binding sites with 1 x TBS 5 % milk powder, the membrane was incubated for at least 2 h at room temperature or over night at 4°C with a suitable directly labeled antibody or an unlabeled primary antibody, diluted in 1 x TBS, 0.5 % Triton-X 100, 3 % milk powder. After washing with 1 x TBS 0.5 % Triton-X 100 (secondary antibody) or 1 x TBS 0.1 % Triton-X 100 (primary antibody), the membrane was likewise incubated with the respective secondary antibody or developed by incubation with TMB in order to detect the separated protein.

2.2.6.2 Nonequilibrium pH Gel Electrophoresis (NEPHGE)

NEPHGE is a modification of isoelectric focusing running with inverted polarity. Samples were diluted to the desired concentration with ultra pure water and mixed with IEF sample buffer at the rate of 1:2. Samples were loaded together with an appropriate marker (IEF marker, Serva) onto a precast IEF Gel (NuPAGE, Invitrogen). NEPGHE was run in an XCell Surelock gel chamber (Novex, Invitrogen) with 40 mM glutamic acid being the anode buffer and 20 mM NaOH being the cathode buffer. Separation was performed by a gradual increase in voltage (60 min 100 V, 60 min 200 V, 10 min 500 V) and constant current and power. After separation, the gel was fixated in 12 % TCA for 30 min. The gel was then washed five times with ultra pure water for 10 min at a time and finally stained with Coomassie staining solution (Simply Blue Stain, Invitrogen) over night. After discoloration of background staining with ultra pure water, the result was photo-documented using a Biospectrum AC Imaging System.

2.2.6.3 Thermal stability

Thermal stability was determined by dynamic light scattering. Therefore, 100 µg of the respective protein were diluted in PBS to a final volume of 1 ml, sterile filtered and

transferred to a quarz cuvette. At a rising temperature gradient from 30 to 90°C (1°C steps with 2 min equilibration time), dynamic laser light scattering intensity (kcps) was measured. From these measurements, the protein specific melting point was determined as the temperature when an explicit increase in the measured light scattering intensity occurred.

2.2.6.4 Size Exclusion Chromatography (SEC)

SEC was performed on a Waters or a Beckman Coulter HPLC-System. The purified fusion protein was analyzed on a Bio-Sep-Sec 200 or a TSK gel G3000SWXG column at a flow rate of 0.5 ml/min with PBS as mobile phase. As a size marker a blend of the following proteins was used:

1) thyroglobuline (669 kDa), apoferritin (443 kDa), β-amylase (200 kDa), bovine serum albumin (67 kDa), carbonic anhydrase (29 kDa) and cytochrome c (12.4 kDa),
2) thyroglobulin (669 kDa), γ-globulin (158 kDa), Ovalbumin (44 kDa), Myoglobulin (17 kDa), Vitamin B12 (1.4 kDa).

2.2.6.5 Cation exchange chromatography (CEX)

CEX was performed by HPLC using a TSKgel CM-STAT 7 µm column with 20mM MES pH 6.0 as mobile phase and 20 mM MES, 1 M NaCl, pH 6.0 as elution buffer. System flow rate was set to 0.8 ml/min, column temperature was set to 28°C. The gradient was created as follows:

Time	Flow [ml/min]	% pump A 20 mM MES, pH 6.0	%pump B 20 mM MES, 1 M NaCl, pH 6.0
Initial	0.8	95	5
7.0		85	15
7.1		0	100
7.9		0	100
8.0		95	5
10.0		95	5

2.2.7 Functional characterization

2.2.7.1 Serum Stability

Purified protein was diluted to a concentration of 10 µM in PBS 20% human serum and incubated at 37°C, 5 % CO_2 and 21 % O_2 for ten days with regular sampling. Samples were stored at -20°C until measurement. Stability, i. e. ability to bind to TNFR1, of both the divalent and the monovalent antibody derivative, were analyzed by ELISA.

2.2.7.2 Affinity measurement

Affinity of both the mono- and divalent antibody derivatives for human TNFR1 were determined by quarz cristal microbalance (QCM) on a A100 C-Fast System (Attana, Sweden). Binding studies were performed on recombinant human TNFR1, immobilized via amine coupling to a carboxyl sensor chip according to the manufacturer´s protocol, resulting in a 27 Hz baseline. Different concentrations were tested (15.6 nM - 250 nM) at a constant temperature of either 25 °C or 37 °C. The system was run at a flow rate of 25 µl/min. All measurements were performed in PBS 0.1 % Tween20, pH 7.4. The sensor chip was regenerated between the individual measurements with 5 mM NaOH, every third measurement was a blank. Data were collected by integrated Attester 3.0 (Attana, Sweden) and analyzed by ClampXP [162]. A mass transport model was fitted to the data [161].

2.2.7.3 Enzyme linked immune absorbent assay (ELISA)

The respective capture antibody was coated to high binding 96-well polystyrene microtiter plates (NUNC, Thermo Scientific, Waltham, USA) by incubation overnight at 4°C. Remaining binding sites were blocked for 2 h at room temperature either with PBS 2% milk powder or PBS 3% BSA. Samples were applied in appropriate dilutions and incubated for another hour at room temperature. Protein not bound to the capture antibody was removed by a washing step (5 x 200 µl/well PBS 0.05% Tween20). Bound protein was detected by the following incubation with the respective secondary antibody conjugated to horse radish peroxidase (HRP). Non bound antibody was removed by another washing step. Upon incubation with HRP substrate 3,3’,5,5’-tetramethylbenzidine (TMB), the enzyme mediated conversion to 3,3’,5,5’-tetramethylbenzidine diimine, resulting in a colour change of the

solution from transparent to blue. The reaction was stopped by addition of 3 M HCl or 1 M H_2SO_4. Absorbance was measured at 450 nm and for plate correction at 690 nm in an ELISA reader.

2.2.7.4 Multiplex Assay

The method is based on the principles of a sandwich ELISA. A Human Proinflammatory 9-Plex Kit for the simultaneous detection of up to nine cytokines (GM-CSF, IFN-γ, TNFα, IL-1β, IL-2, IL-6, IL-8, IL-10 and IL-12p70) was used. In this kit, capture antibodies were coupled to nine spots per well in a 96-well multiplex plate ex works. In brief, samples are loaded onto the plate in appropriate dilutions next to a calibrator blend of all nine cytokines after blocking of free binding sites. All samples were incubated for 2 h at RT under shaking. Non bound protein was washed away and a blend of sulfo-tag labeled secondary antibodies, specific for the respective cytokine was added. After additional two hours of incubation unbound antibody was washed away and cytokines were detected by the aid of a specific reading buffer. In this step, photons are emitted upon an electrochemical trigger which can be measured as a function of the amount of analyte in the respective sample.

2.2.7.5 Flow Cytometry

Mouse embryonic fibroblasts stably transfected with either TNFR1-Fas or TNFR2-Fas were seeded in a 96-well V-shaped microtiter plate at a density of $3x10^5$ cells/well, resuspended in PBA. Cells were pre-incubated with both antibody derivatives for 2h and then stained with the indicated antibodies. All steps were carried out at 4°C (Benedict et al., 1997). Samples were analyzed by flow cytometry (Cytomics FC500, Beckmann-Coulter, Krefeld, Germany). Data was visualized by WinMDI V2.9 and mean fluorescent intensities were analyzed and fitted in GraphPad Prism 5 (La Jolla, USA).

2.2.7.6 Cytotoxicity

Neck cancer cell line Kym-1 expressing TNFR1 as well as TNFR2 were inoculated into a 96-well plate at a density of 10^4 cells/well. After incubation for 23 h, cells were incubated with antibody in triplicates in the concentrations indicated in the respective figure. After another hour of incubation, TNF was added in a concentration determined earlier to reliably kill 90 % of Kym-1 cells in the same experimental setup (LD_{90}). The approaches were

incubated for 23 hours before detection reagent CCK-8 was added to the wells. After further three hours of incubation, optical density (OD) was measured at λ = 440 nm and a reference wavelength of 700 nm (Tecan Infinite M200).

2.2.7.7 Human whole blood assay

Freshly sampled human whole blood from healthy donors was processed within 30 min after withdrawal. 450 µl/well were inoculated into 12-well plates and equilibrated at 37°C. Cells were then pre-incubated with serial dilutions of both antibody derivatives (50 µl) and incubated for another hour. Then cells were stimulated with the indicated concentration of TNF (50 µl) and incubated for further 4 h after which the blood samples were spun down. Serum was collected for the direct use in IL-6 and IL-8 ELISA or stored at ≤ -65 °C until measurement.

2.2.7.8 IL-6 and IL-8 assay

For TNF-mediated release of IL-8, HT1080 cells were seeded into 96-well plates at a density of 2 x 10^5 cells/well and incubated overnight. The next day, along with medium exchange in order to remove constitutively released IL-8, cells were stimulated with serial dilutions of TNF. This was done in combination with or without the antibody derivatives. Also the antibody derivatives alone were tested. The cell culture plates were incubated for additional 18 h and were then centrifuged 5 min at 209 g. The supernatant was used for determination of IL-8 levels by ELISA (Immunotools, Friesoythe, Germany). For TNF-mediated IL-6 release, the same experiment was performed with HeLa cells. These supernatants were used for IL-6 ELISA (Immunotools, Friesoythe, Germany)

3 RESULTS

3.1 Development of research cell lines for three different structure variants of IZI06.1

Three different constructs of the humanized TNFR1 specific antibody H398 (IZI-06.1) were in question to generate a promising therapeutic. These were a full length IgG, a scFv-HSA and a Fab-HSA fusion protein (Figure 3-1). The scFv-HSA and the Fab-HSA are composed of the respective antibody fragment of humanized H398 fused to HSA by a GGGS linker. A major requirement for the full length IgG was to not induce ADCC or CDC. Therefore an IgG4 Fc was considered as a backbone for H398, since the low affinity for the FCγRI would ensure for low ADCC and CDC activity. This was finally neglected, because it was found recently that IgG4 is capable of interchanging Fab fragments and by that loses its bivalency or possibly, and more critically, gains cross reactivity to other not predictable targets in vivo [164]. So it was decided instead to generate an antibody of the IgG1 subtype with silenced ADCC and CDC activity. For this purpose, an engineered IgG1 Fc region was used (pFuse-hIgG1e3-Fc2, Invivogen) with residues of IgG2 (position 233-236) and IgG4 (positions 327, 330 and 331) being introduced into the original IgG1 Fc part of the allotype G1m17,1 [11]. A decision for one of these constructs will be made upon data from initial biochemical and functional characterization. From the final candidate, a fully GMP compliant cell line will be developed.

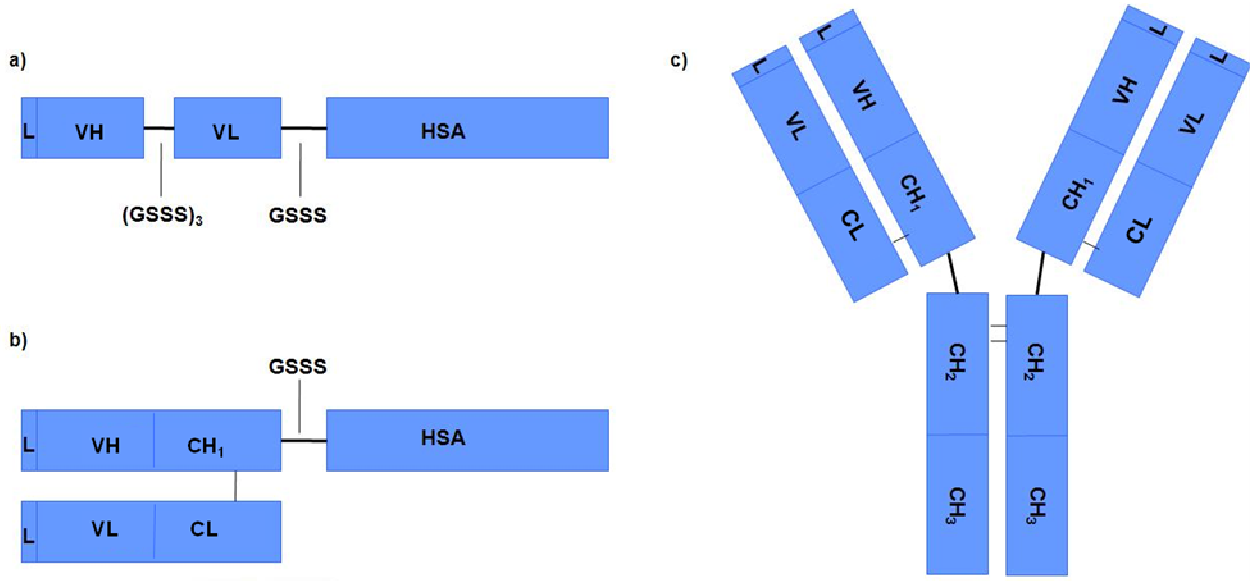

Figure 3-1 **Composition of the different IZI06.1 structure variants.** a) scFv-HSA, b) Fab-HSA, c) IgG1. GGGS – glycine serine linker, L – leader sequence, VH – variable domain of the heavy chain, VL – variable domain of the light chain, CH_1,CH_2, CH_3 – constant domain 1, 2 and 3 of the heavy chain, HSA – human serum albumin

3.1.1 Cloning of the vector constructs

In order to generate sufficient protein for the initial biochemical and functional characterization of the respective TNFR1 antagonist, research cell lines were developed by the use of the CEMAX System. CEMAX is a patent pending technology developed by Celonic for rapid cell line generation by site directed integration of an expression cassette into a hot spot of the CHO genome [77]. The GOI is integrated by a homologous recombination mechanism induced by artificially introduced DNA double strand breaks. The system comprises a shuttle vector into which the GOI is cloned and which features homologous sequence sections necessary for integration. The HSA fusion proteins were cloned via *BamHI* and *NotI* into pCV072. The light chain of the IgG was cloned via *BamHI/NotI* into pCV072, while the heavy chain was cloned via *KasI/NheI* into pFuse-hIgG1e3-Fc 2. From pFuse, the complete heavy chain (with manipulated Fc part) was cloned 5' to the light chain via *SwaI* into pCV072 from step one. All cloning steps were performed at the Institute of Cell Biology and Immunology at the University of Stuttgart.

3.1.2 Development of research cell lines

The CEMAX host cell line is CHO-K1 based and adapted for growth in suspension. Clone 14-CHO-S/CV063/25.004 was thawed and subcultivated for at least three passages. For each transfection approach, 5×10^6 cells were used. A combination of 0.17 pmol of the respective plasmids and 2.26 pmol of a plasmid vector for expression of endonuclease I-SceI was transfected by nucleofection. The endonuclease introduces double strand breaks into the host cell genome and intrinsic DNA repair mechanisms (homologue recombination) allow for site directed integration of the GOI. Since with a recombination frequency of $1\text{-}10 \times 10^{-6}$ targeted integrations are very rare, only a few cells will be positively transfected and survive selection while the bulk of cells will not. Therefore, two approaches were performed to ensure clone growth. In one approach, cells were seeded directly after transfection into 96-well plates at a density of 4000 cells per well and in the other approach, cells were inoculated to 150 mm cell culture plates. By spreading cells into 96-well plates the probability that a grown colony is single cell derived and not cross contaminated is higher than in the 150 mm plates from where clones were picked via cloning cylinders. Both approaches were performed in the presence of FCS. Upon incubation with FCS, viable cells got adherent and dying cells could be efficiently

removed by medium exchange. Positively transfected cells were selected by incubation with a combination of 0.8 mg/ml G418 and 0.2 mg/ml Zeocin. A set of 13 to 25 pools were picked from the respective approach by trypsinization and expanded under constant selection pressure. In the course of expansion, cells were re-adapted to suspension by cultivation with serum free medium.

3.1.3 Characterization of clones

The first criterion for suitability of the different constructs was the growth of the selected pools. Growth was different for the individual constructs. The IgG1 and the scFv-HSA pools grew well and were easy to expand whereas only 4 out of 18 Fab-HSA pools could be expanded. In the following, the stable pools were tested for their specific productivity under comparable conditions (CSP-test, view methods chapter 2.2.3.5). Cells were incubated for at least four days. IgG titers were measured in a hIgG Fcγ specific ELISA and the protein levels of both fusion proteins in a TNFR1/HSA specific ELISA. The complete antibody and the scFv-HSA fusion protein were expressed at a productivity ranging between 8-10 pg/c/d (best producers, Figure 3-2, Figure 3-3). From the four clone pools that could be expanded for Fab-HSA, only two showed a detectable protein expression that was in the range of 0.3-1 pg/c/d (Figure 3-4). No major differences in cell growth (as measured as PDT and maximum cell density) could be observed between the pools of the different constructs, once a stable cultivation was established.

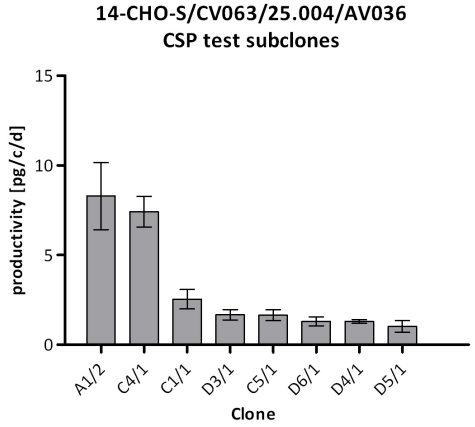

IgG CSP Test	max. vcd [c/ml]	Mean PDT [h]	Titer at d4 [µg/ml]
A1/2	2.1E+06	34	34
C4/1	2.6E+06	36	37
C1/1	1.4E+06	51*	8
D3/1	0.9E+06	57*	4
C5/1	1.7E+06	55	6
D6/1	1.4E+06	44	4
D4/1	1.1E+06	53	3
D5/1	1.0E+06	56*	3

Figure 3-2 **Cell specific productivity of clones expressing the IgG1**. Three day 6-well cultivation of respective clones. Data represent mean ± SD of productivity from the daily intervals. Titers were measured by Fcγ specific ELISA. * One timepoint excluded, since there was no cell growth and PDT became negative

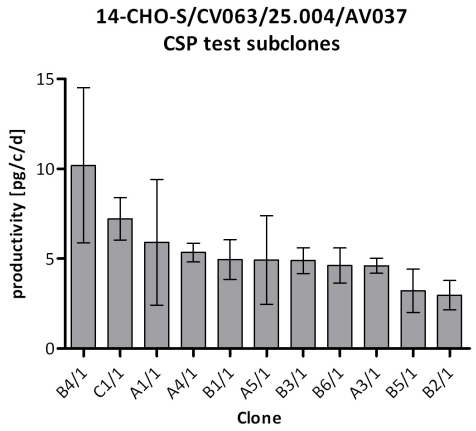

scFv-HSA CSP Test	max. vcd [c/ml]	Mean PDT [h]	Titer at d4 [µg/ml]
B4/1	1.2E+06	71	21
C1/1	2.5E+06	59	24
A1/1	1.7E+06	50	31
A4/1	2.7E+06	41	26
B1/1	3.1E+06	45	21
A5/1	1.4E+06	43	15
B3/1	2.6E+06	57	26
B6/1	1.3E+06	49	13
A3/1	1.7E+06	45	15
B5/1	2.7E+06	31	13
B2/1	2.1E+06	35	12

Figure 3-3 **Cell specific productivity of clones expressing scFv-HSA.** Three day 6-well cultivation of respective clones. Data represent mean ± SD of productivity from the daily intervals. Titers were measured by TNFR1- and HSA-specific ELISA.

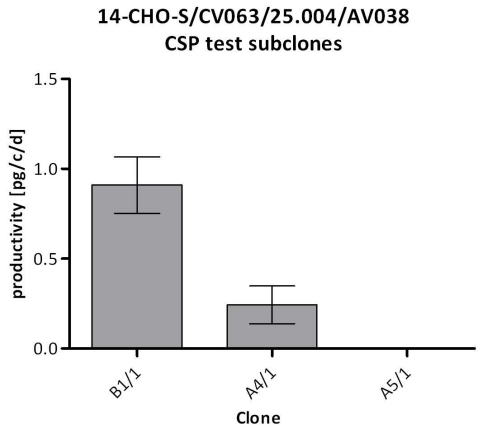

Fab-HSA CSP Test	max. vcd [c/ml]	Mean PDT [h]	Titer at d4 [µg/ml]
B1/1	3.1E+06	32	5
A4/1	2.6E+06	35	1
A5/1	1.8E+06	64	0

Figure 3-4 **Cell specific productivity of clones expressing Fab-HSA.**Three day 6-well cultivation of respective clones. Data represent mean ± SD of productivity from the daily intervals. Titers were measured by TNFR1- and HSA specific-ELISA.

For each construct the clone with the best combination of productivity, growth and titer achieved in the CSP test was tested in batch and standard fed batch cultivation without any medium and feed optimization. The respective clones were C4/1 for the full length IgG, A1/1 for scFv-HSA and B1/1 for Fab-HSA. Initially, a standard protocol was employed for fed batch cultivation that more or less suits most cell lines. All batches were inoculated at a cell density of 3×10^5 cells/ml in a volume of 54 ml of CM1035, supplemented with 4 mM glutamine, 0.2 mg/ml Zeocin and 0.6 mg/ml Geneticin, respectively. At days 2, 4, 5, 8 and 10, 1.2 ml feed (IS CHO Feed-CD XP, Irvine Scientific, Santa Ana, CA US) was added to the fed batches and 1.2 ml medium was added to batches, respectively. Growth profiles are given in

Figure 3-5, development of integrated viable cell density and product titer in Figure 3-6. An overview on the main cultivation characteristics is given in Table 3-3.

a)

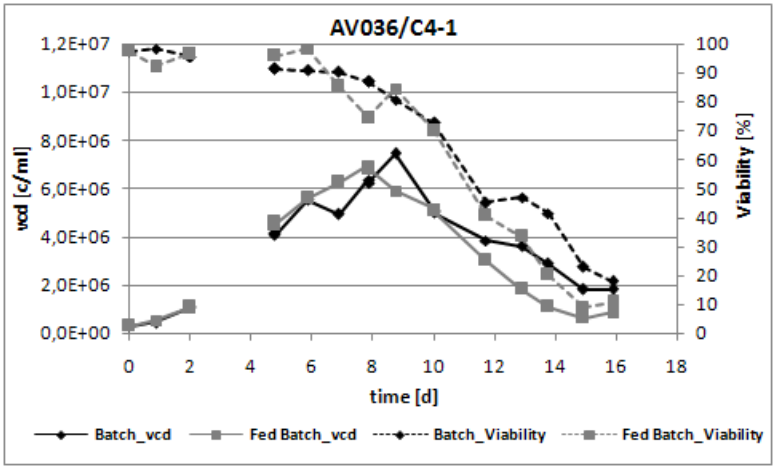

b)

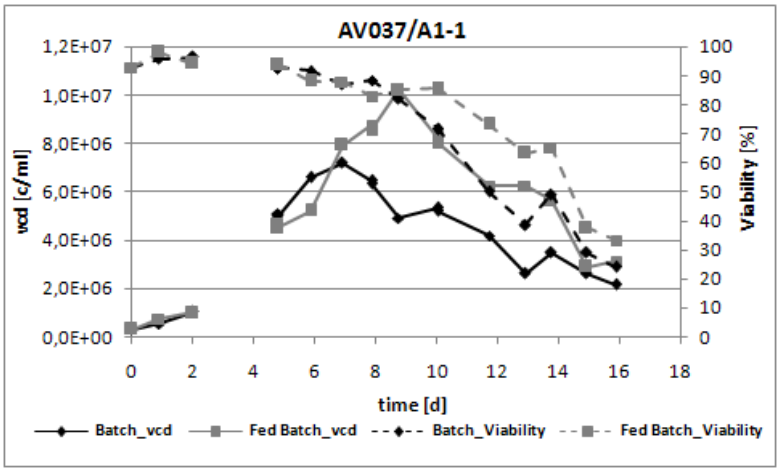

c)

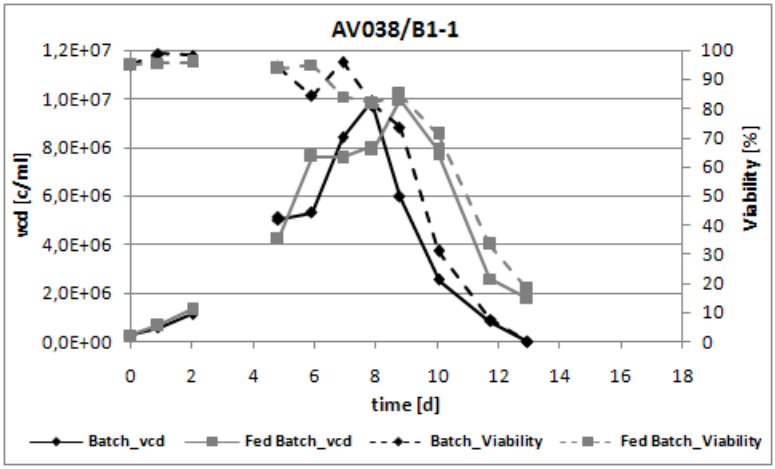

Figure 3-5 **Comparison Batch and Fed Batch cultivation** of cell lines 14-CHO-S/CV063/25.004/AV036/C4-1 (IgG1, a), 14-CHO-S/CV063/25.004/AV037/A1-1 (scFv-HSA, b) and 14-CHO-S/CV063/25.004/AV038/B1-1 (Fab-HSA, c). Culture was inoculated with 0.3 x 10^6 cells/ml and grown until viability dropped below 20%. In Fed Batch mode, cells were fed in total 10% of the end volume with IS CHO-Feed CD XP in 5 steps at days 2, 4, 5, 8 and 10. The Batch volume was adjusted with an equal amount of medium.

a)

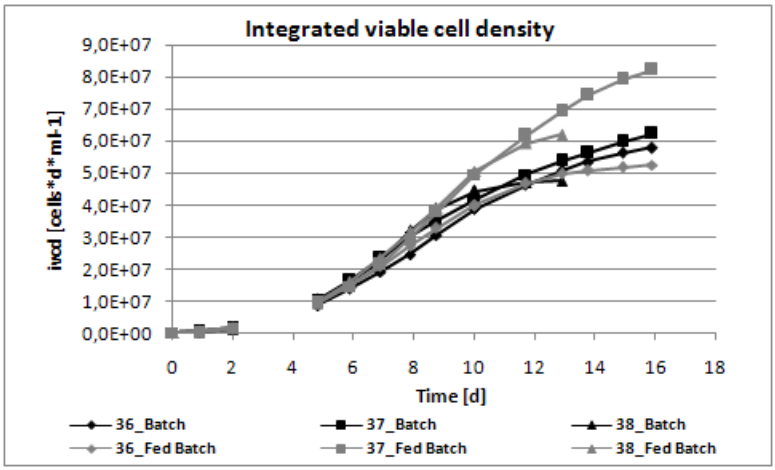

b)

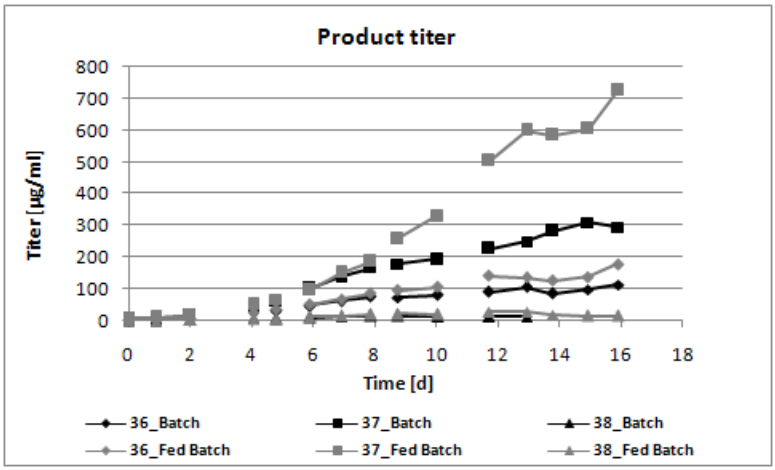

Figure 3-6 **Integrated viable cell density (a) and product titer (b)** of batches and fed batches of cell lines 14-CHO-S/CV063/25.004/AV036/C4-1 (IgG1), /AV037/A1-1 (scFv-HSA), /AV038/B1-1(Fab-HSA). IgG titer were determined by IgG specific ELISA, those of the fusion proteins by HSA specific ELISA. ivcd – integrated viable cell density.

For the IgG expressing cell line, this feeding strategy made no difference in maximum viable cell density, PDT, integrated viable cell density or cultivation time. Instead, growth of the cell lines for the expression of scFv-HSA and Fab-HSA could be enhanced, even if more pronounced for the scFv-HSA than for the Fab-HSA cultivation. Cultivation period at a viability of > 80 % was increased by one day. Maximum viable cell density was increased mainly for the scFv-HSA (7.2×10^6 c/ml to 1.02×10^7 c/ml), whereas the integrated viable cell density was increased for both constructs by 19 % and 29 % cells x ml x d^{-1}, respectively. PDT increased in fed batch cultivation compared to the batch cultivation. Protein expression was best for scFv-HSA, where a maximum titer of 295 mg/l was reached for the batch cultivation and 724 mg/l for the fed batch cultivation. The maximum titer for the full length

IgG was 113 mg/l in the batch and 178 mg/l in the fed batch. Fab-HSA was produced less well as expected from cell specific productivity. A titer of 16 mg/l was reached in the batch and 28 mg/l in the fed batch. The titer measured in samples of the last days of culture have to be regarded critically since the then low viability causes cell rupture and subsequent release of intracellular proteins like proteinases. From all three batches, samples from day 5 to 14 were analysed via Western Blot for product quality and integrity (Figure 3-7).

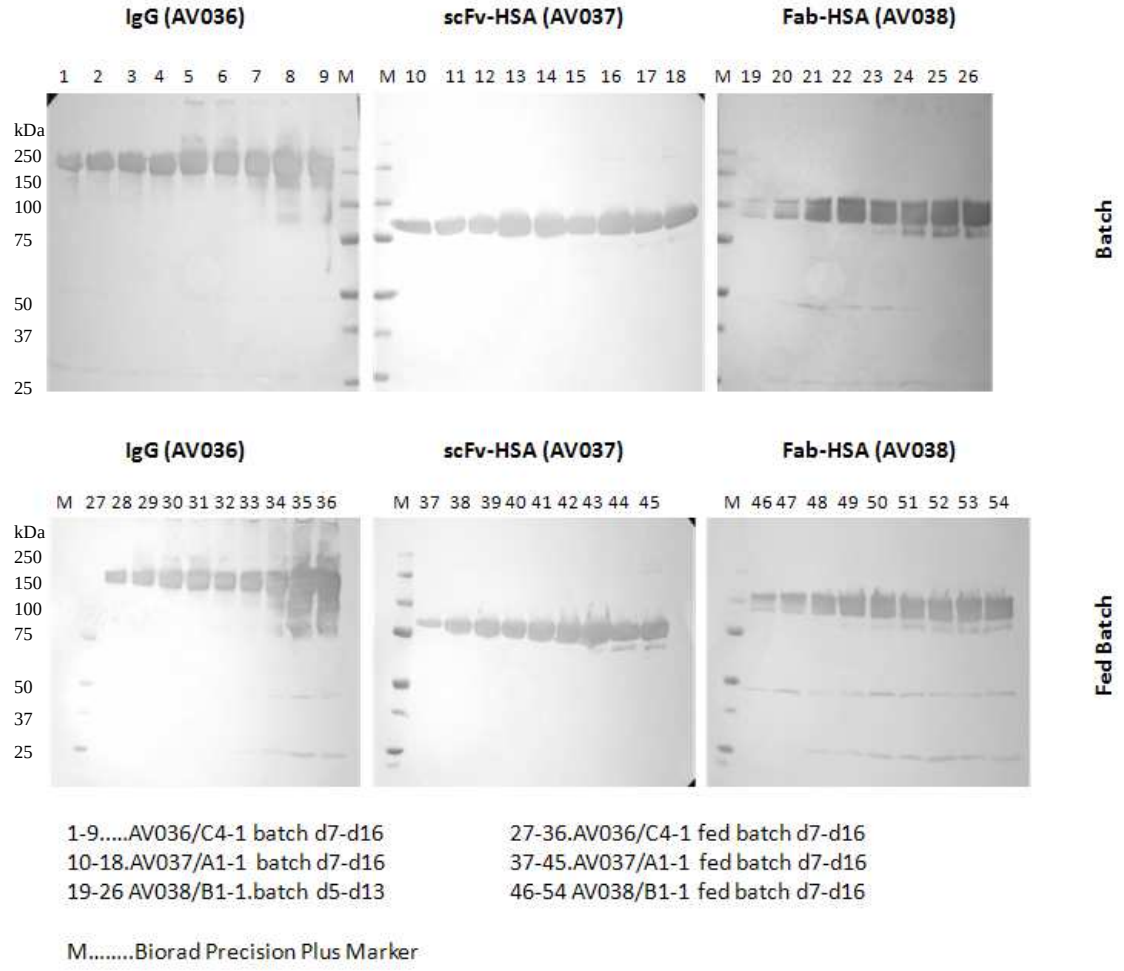

Figure 3-7 **Western Blot analysis of supernatants from batches and fed batches of cell lines 14-CHO-S/CV063/25.004/AV036/C4-1 (IgG), /AV037/A1-1 (scFv-HSA) and /AV038/B1-1 (Fab-HSA)**. Western Blots from supernatants of AV036/C4-1 were co-incubated with an IgG Fcγ specific and a kappa light chain specific antibody, those of AV037/A1-1 and AV038/B1-1 with an HSA specific and a kappa light chain specific antibody, resp. Loaded sample volume was equal for all lanes.

The proteins migrated at an apparent molecular mass of ~ 160 kDa (IgG), ~ 115 kDa (Fab-HSA) and ~90 kDa (scFv-HSA), respectively. An increase of product is detectable with longer cultivation time and also in samples from the fed batches compared to those of the batches. Blots were incubated with a combination of antibodies (against human IgG or HSA

in combination with an antibody against the human kappa light chain) in order to detect free light chains resulting from incomplete assembly or degradation. In a control, all antibodies were tested individually to proof their functionality (not shown). All antibodies worked with the three proteins, except the kappa light chain antibody did not recognize the scFv-HSA. For this protein, though, no free light chains are expected. Samples from the batches as well as from the fed batches of the IgG and Fab-HSA showed the occurrence of light chains (free light chains migrating at ~ 25 kDa and Fab fragments migrating at ~ 50 kDa), resulting probably from a low viability in the last days of the culture. Also the Fab-HSA appears not as a single band but at least as a double band.

In general, the correct protein was expressed in all batches, therefore these pools are suitable for a small-scale production. Batches of a volume of 800ml were inoculated at a density of at least 0.3×10^6 c/ml and cultivated until the viability was nearly or scarcely dropped below 80% in order to prevent product degradation by proteases. The supernatant was harvested and proteins were purified via Protein A (IgG) or Blue Sepharose (scFv-HSA, Fab-HSA). The purified proteins were then analyzed via SDS-PAGE and Western Blot to check for identity, purity and integrity (Figure 3-8, Figure 3-9, Figure 3-10). The full length antibody and the scFv-HSA fusion protein migrated at the expected size (Atrosab ~160kDa, scFv-HSA ~97kDa). The preparation of the Fab-HSA fusion protein revealed several bands apart from the fully assembled protein. Since they were detectable via Western Blot also, they might indicate an incomplete protein assembly or degradation. The IgG preparation showed less impurities (determined by optical densitometry) compared to the preparations of both fusion proteins. In total, 6.4 mg of the IgG, 10.4 mg of the scFv-HSA and 5 mg of the Fab-HSA were prepared and could be delivered to the IZI, University of Stuttgart, where initial tests were performed to assess the functionality of the three TNFR1 antagonists [232].

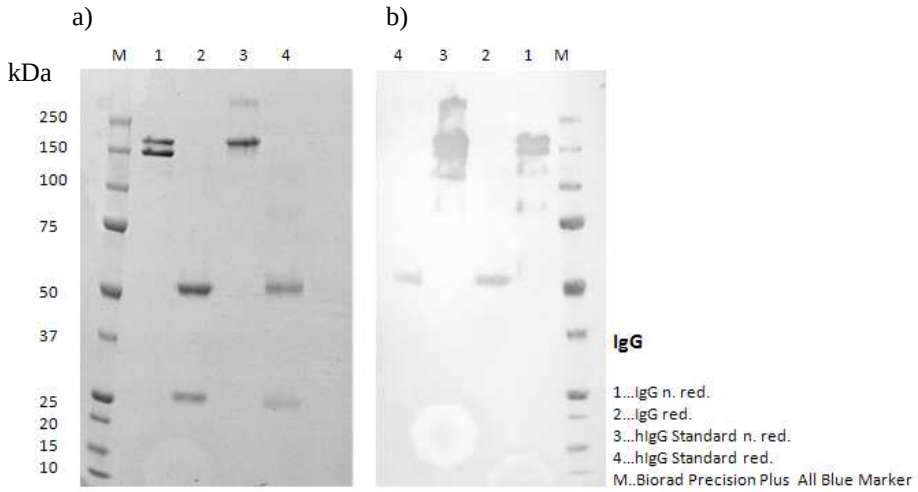

Figure 3-8 **Western Blot (a) and SDS-PAGE (b) of final preparations of ATROSAB** under reduced (red.) and non-reduced (n.red.) conditions. Protein was detected via an IgG Fcγ spec. antibody in western blot, the 4-12% SDS gel was Coomassie stained.

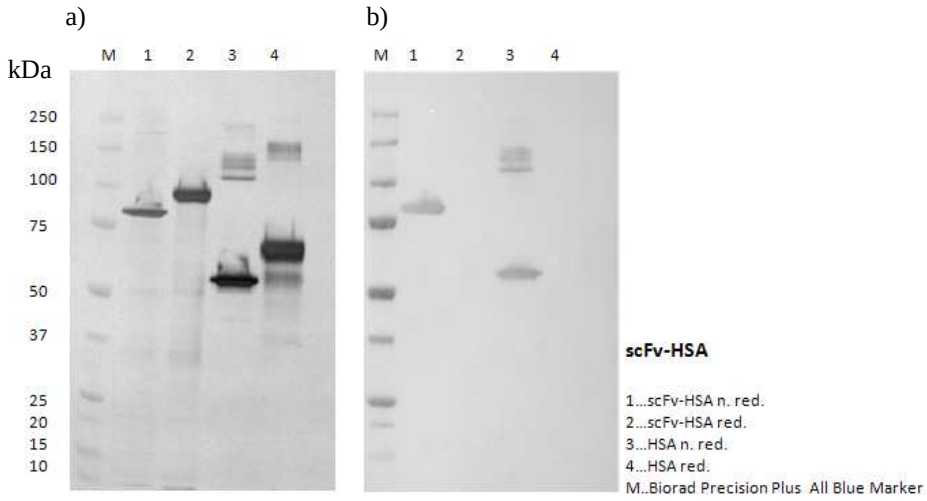

Figure 3-9 **Western Blot (a) and SDS-PAGE (b) of final preparations of scFv-HSA** under reduced (red.) and non-reduced (n.red.) conditions. 600 ng scFv-HSA and 800 ng HSA were applied per lane. Protein was detected via an antibody specific for HSA in western blot and 4-12% SDS gel was silver stained.

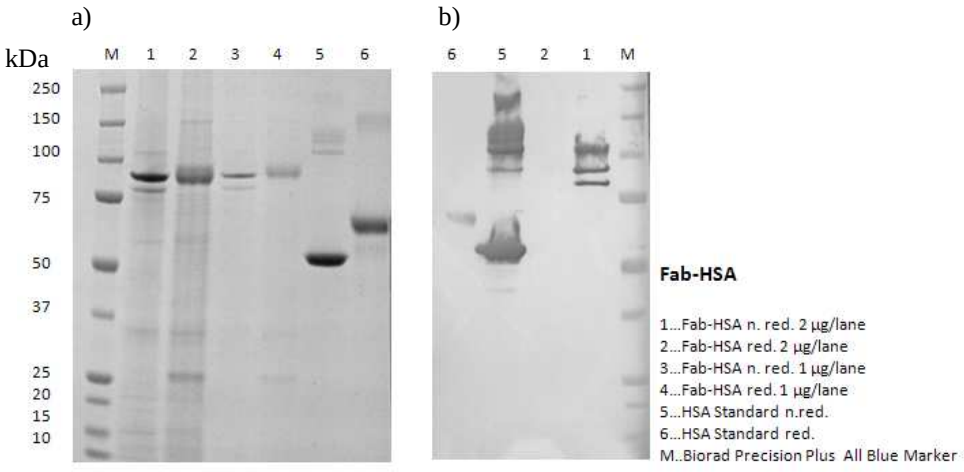

Figure 3-10 **SDS PAGE (a) and western blot (b) of final preparations of Fab-HSA** under reduced (red.) and non-reduced (n.red.) conditions. 2 µg and 1 µg Fab-HSA were applied per lane in SDS-PAGE and 800 ng per lane in western blot. Protein was detected via an antibody specific for HSA in western blot and 4-12% SDS gel was Coomassie stained.

3.2 Evaluation of monovalent TNFR1 inhibitor scFv-HSA

From functional tests at the Institute of Cell Biology and Immunology, Universtity of Stuttgart, the full length antibody emerged as the most favourable design variant because of its high affinity towards hu-TNFR1. However, the influence of composition, valency and molecular mass on the applicability in TNF-mediated disease remained to be evaluated in more detail. For this reason, monovalent scFv-HSA was compared to the full length, bivalent IgG (termed ATROSAB) with respect to TNFR1 specificity, affinity, stability, plasma half life and the ability to inhibit propagation of TNF-mediated inflammation. Fab-HSA was not considered because of the difficulties in expression and purification.

3.2.1 Production of scFv-HSA fusion protein

In order to generate sufficient protein, cell line 14-CHO-S/CV063/25.004/AV037/B4-1 was thawed and expanded for a small scale production. An uncontrolled 800 ml fed batch was performed from which in total 30 mg protein were purified by affinity chromatography (Cibacron Blue 3G). The purified protein was dialyzed against phosphate buffered saline, sterile filtered and stored at 2-8°C. It was then analyzed on SDS-PAGE and via HP-SEC for correct assembly and purity (Figure 3-11 and Figure 3-12, resp.). In SDS-PAGE, scFv-HSA migrated at the correct molecular mass and no impurities could be detected. Protein of higher molecular weight was detected in the sample of a HSA preparation (MW HSA ~67 kDa), which was included as a control. Analysis by HP-SEC revealed also for scFv-HSA portions of protein with higher molecular mass. Most likely aggregation of HSA is responsible, since similar observations were published for HSA earlier [135].

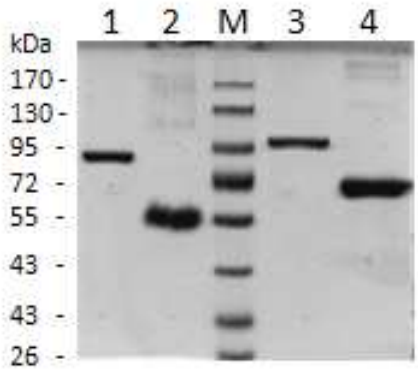

Figure 3-11 **SDS-PAGE analysis** (12% tris-acetate gel, Coomassie staining) of 3 µg scFv-HSA (lanes 1 and 3) and HSA (lanes 2 and 4) under non reduced conditions (lanes 1 and 2) or reduced conditions (lanes 3 and 4).

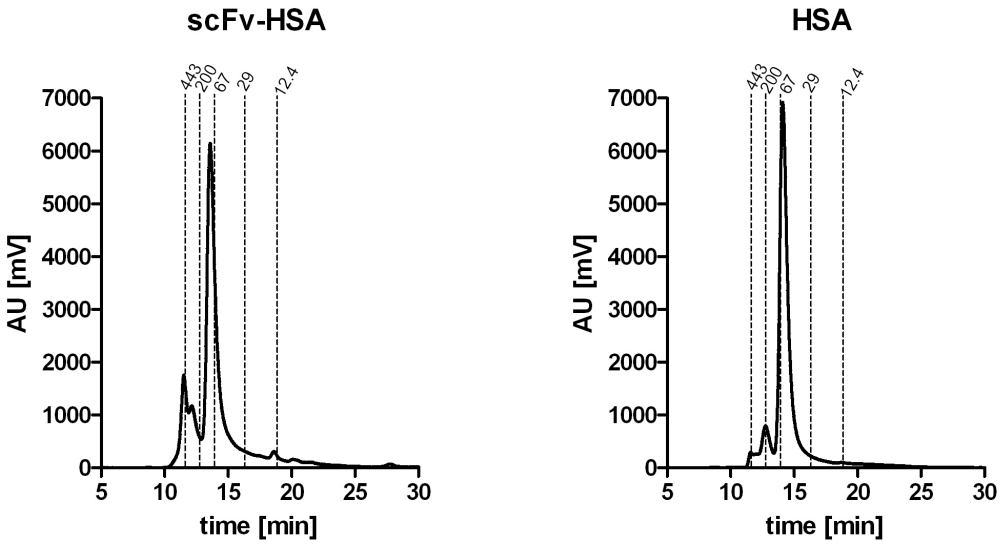

Figure 3-12 **Biochemical properties of scFv-HSA.** Size exclusion chromatography of scFv-HSA and HSA on a BioSep-SEC S2000. The dotted lines indicate retention times and MW of the standard proteins.

3.2.2 Biochemical and functional characterization of the scFv-HSA fusion protein

The generated protein was tested for its bioactivity in comparison to ATROSAB. All following results are summarized in Table 3-8.

3.2.2.1 Thermal stability

First, thermal stability of both proteins was tested. Therefore, the specific melting point was determined for each protein by dynamic light scattering (Figure 3-13). The monovalent format revealed a melting point of about 60°C, which is higher than with its single component scFv (~40°C), but lower than with HSA alone (~73°C). Fusion to HSA obviously stabilizes the antibody fragment. However, the full length antibody is significantly more stable than its monovalent derivative with a melting point of about 80°C.

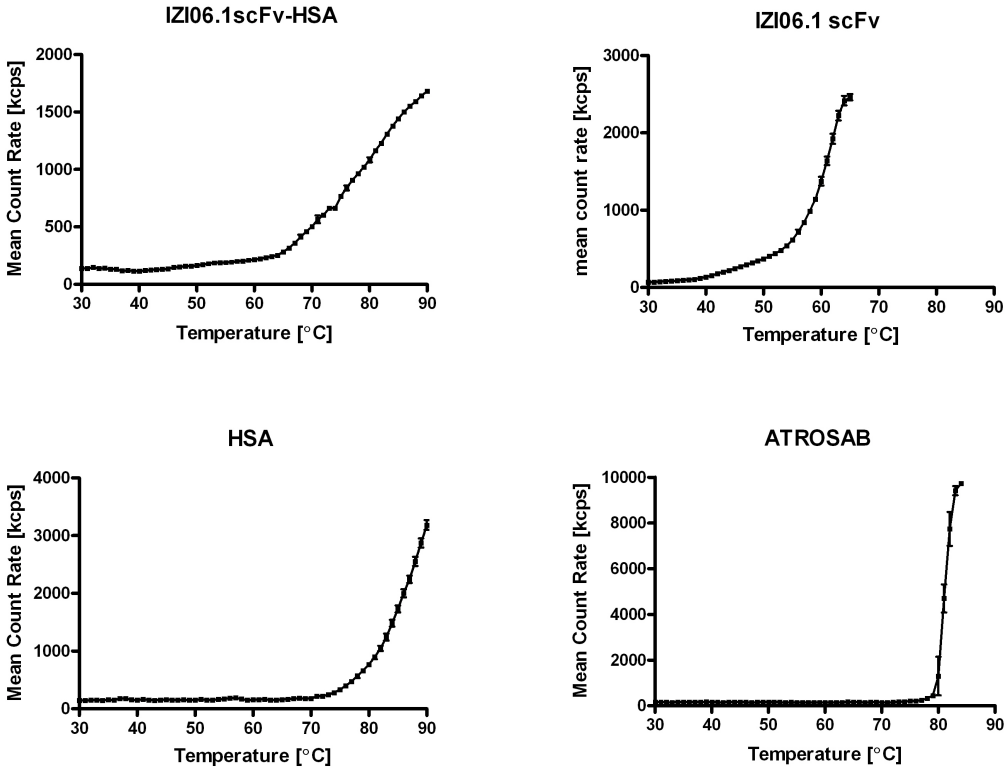

Figure 3-13 **Thermal stability of scFv-HSA, ATROSAB, IZI06.1 and HSA.** Course of protein denaturation with rising temperature, measured by dynamic light scattering on a Zetasizer.

3.2.2.2 Binding specificity and affinity

Next, binding to human TNFR1 was tested in ELISA. Serial dilutions of every format were tested (17 nM - 1 µM). Half maximal binding to an immobilized hTNFR1-Fc fusion protein (1 µg/ml) was determined for the monovalent scFv-HSA at concentrations of 4.6 nM and for ATROSAB at a sub-nano molar level of 0.29 nM (Figure 3-14-A). Results from the ELISA were confirmed by quartz crystal microbalance (QCM) affinity measurements. Here, half maximal binding was reached for scFv-HSA at a concentration of 29 nM (Figure 3-14-B). ATROSAB was demonstrated earlier to show half maximal binding at 0.35 nM [233]. For further proof for selective binding to TNFR1, mouse embryonic fibroblasts stably transfected with either TNFR1 or TNFR2, were incubated with both constructs (0-333 nM). Binding was determined via flow cytometry. Both, scFv-HSA as well as ATROSAB showed selective binding to TNFR1 but not to TNFR2 (Figure 3-14-C). Again, half maximal binding was determined. Half maximal saturation of receptors was reached at a concentration of 8.6 nM for scFv-HSA and at 0.19 nM for ATROSAB (Figure 3-14-D). Taken together the data from ELISA, QCM and flow cytometry, ATROSAB shows a higher affinity towards TNFR1. Nevertheless, both constructs bind specifically to only TNFR1.

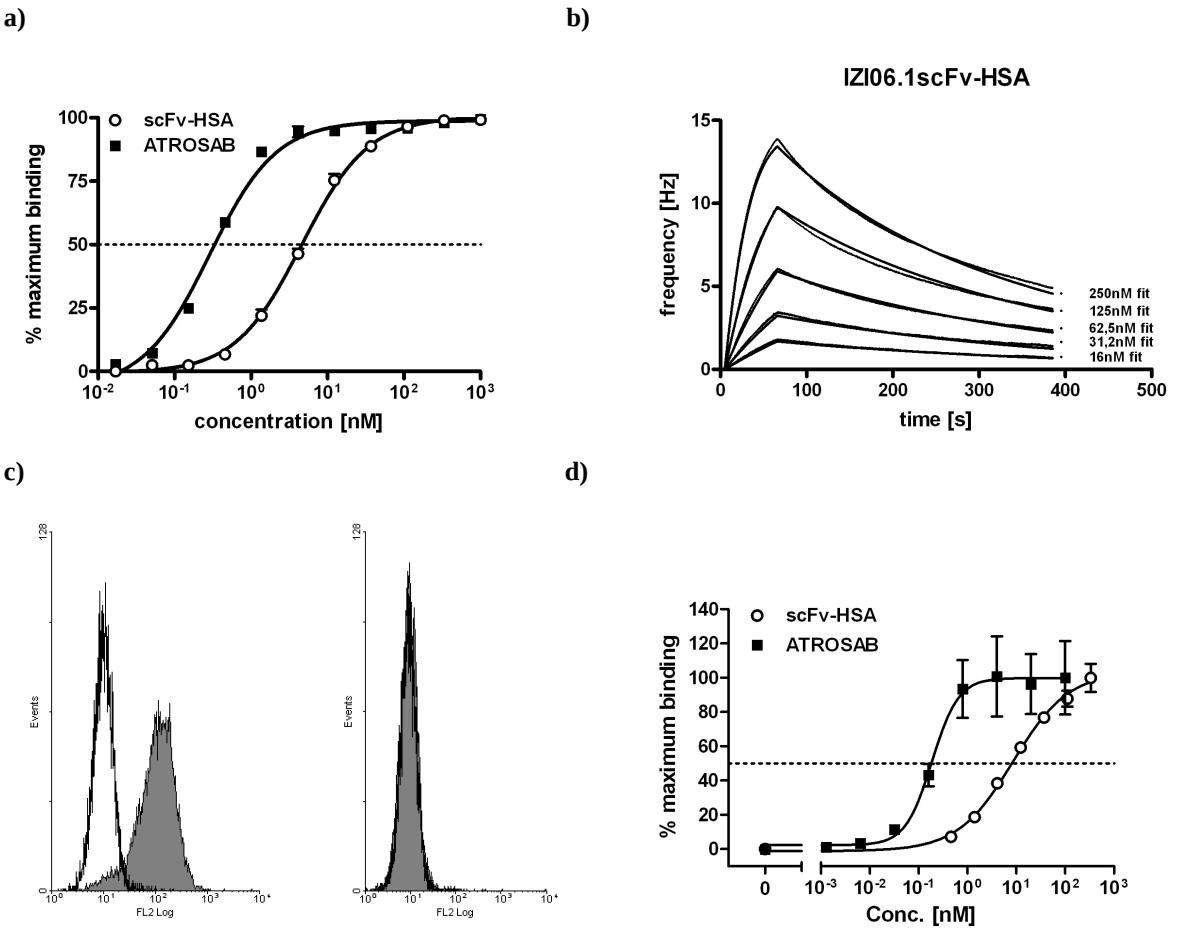

Figure 3-14 **Binding specificity and affinity of scFv-HSA.** Binding of scFv-HSA (o) and Atrosab (■) to TNFR1 and TNFR2, (a) binding affinity to hTNFR1-Fc (1µg/ml coated) in ELISA, (b) determination of binding affinities by QCM, raw data and fit are shown, (c, d) flow cytometry analysis of binding to MEF-TNFR1 and –TNFR2 cells, either with 1 µM (c, histogram) or serial dilutions (d) of scFv-HSA and ATROSAB, resp. Mean fluorescent intensity and ELISA data were normalized (values of untreated control becomes 0%, largest value becomes 100%) and fitted, EC50 values were determined (n=3).

3.2.2.3 Functional inhibition of TNF induced IL-6 and IL-8 release

After confirmation of specificity and binding affinity, the ability of both constructs to inhibit TNF-mediated release of inflammatory cytokines from HT1080 (IL-8) and HeLa (IL-6) cells was investigated. After 18 h of incubation with 10 pM TNF, an IL-6 titer of around 300 pg/ml was measured in the supernatant of HeLa cells. HT1080 cells stimulated with 100 pM TNF for the same incubation period released IL-8 in the range of 4000 pg/ml. Co-incubation of TNF with serial dilutions of both constructs (2 µM to 0.03 nM for IL-6 release from HeLa and 1 µM to 0.02 nM for IL-8 release from HT1080) inhibited cytokine release to control levels (100 pg/ml IL-6, 500 pg/ml IL-8, Figure 3-15).

For scFv-HSA, an IC_{50} of 266 nM for the inhibition of IL-6 release and 339 nM for the inhibition of IL-8 release was determined. However, 6 to 7 fold less ATROSAB was

necessary to reach half maximal inhibition of cytokine release (41 nM for IL-6 and 53 nM for IL-8). When incubated with ATROSAB alone, a small peak of IL-6 and IL-8 secretion could be observed in HeLa and HT1080 cells, respectively, at around 10 nM. This peak equals approximately 2% of the maximum cytokine response in the TNF control and could not be observed with scFv-HSA, neither in HeLa nor in HT1080 cells (Figure 3-16).

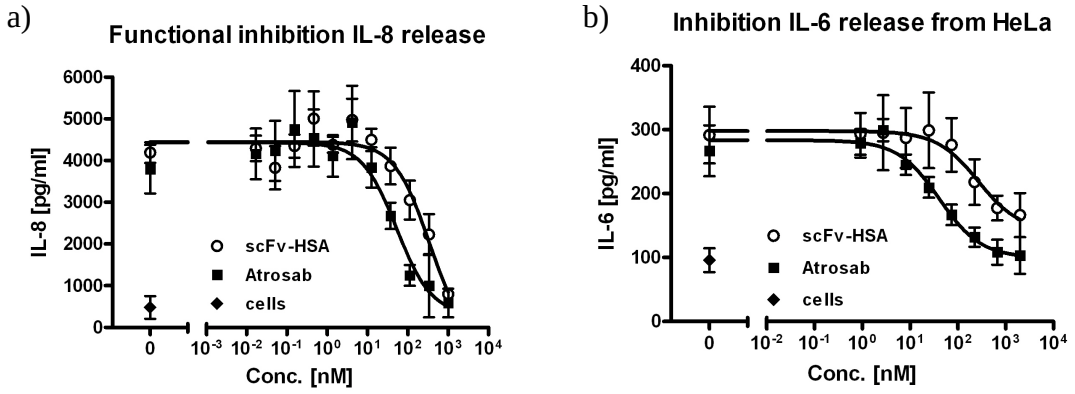

Figure 3-15 **Inhibition of TNF-induced cytokine release by scFv-HSA** (o) **and ATROSAB** (■)**.** a) Inhibition of TNF-induced IL-8 release from HT1080 cells in the presence of 100 pM TNF. Block shift transformation was applied due to different basal cytokine levels in the individual experiments. b) Inhibition of TNF-induced IL-6 release from HeLa cells in the presence of 10 pM TNF. All (n=3).

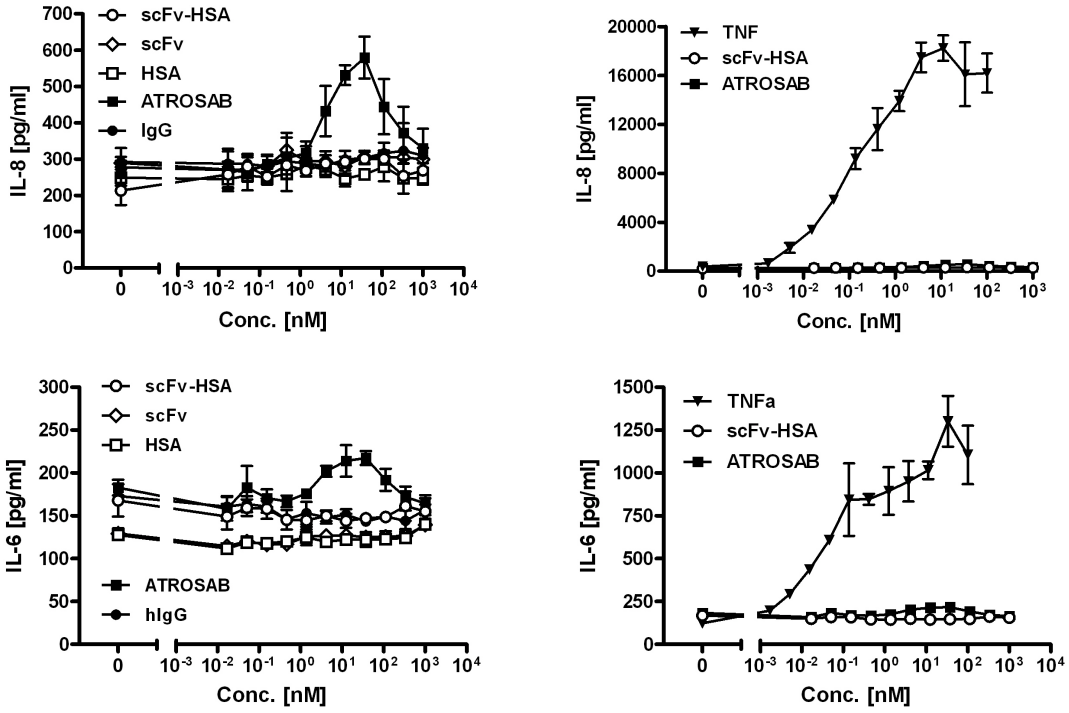

Figure 3-16 **Cytokine release upon individual stimulation with either TNF or scFV-HSA and ATROSAB.** Cytokine release from HeLa (IL-6) and HT1080 (IL-8) cells upon stimulation with 100 nM TNF or serial dilutions of scFv-HSA (o), Atrosab (■) and control proteins (IgG •, scFv ◊, HSA □), respectively. Block shift transformation was applied due to different basal cytokine levels in the individual experiments (n=3).

3.2.2.4 Pharmacokinetics

CD1 female mice were treated i.v. with an initial dose of 25 µg/ml of scFv-HSA and ATROSAB. Serum concentrations decreased for both constructs bi-exponentially. The β-serum half-life was determined to be 1.2 ± 0.1 days for scFv-HSA and 8.3 ± 2.4 days for ATROSAB (Figure 3-17). AUC for terminal half-life was determined as 522 µg/ml*h for scFv-HSA and 1013 µg/ml*h for ATROSAB.

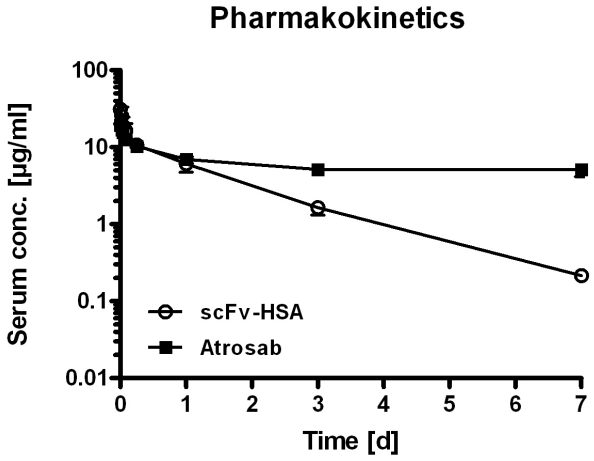

Figure 3-17 **Pharmakokinetics** of scFv-HSA and ATROSAB in female CD1 mice. Serum clearance following a single i.v. injection of 25 µg protein (n=3). Protein levels were determined by ELISA.

3.3 Development of a regulatory compliant production cell line for ATROSAB

Based upon the data generated from the different structure variants of IZI06.1, a regulatory compliant cell line was chosen to be developed from the full length IgG. This cell line is dedicated to be used for the production of clinical grade protein. Therefore all used material was documented and of animal free origin. FCS was completely omitted during cell line development. Celonic cell line 23-CHO-S was used as the host cell line, a CHO-K1 derived cell line adapted to growth in suspension under serum free conditions. The expression vector was adapted and optimized for the expression in CHO.

3.3.1 Vector construction pCV107

For the generation of a plasmid vector that facilitates the high level expression of IZI06.1-IgG (termed ATROSAB) in Chinese hamster ovary cells (CHO), coding sequences from the CEMAX expression vector were cloned into a pcDNA3 based vector backbone. The backbone comprises besides sequences for plasmid propagation and maintenance in *E. coli* a

framework for the expression of the recombinant protein in mammalian cells. This framework consists of the commonly used, strong constitutive promoter region of the human cytomegalovirus immediate early (CMV) genes including an intron A sequence. Enclosure of such a sequence in the 5' untranslated region was shown to enhance heterologous gene expression [42]. A proximate multiple cloning site (MCS) facilitates the insertion of the gene of interest (GOI). Downstream of the GOI, a polyadenylation signal from the bovine growth hormone is included. For a co-selection in eukaryotic cells, a gene cassette for aminoglycoside phosphotransferase was inserted, which confers resistance to Geneticin (G418). Here, the gene is flanked 5' by the simian virus promoter (SV40) and 3' by the respective polyadenylation signal. The coding sequences (CDS) for the IgG1 heavy chain was then excised from CEMAX expression vector AV036 by restriction with *NheI* and *EheI* and inserted into the *EcoRV* and *XbaI* digested vector backbone. In the second step, the CDS for the light chain was excised from AV036 by restriction with *BamHI* and *NotI* and ligated to the likewise digested second vector backbone. A mouse Ig kappa light chain signal sequence was inserted 5' along with the respective CDS. This resulted in two separate expression vectors with both the heavy and the light chain being put under control of the enhanced CMV promoter. In the last step, both vectors were fused. Therefore, the whole expression cassette for the IgG heavy chain (comprising the CMV promoter, the Ig kappa leader peptide, the cds and a BGHpA signal) was excised by restriction with *SspI* and *NaeI* and ligated 5' to the light chain gene cassette of the second intermediate vector, which was linearized by restriction with *MfeI* and treated with *DNA Polymerase Large Fragment* in order to fill in 5' overhangs. These steps resulted in a bi-cistronic expression vector (pCV107) with both gene cassettes (heavy and light chain) being orientated in the same direction. The heavy chain gene cassette is thereby located 5' to the light chain gene cassette in order to assure for sufficient expression of the large heavy chain. Transfection grade plasmid DNA was prepared and checked for quality and identity (Figure 3-19). A vector chart and an overview of both gene cassettes are given in Figure 3-18.

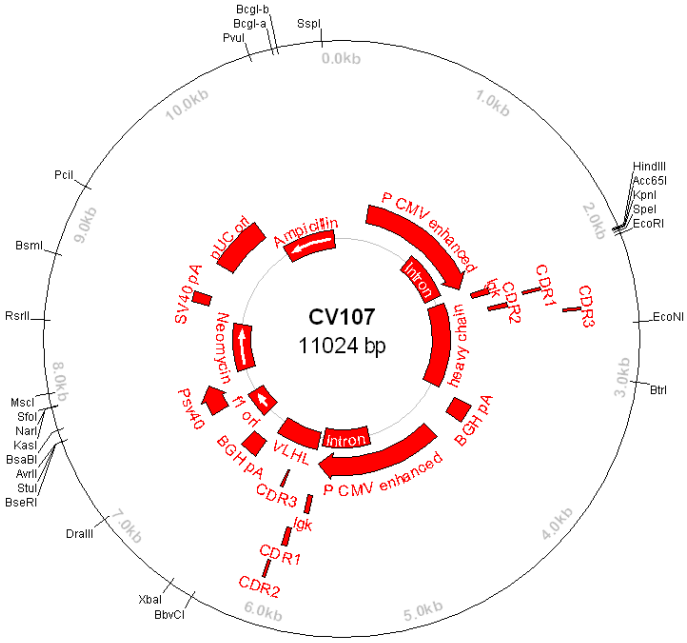

Feature	Name	Function
pCMV enhanced	Cytomegalovirus immediate early promoter, IntronA included	regulated, high level expression of GOI
BGHpA	Bovine growth hormone polyadenylation signal	Polyadenylation signal
Igk	Immunoglobuline kappa light chain leader sequence	Leader sequence for GOI
pUC ori	pUC Origin of replication	Origin of replication in bacteria
F1ori	Bacteriophage F1 origin of replication	Origin of replication in phages
pSV40	Simian virus 40 promoter	Regulated expression of GOI (here antibiotic resistance genes)
SV40pA	Simian virus 40 polyadenylation signal	Polyadenylation signal
Amp/Ampicillin	Beta-lactamase TEM1 gene	Confers resistance to ampicillin
Neo/Neomycin	aminoglycoside phosphotransferase gene	Confers resistance to neomycin

Figure 3-18 **Expression vector pCV107.** Scheme of plasmid vector for the expression of ATROSAB in CHO cells.

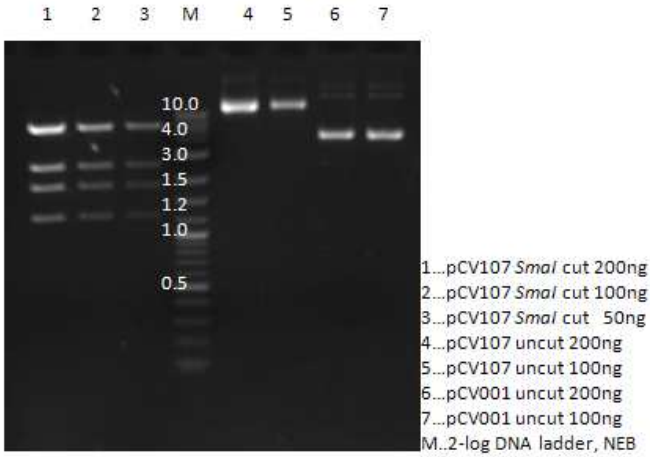

Figure 3-19 **Quality control of plasmid vector preparation for nucleofection.** Identity, concentration and quality were checked by restriction with *SmaI* and compared with a reference plasmid. Predicted fragment sizes were: 5391 bp, 2555 bp, 1838 bp and 1240 bp.

3.3.2 Cell line generation 23-CHO-S/CV107/K20

Cell line RWCB-23-CHO-S 20.10.08 was thawed and cultivated in 250 ml spinner flasks at 37°C, 5 % CO_2, 21 % O_2, gas flow 2.5 sL/h, 80 rpm stirrer speed using serum-free chemically defined CM1035 cell culture medium containing 4 mM L-glutamine. Cells were expanded and passaged at least 2-3 times before they were used for transfection. Cells were suitable for transfection when growing in the exponential growth phase (1-2 x 10^6 cells/ml) and at a viability of more than 90 %. Here, cells reached a density of 1,58 x 10^6 cells/ml and had a viability of 99 % with 3 passages after thawing. An overview on the different steps in cell line generation is given in Figure 3-20 for convenience.

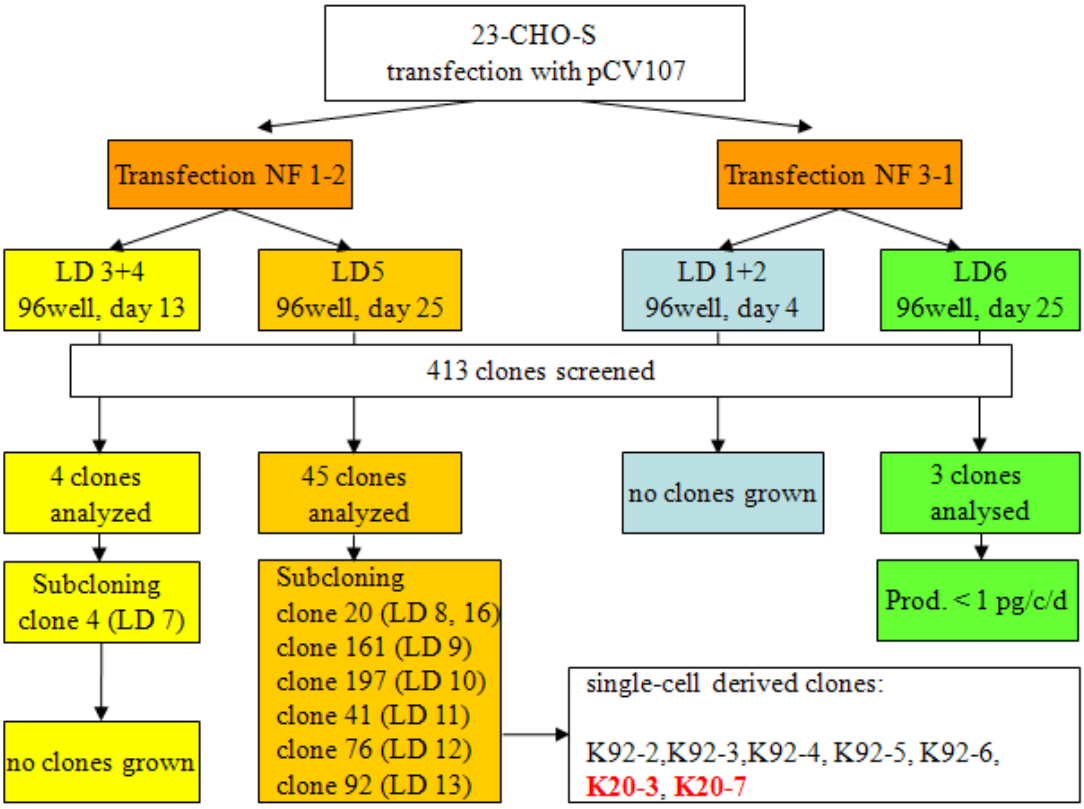

Figure 3-20 **Overview on cell line generation.** Scheme of different cloning steps in the generation of ATROSAB production cell line. K – clone, LD – limited dilution, NF – nucleofection.

In total three different transfections were performed using a nuclefector device (Lonza, Germany). For every nucleofection, three parallel replicates were performed to circumvent any complications regarding the survival of the cells after transfection. One nucleofection approach was performed with 8 µg of supercoiled (sc) plasmid pCV107 (nucleofection 1, NF1), another with 8 µg of the *SspI*-linearized (li) plasmid (NF2). The latter approach directly died after transfection, though, and was repeated (NF3). 24 h after nucleofection with supercoiled pCV107 (NF1), the selection was started by complete medium exchange from

medium without Geneticin to medium containing 0.6 mg/ml Geneticin. Non-transfected cells died within the next twelve days (Figure 3-21). In that course, viability dropped to the minimum of 17 % in replicate 2 (NF1-2, Figure 3-21-A). The characteristic drop in viability during selection was more pronounced as in the selection of cells transfected with the linearized plasmid, where viability dropped to 30 % in NF3-1 at day 7 (NF3, Figure 3-21-B). Approaches with the most articulate drop in viability (NF1-2, NF3-1) during selection were further expanded until a stable clone pool was generated. A small primary seed bank was laid down.

a)

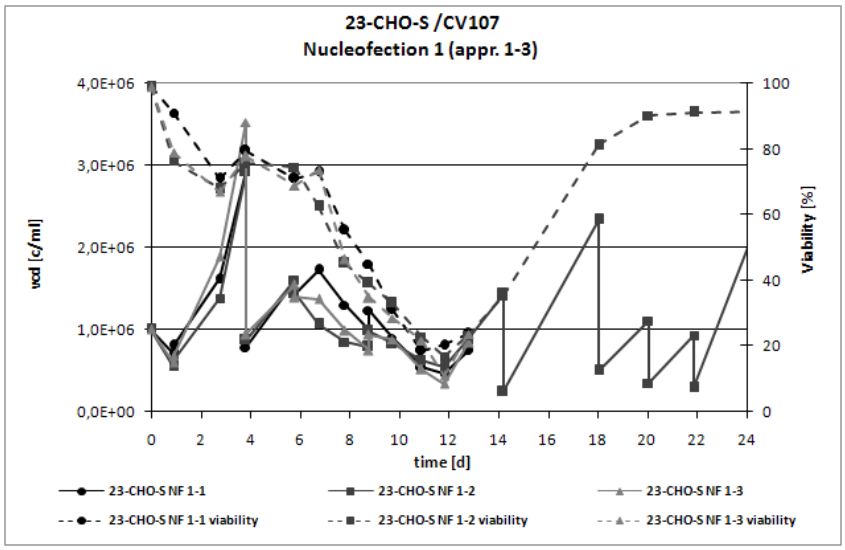

b)

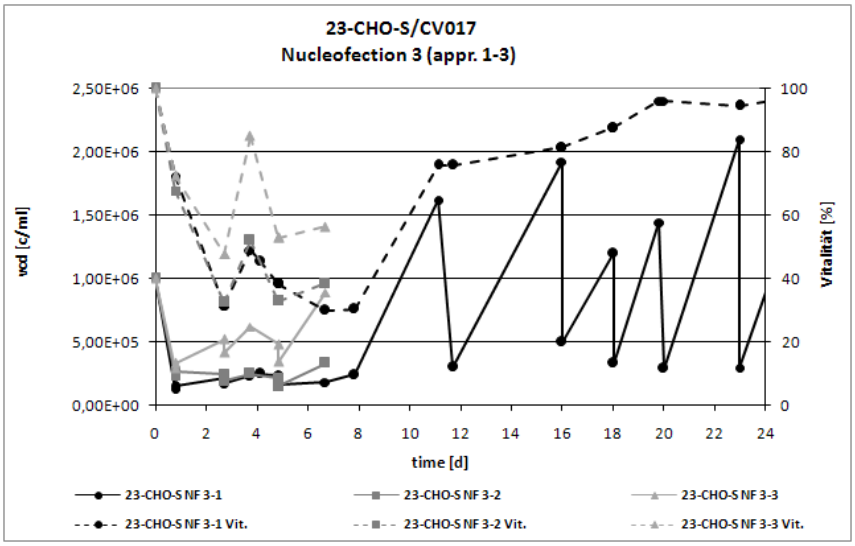

Figure 3-21 **Selection of clone pools for ATROSAB.** Viable cell count and viability of nucleofection 1 (a) and 3 (b), approaches 1-3, during selection process with Geneticin. On day 13, all cultures recovered in NF-1 and NF1-2 was cultivated until the clone pool fully recovered. From NF-3, approach NF3-1 was expanded. Vcd – viable cell density, NF – nucleofection.

Both fully recovered clone pools were then subjected to a 3-day 6-well cultivation under identical conditions to determine their specific productivity (measured by hIgG specific ELISA, Figure 3-22). No significant differences could be observed between the clone pools generated with either supercoiled (0.27 pg/c/d, NF1-2) or linearized (0.31 pg/c/d, NF3-1) plasmid DNA. Finally, the clone pool derived from NF1-2 was chosen for the first cloning step, because the lower viability during selection than in NF3-1 might account for a more stable clone pool.

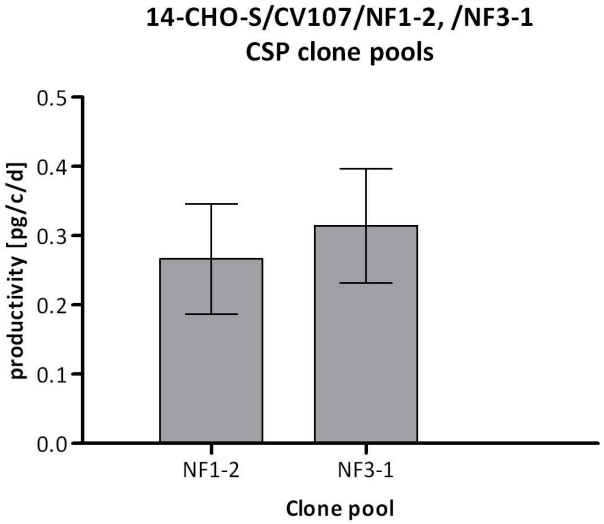

Figure 3-22 **Cell specific productivity of clone pools** generated from nucleofection 1 (supercoiled plasmid) and 3 (linearized plasmid). Data represent mean ± SD of productivity from the daily intervals. NF – nucleofection

In order to check for correct expression, a western blot was performed from samples taken during the transient expression phase in NF1-2 post transfection (days 1, 3 and 4, Figure 3-23). Detection with a human IgG Fcγ specific antibody revealed that cells were expressing the desired product. Interestingly, instead of one distinct band, two separate bands were recognized by the antibody.

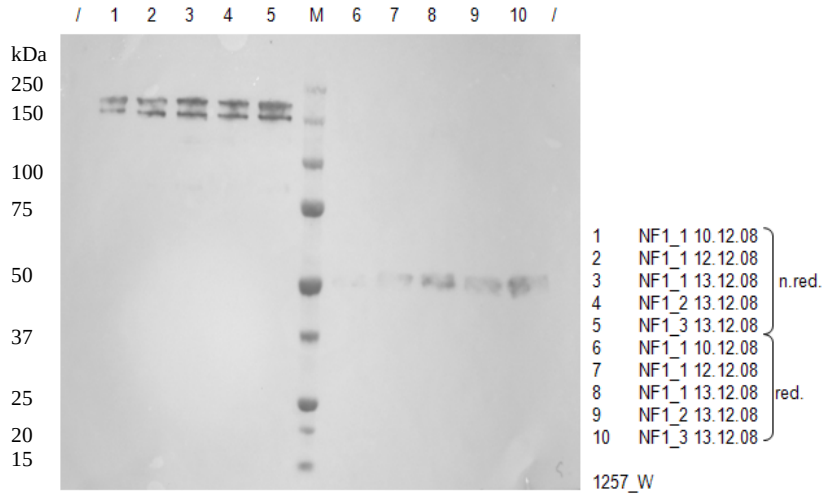

Figure 3-23 **Transient expression of ATROSAB (NF1)**. Western blot of transient expression of ATROSAB at day 1,3 and 4. Lanes 1-5 represent non reduced samples, lanes 6-10 the reduced samples. M – Precision All Blue Marker (Biorad). ATROSAB was detected by an antibody specific for the IgG Fc domain.

Cells from NF1-2 were subjected to limiting dilution cloning when, at day 13 post transfection, a slight increase of viability from 17 % to 23 % was observed and positively transfected cells began to expand. Cells were spread into 96-wells with a statistical density of 0.3 cells/well (35 plates) and 1 cell/well (15 plates). All plates were examined microscopically and only wells with one distinct cell were further observed.

After 24 days, all 50 plates did not show any cell growth. Therefore, the fully recovered, cryo-preserved clone pool of NF1-2 was thawed and another limited dilution (50 plates) was seeded with statistically 3 cells/well. This approach was not examined for single cells. After 11 days, the first clones could be transferred to 12-well successfully. At this stage, grown clones represent “mini-pools”, since it was not discriminated between clones grown from wells with single cells and those with more than one cell. In total, 413 clones from wells with detectable cell growth could be transferred in multiple steps from 96-well to 12-well plates on day 13 and 15 after seeding. Confluence was documented for every well. During transfer, ELISA analysis of the 96-well supernatants was performed to discriminate between potential high producers and clones that produced no or merely low amounts of protein (Figure 3-24). For calculation of the final IgG titer, the confluence at the day of sampling was taken into account before the different clones were compared.

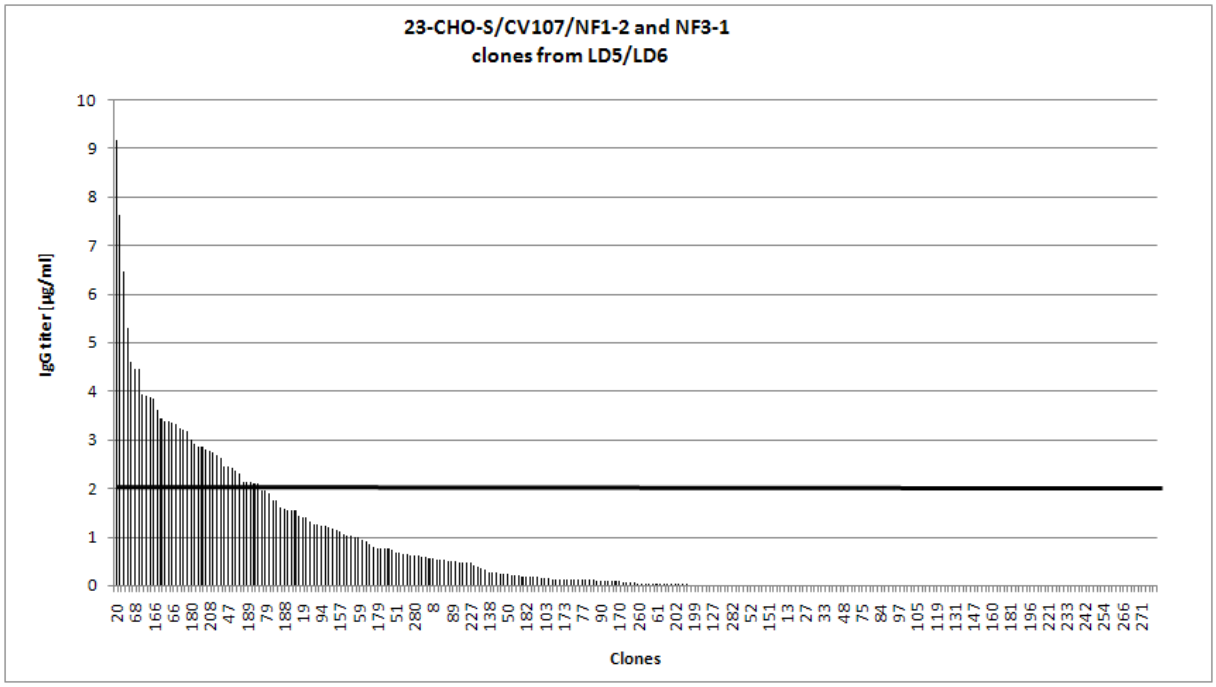

Figure 3-24 **Discrimination of clones by IgG titer from 96-well supernatants.** Determination of IgG titer by ELISA from 96-well supernatants of limited dilutions 5 and 6. Titers are corrected for individual confluences at the time of sampling. The black line indicates the threshold of 2µg/ml IgG. Only clones with detectable protein expression are shown and only every 5th clone number is given.

From these 413 clones, 39 showed an IgG titer of over 2 µg/ml. They were subsequently expanded and analyzed for their specific productivity in small three day cultivations (6well, CSP test). Results are shown in Figure 3-25-a. Eight clones were regarded as potential high producers (1.7 – 4.8 pg/c/d) and taken into account for sub-cloning (K20, K161, K41, K197, K76, K169, K172, K92). For a final decision, the results of T-flask and spinner cultivation were also considered. Productivity from all growth phases was included. These results present a slight different picture in the ranking of productivity, although also here, clone K20 performed best (13 pg/c/d, Figure 3-25-B). All other clones showed a similar productivity between 2 and 3 pg/c/d. The ranking from this experiment would be K20, K197, K161, K41, K169, K92, K172 and K76.

a) b)

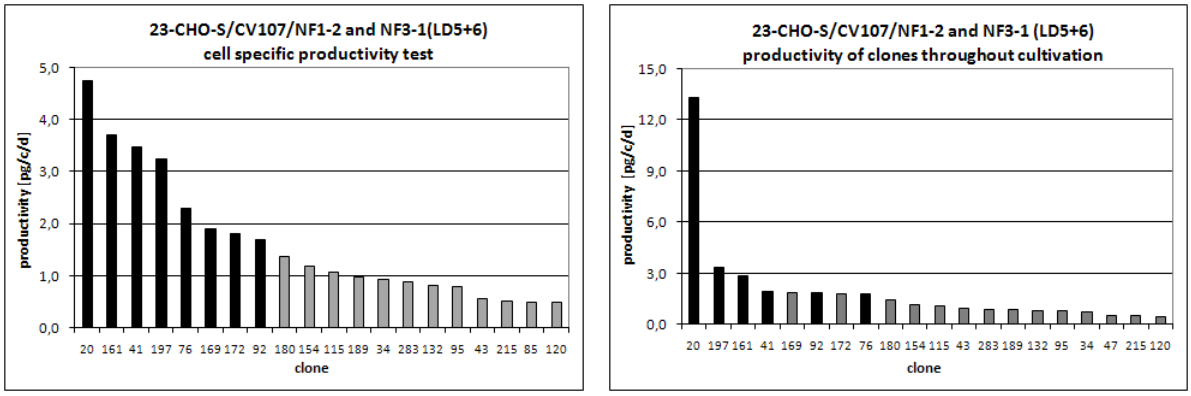

Figure 3-25 **Test for cell specific productivity.** Cell specific productivity as determined from a 3-day 6-well cultivation (a) and from cultivation during expansion (b). Data represent means of productivity from the daily intervals. Titers were measured by IgG Fc domain specific ELISA.

Finally, the following six clones were sub-cloned by limiting dilution: K20, K197, K161, K41, K92 and K76. In this step, cells were seeded at the single cell level to finally obtain a single cell derived cell line. Since the last singling was not successful, different approaches were tested beforehand in order to promote single cell growth in limiting dilution. At the single cell level, cells are more sensitive to stress, like major changes in temperature, pH or osmolality. This makes limiting dilution a delicate step in cell line development and all additional stress is preferably avoided. In a first approach the serum free, chemically defined medium was enriched by various supplements. Cells were seeded into 96-well plates either suspended in medium containing 0.3 % pepton, 0.2 and 2 % hydroxyethyl starch (HES-70, HES-450), conditioned medium or medium at pH 6.8. As a control, also an approach with medium containing 2 % FCS was performed. Wells were checked microscopically for single cells. Only these wells were monitored. The control revealed a cloning efficiency of 13 % (grown clones in relation to wells with only one cell documented), whereas the approach with pepton only resulted in 3 % grown single cell clones, all other approaches failed. In a second approach it was tested whether it would be beneficial to refrain from the use of antibiotics during limiting dilution. But as mentioned earlier, these “clones” represent mini-pools that may originate from more than one cell and therefore are not completely homogenous. When omitting the antibiotic, poorly transfected cells have an advantage in survival since they are not burdened with recombinant protein expression. This could result in a high amount of clones to be screened, with in part poor producing clones. So, in parallel to product titer analysis, the most promising clone K20 was transferred into spinner culture to test the stability of productivity without Geneticin (G-418). The culture without the antibiotic reached higher cell densities as expected (maximum viable cell density of 4.8×10^6 c/ml without

compared to 3.3 x 10^6 c/ml with G-418). Viability and, most important, productivity was not affected by addition or omission of G-418, though (16.7 pg/c/d with G-418 compared to 16.1 pg/c/d without G-418, Figure 3-26). Therefore, G-418 was omitted during seeding of limited dilutions for sub-cloning.

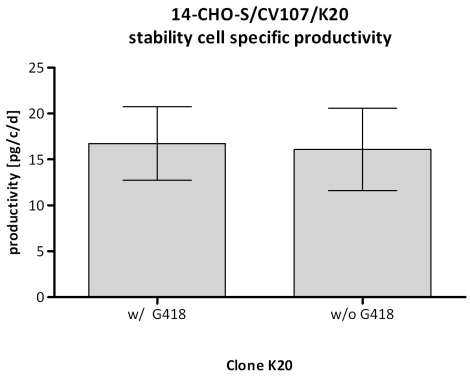

Figure 3-26 **Cell specific productivity of cell line 14-CHO-S/CV107/K20-3 when incubated with or without geneticin.** Samples were taken from a 3-day 6-well cultivation and titers were determined by IgG specific ELISA. Data represent the mean ±SD from the daily intervals.

In total, 80 96-well plates were inoculated with either 0.3 or 1 cell per well. Each well was checked microscopically for single cells, in total 1173 single cells were documented, and only these were further monitored. From these, a sum of ten clones survived limiting dilution and could be expanded. Each clone was tested for its cell specific productivity (Figure 3-27). Sub clones of K20 showed a productivity between 10.7pg/c/d (K20-3) and 7.8pg/c/d (K20-7, K20-10, K20-11) and were therefore considered to be the most promising production clones. All other clones exhibited a low specific productivity below 2 pg/c/d. From all clones, small cell banks were cryo-preserved.

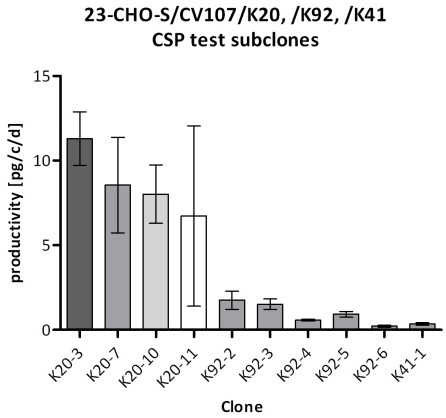

Figure 3-27 **Cell specific productivity of K20 derived single cell sub-clones.** Samples were taken from a three day 6-well cultivation, IgG titer was determined via IgG specific ELISA. Data represent mean ± SD of productivity from the daily intervals.

3.3.2.1 Characterization of potential producer clones

In order to make a choice between the four single cell clones derived from K20, batch cultures were performed. They were analyzed in terms of peak viable cell density, longevity, growth and product titer (Figure 3-28 to Figure 3-32, Table 3-4). For a viability ≥ 80 %, highest maximum cell density was reached with clone K20-7 (9.3×10^6 c/ml), K20-3 showed the longest cultivation period with nine days. Integrated viable cell density was highest for K20-7 with 3.7×10^7 c*d*ml^{-1}, as well as product titer (276 µg/ml). In turn the highest final titer was achieved with K20-3 (350 µg/ml). Clones K20-10 and K20-11 were excluded from further testing.

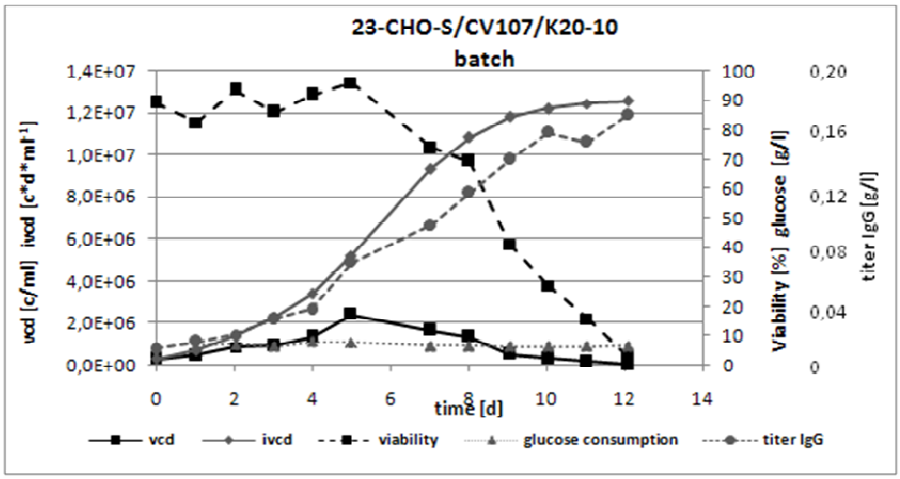

Figure 3-28 **Growth profile clone K20-10.** Viable cell density (vcd), viability, integrated viable cell density (ivcd), glucose consumption and accumulated product are shown during batch cultivation (spinner flask). Inoculation density 0.3×10^6 c/ml.

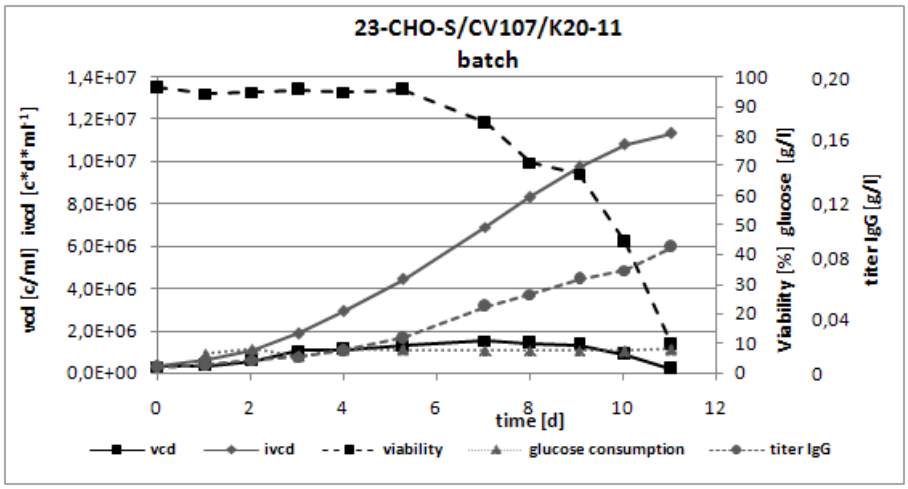

Figure 3-29 **Growth profile clone K20-11.** Viable cell density (vcd), viability, integrated viable cell density (ivcd), glucose consumption and accumulated product shown during batch cultivation (spinner flask). Inoculation density 0.3×10^6 c/ml.

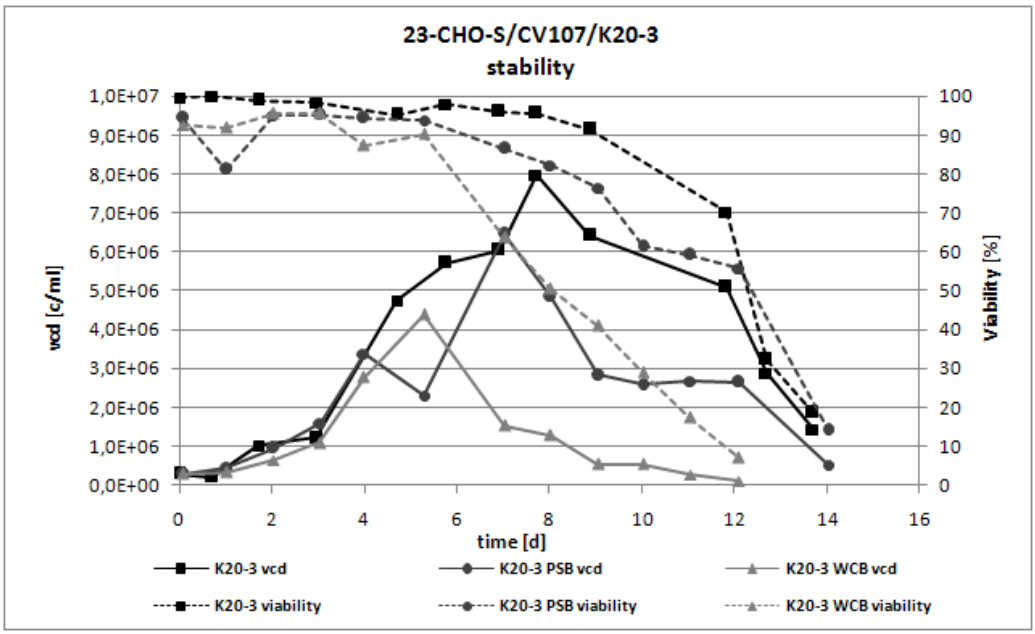

Figure 3-30 **Growth profile clone K20-3.** Comparison of cells never subjected to cryopreservation, from a primary seed bank (PSB) and from a working cell bank (WCB). Viable cell density (vcd) and viability shown during batch cultivation (spinner flasks). Inoculation density 0.3 x 10^6 c/ml.

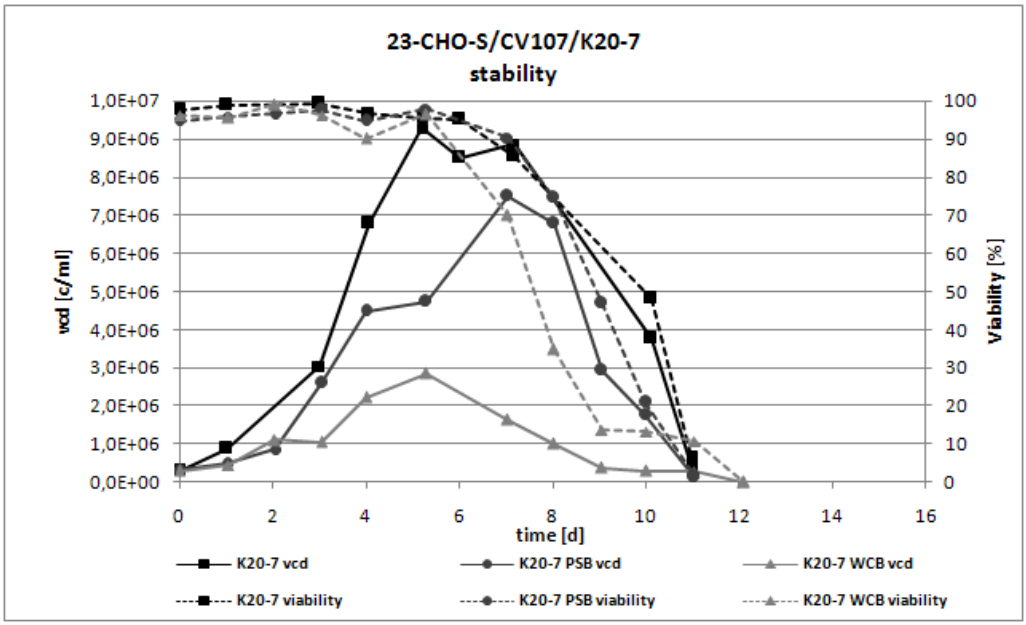

Figure 3-31 **Growth profile clone K20-7.** Comparison of cells never subjected to cryopreservation, from a primary seed bank (PSB) and from a working cell bank (WCB). Viable cell density (vcd) and viability shown during batch cultivation (spinner flasks). Inoculation density 0.3 x 10^6 c/ml.

a)

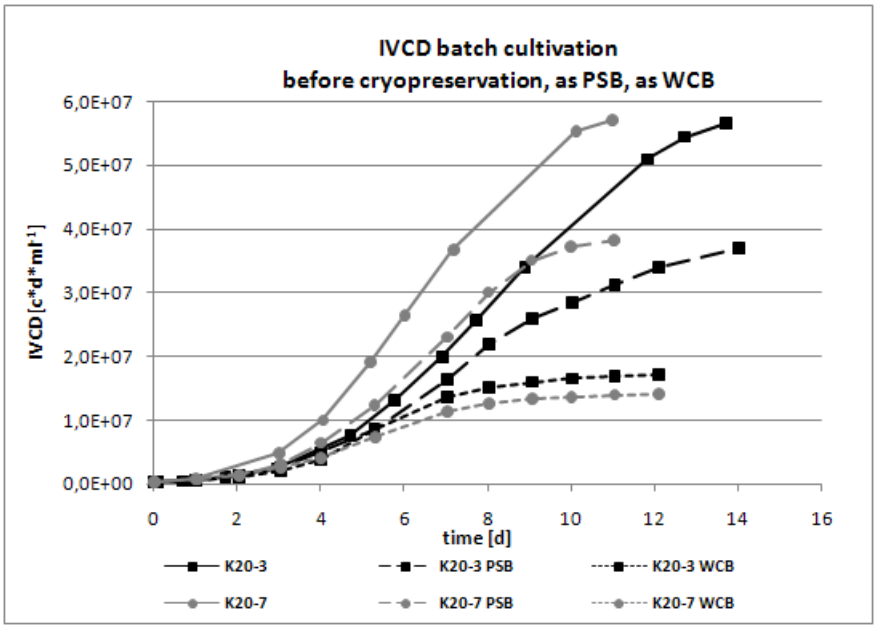

b)

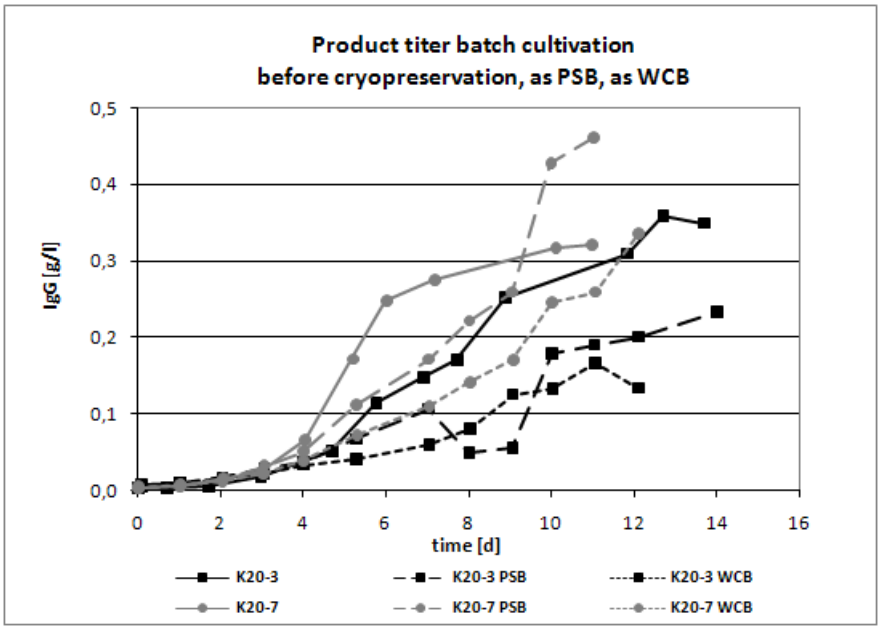

Figure 3-32 **IVCD (a) and product titer(b) from batch cultivation of clones K20-3 and K20-7**. Originator cultures before cryopreservation, PSB and WCB were compared, resp. Product (ATROSAB) titer was determined by IgG Fc domain specific ELISA from supernatant of the daily samples.

3.3.2.2 Stability of protein expression

To further characterize K20-3 and K20-7, population doubling time (PDT) and viability was determined throughout routine cultivation over a period of nine passages. Viability was stable at ≥ 90% and mean PDT was 26 h for K20-3 and 37 h for K20-7. Samples were taken in

parallel to analyze IgG titer and determine the clone specific productivity. Both clones exhibited a comparable productivity of 15 ± 6 pg/c/d, calculated as the mean from the whole period (Data not shown). In both cultures, cells tended to form aggregates.

Additionally, the influence of cryopreservation on cell line performance was investigated. So, in parallel to batch cultivation of cells from the original culture, vials of the primary seed bank and a working cell bank were thawed and also cultivated in batches. Batches were performed in a non pH and DO controlled spinner system. From samples of the first three days, productivity was determined and compared. No major difference could be observed between the two clones. Also no loss in productivity could be observed due to cryopreservation either (8.4 pg/c/d PSB K20-3 compared to 9.9 pg/c/d WCB K20-3, 8.4 pg/c/d PSB K20-7 compared to 8.2 pg/c/d WCB K20-7, data not shown). This was confirmed by results from individually performed CSP tests in 6-wells lasting three days as well (Figure 3-33). Productivity of the PSB and of the WCB was similar; yet, K20-3 exhibited a higher productivity than K20-7 (10.2 pg/c/d PSB K20-3 compared to 9.2 pg/c/d WCB K20-3, 7.3 pg/c/d PSB K20-7 compared to 6.7 pg/c/d WCB K20-7). In this experiment, the productivity of the original cultures were significantly lower compared to what was measured earlier and also compared to the thawed cultures.

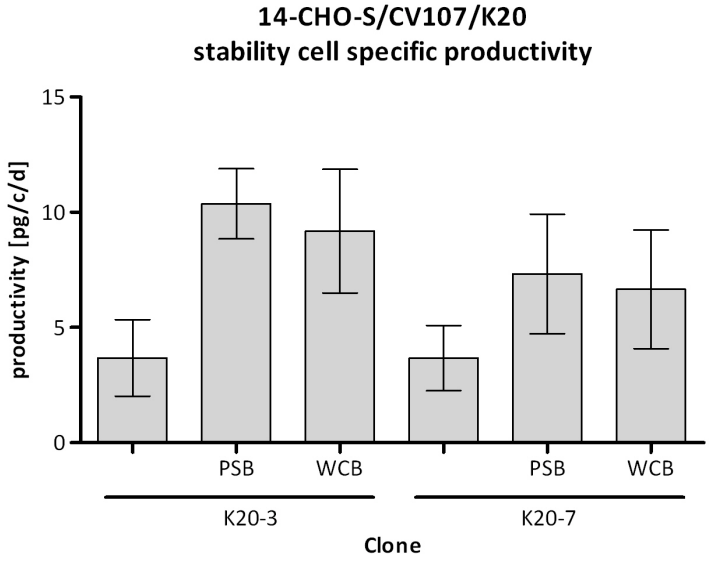

Figure 3-33 **Cell specific productivity of cell line 23-CHO-S/CV107/K20-3 and /K20-7 throughout various stages of cryo-preservation.** Samples were taken from a three day 6-well cultivation, IgG titer was determined via IgG specific ELISA. Data represent mean ± SD of productivity from the daily intervals.

The overall performance of the thawed cultures differed compared to the original cultures as observed for culture longevity, accumulated cell densities, peak maximum viable cell densities and achieved product titer. However, both clones behaved similarly. All main characteristics are summarized in Table 3-5. The cultivation period with viabilities higher than 80% was shorter for the cultures that had undergone cryopreservation (from nine to five days for K20-3 and seven to five days for K20-7). Peak maximum viability dropped from 8-9 x 10^6 c/ml to 3-5 x 10^6 c/ml (except for K20-7 PSB, which was nearly comparable to that of the original culture). Accumulated cell densities dropped likewise from 2.6 x 10^7 c*d*ml^{-1} to 8.5 x 10^6 c*d*ml^{-1} for clone K20-3 and 3.7 x 10^7 c*d*ml^{-1} to 7.4 x 10^6 c*d*ml^{-1} for clone K20-7. This equals a three to five fold reduction. The product titer was reduced accordingly up to six fold for K20-3 (253 µg/ml to 41 µg/ml) and four fold for K20-7 (276 µg/ml to 74 µg/ml). In order to determine the product quality in terms of possible degradations or aggregations, a western blot was performed from routinely taken samples during these batches. As a result, clone K20-7 showed an earlier accumulation of degradates in cultivation (e.g. day two and three, Figure 3-34).

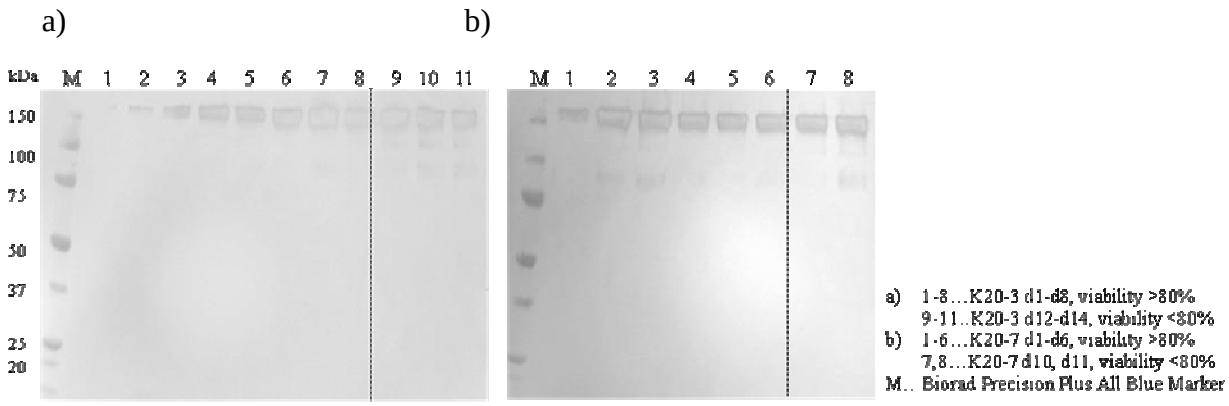

Figure 3-34 **Qualitative determination of product quality** from samples of batches with K20-3 and K20-7. Western Blot from a 4-12% BisTris SDS-Gel, ATROSAB was detected by an IgG Fc domain specific antibody. The dotted line indicates drop of viability below 80% during cultivation. 800 ng protein were loaded per lane (except days 1-5 in a and day 1 in b, due to low product titers in the beginning of the culture).

3.3.3 Cell line generation 23-CHO-S/CV107/K20-3/CV108/K35-1 and /K35-2

In order to further enhance productivity of the obtained clones, cell line 23-CHO-S/CV107/K20-3 was re-transfected. Therefore the expression vector was adapted in a way to allow for a selection that discriminates between the parental, once transfected, cell line and clones being successfully re-transfected.

To allow for an effective selection of re-transfected clones, the resistance gene of pCV107 was exchanged from the *hph* gene (conferring resistance to neomycin) to the *aminoglycoside phosphotransferase* gene (conferring resistance to hygromycin). Therefore, pCV107 was digested with *BsmI* and *StuI*, by which part of the resistance gene cassette was excised. A plasmid vector containing the *aminoglycoside phosphotransferase* gene (pCV050) was digested likewise to generate the insert which was then ligated to the pCV107 backbone. From this vector (pCV108), transfection grade plasmid DNA was generated that was used in the following for a re-transfection of 23-CHO-S/CV107/K20-3.

One vial of ATROSAB production cell line 23-CHO-S/CV107/K20-3 (RWCB, P48, 22.04.2009) was thawed and expanded for transfection. After three passages, cells were subjected to transfection, with either supercoiled pCV108 (NF1) or *PciI*/*SspI* linearized pCV108 (NF2). Therefore, $2x10^6$ cells were transfected with 8 µg of the respective plasmid DNA by nucleofection, following a 23-CHO-S optimized protocol, and resuspended in 2ml culture medium. Each nucleofection comprised three approaches (NF1-A, -B, -C, Figure 3-35-a and NF2-A, -B, -C, Figure 3-35-b) in case an approach failed to recover from transfection. Selection with 0.4 mg/ml Hygromycin B was started 48 h after transfection only for NF2-C, since the overall cell densities and viabilities were unusually low in all other approaches. The remaining approaches were allowed to recover before at day five post transfection selection was started. Approach NF1-B, exhibiting only 2 % viable cells, was discarded. Selection pressure was likewise set to 0.4 mg/ml Hygromycin B and added to the culture medium. All nucleofection approaches were cultivated until positively re-transfected cells began to expand. At day 13, all approaches of NF2 began to recover. Viability of approach NF2-C increased from a minimum viability of 19 % (d 12) to 34 %. This approach was used at day 14 with a cell density of 5.6×10^6 c/ml, viability of 44 % and passage 54 for seeding of Limited Dilution 1. At day 16, the remaining approaches of NF1 began to recover, too. Viability of NF1-A increased from 13 % (d 14) to 38 %. This approach was used at day 16 with a cell density of 6.8×10^5 c/ml, viability of 38 % and passage 55 for seeding of Limited Dilution 2. All nucleofections were further cultivated until cells fully recovered.

a)

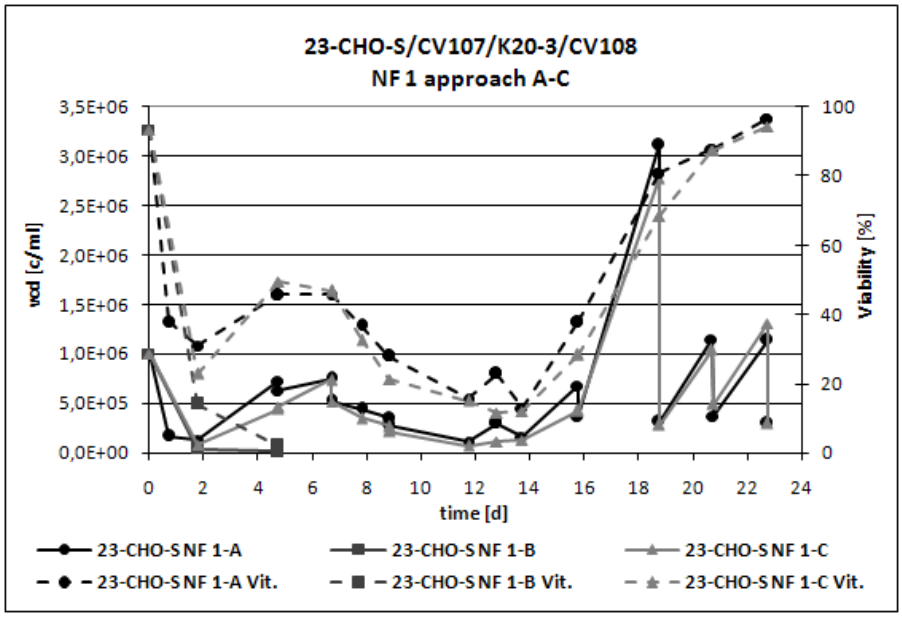

b)

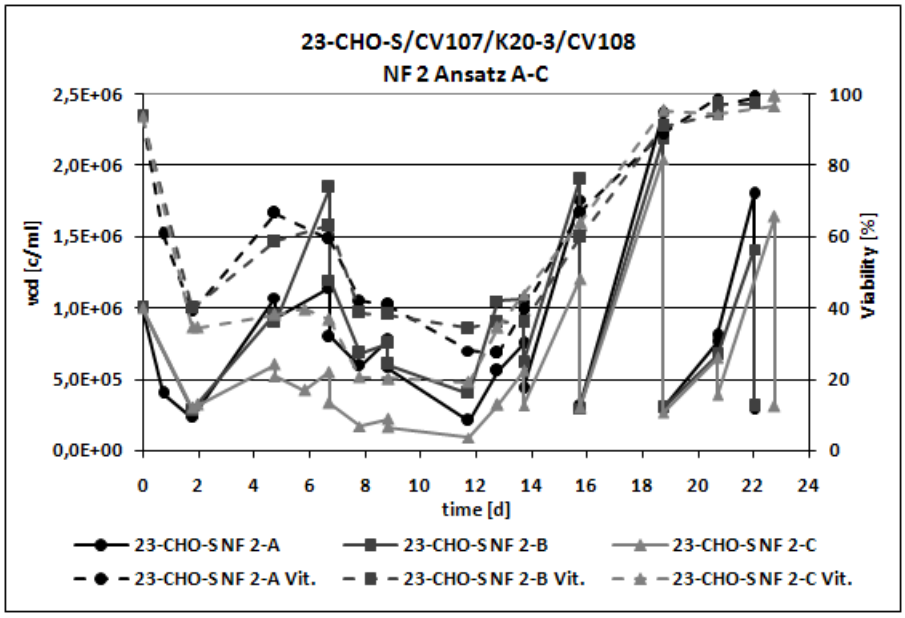

Figure 3-35 **Selection process of cell line 23-CHO-S/CV107/K20-3 transfected with plasmid vector CV108.** In NF1 (a), cells were transfected with supercoiled DNA, in NF-2, plasmid DNA was linearized prior to transfection. Selection with 0.4 mg/ml Hygromycin B was started 48 h post transfection for approach NF2-C, for all other approaches, selection was started at day 5.

These clone pools were tested for their specific productivity in order to get an impression, whether re-transfection was successful (Figure 3-36). In all clone pools an increase in productivity compared to K20-3 could already be observed (11 – 18 pg/c/d).

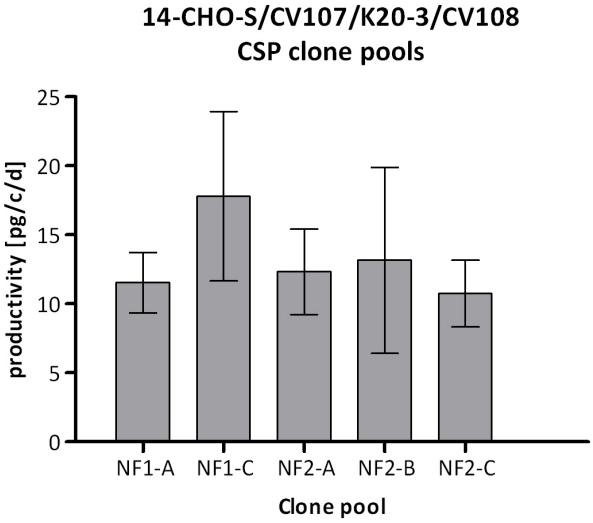

Figure 3-36 **Test for cell specific productivity of clone pools generated from nucleofection 1 (NF1) and 2 (NF2).** Fully recovered clone pools were subjected to a three days 6-well cultivation. Daily samples were analyzed in an IgG specific ELISA. Data represent mean ± SD of productivity from the daily intervals.

For both Limited Dilutions, 30 96-well plates were seeded with statistically 3 cells/well under constant selection pressure and incubated for one week without any manipulation. Wells were not checked for clonality at this timepoint, so clones grown from this limited dilution might resemble “mini-pools”. After this week, medium was added and incubated for an additional week. At this time point, first clones were visible. Clones were transferred from 96-well to 12-well. For a rough estimation of production capacity, the IgG titer of the 96-well supernatants was determined via ELISA and charged against the individual confluence at the day of transfer (Figure 3-37). Altogether 178 clones were transferred from 96-well plates. The threshold for further expansion was set to 50 µg/ml.

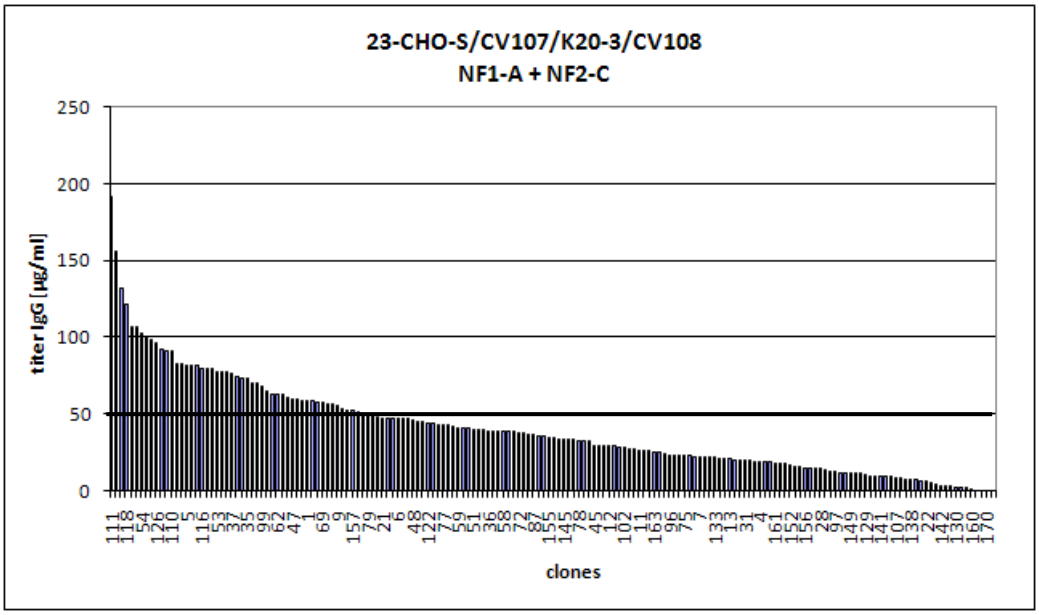

Figure 3-37 **ATROSAB titer from clones that survived limiting dilution at the day of transfer from 96- to 24-well.** Samples were taken from 96-well supernatant and measured in an IgG specific ELISA. Results were corrected for the individual confluence at the day of sampling. Threshold for further expansion was set to 50 µg/ml (black line).

47 clones were expanded and tested for their cell specific productivity (Figure 3-38). Nearly all clones exhibited a significant higher productivity than clone K20-3, (22-31 pg/c/d for the best ten clones compared to 10pg/c/d of K20-3). Based on the results of this CSP tests, five clones were chosen to proceed with (K35, K43, K74, K99 and K154). Identity and integrity of the respective product of each clone was verified by Western Blotting (Figure 3-39).

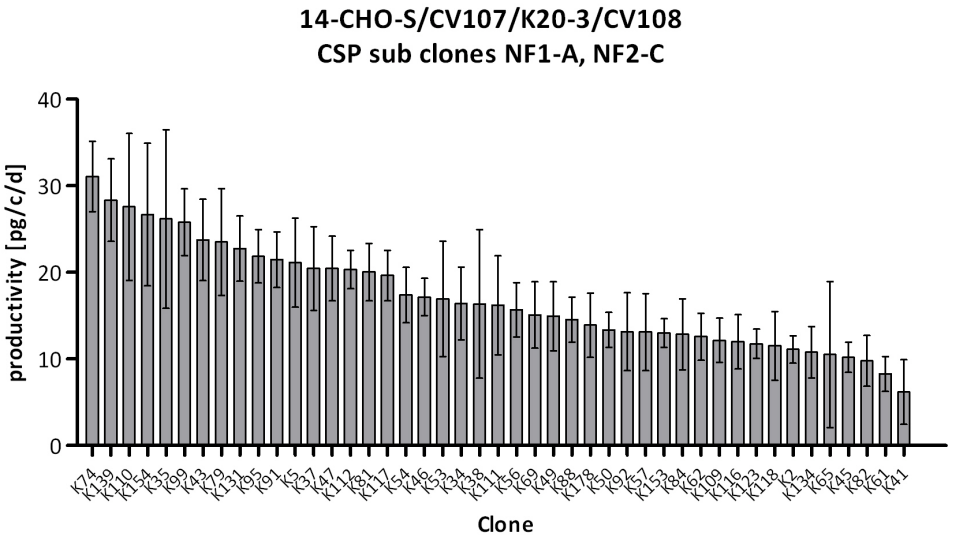

Figure 3-38 **Test for cell specific productivity from 47 clones expanded after transfer from 96-well.** All clones were subjected to a three days cultivation in 6-wells. ATROSAB titer was determined from daily samples via IgG specific ELISA. Data represent mean ± SD of productivity from the daily intervals.

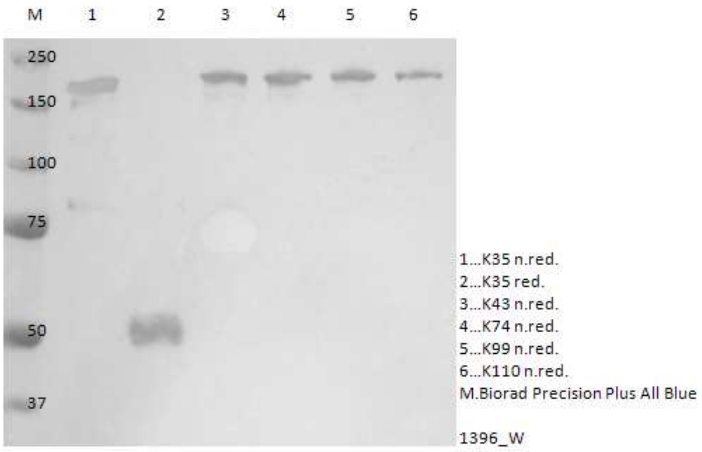

Figure 3-39 **Western Blot of supernatants from five clones selected for limiting dilution.** Samples were taken from the last day of the above CSP test and detected by an antibody specific for the IgG Fcγ domain. Supernatant from clone 35 was applied under reduced and non reduced conditions; all other samples were applied under non reducing conditions.

All five clones from cloning step I were expanded for sub-cloning via Limited Dilution aiming at the generation of a fully single cell derived cell line. From all clones, ten 96-well plates were seeded with statistically 1 cell/well. All plates were microscopically checked for the actual number of cells per well within 24 h after seeding. Results were documented. According to cloning step I, the plates were incubated for two weeks before they were checked for cell growth. In total, only six clones accrued from the whole of 50 plates, namely K35-1, K35-2, K35-3, K99-1, K99-2 and K154-1.

3.3.3.1 Characterization of potential producer clones

The resultant six clones were further expanded and subjected to a test for their specific productivity (Figure 3-40). The best clone K35-1 exhibited a productivity of 34 pg/c/d. This is a significant increase of productivity compared to the original clone K20-3, which exhibited a productivity of 10 pg/c/d. In general all generated clones showed elevated levels of expression compared to clone K20-3.

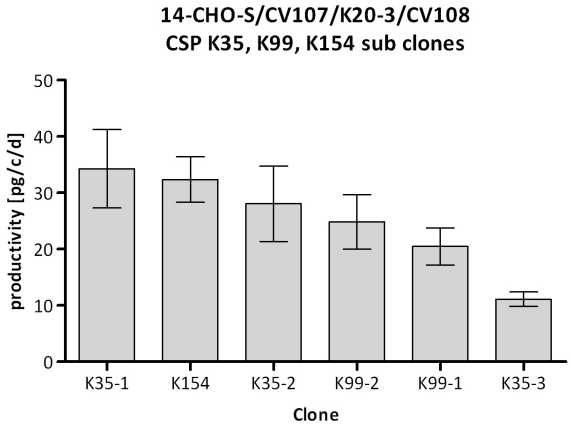

Figure 3-40 **Test for cell specific productivity from six single cell derived clones that survived limiting dilution.** All clones were subjected to a three days cultivation in 6-wells. ATROSAB titer was determined from daily samples via IgG specific ELISA. Data represent mean ± SD of productivity from the daily intervals.

From all clones small batches were performed in order to test their potential as a prospective production cell line. Main criteria were population doubling time (PDT), length of the cultivation period, the maximum viable cell densities and the ATROSAB titer at viabilities higher than 80 % and below 80 % (Figure 3-41 a-f and Figure 3-42). Results are summarized in Table 3-6. The best titer (final as well as at a viability ≥ 80 %) was reached with clones K35-1 and K35-2 (456 µg/ml and 1143 µg/ml for K35-1, 606 µg/ml and 936 µg/ml for K35-2, resp.). The length of the cultivation period was similar in all batches (seven to nine days). Maximum viable cell densities and PDT differed for the individual clone (2 x 10^6 c/ml up to 4.8 10^6 c/ml and 21 h up to 59 h). In general, all achieved cell densities are lower than observed with K20-3, leaving space for improvement. For a comparison, the original clone K20-3 reached higher cell densities (8 x 10^6c/ml) but a lower product titer (250 µg/ml at a viability higher than 80 % and 360 µg/ml below 80 %). K99-1 showed the lowest PDT and the highest viable cell density. But the production ranged far below K35-1 and K35-2. The highest PDT with 59 h accompanied by a mediate product titer and low viable cell density was observed with clone 154-1.

a)

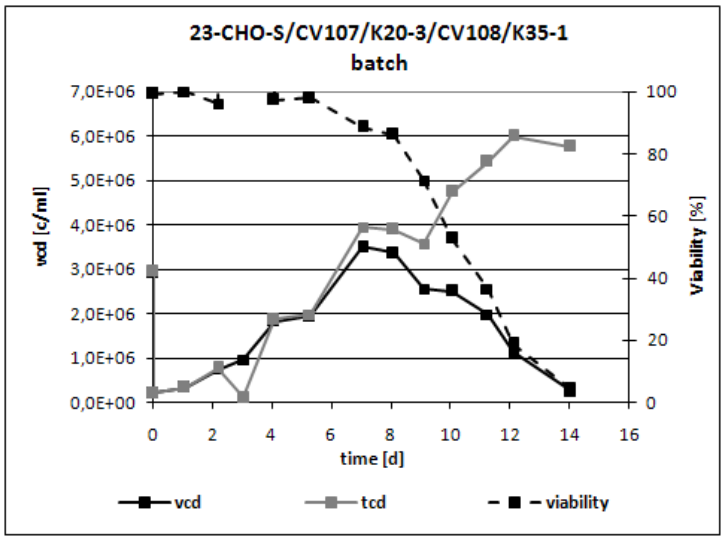

b)

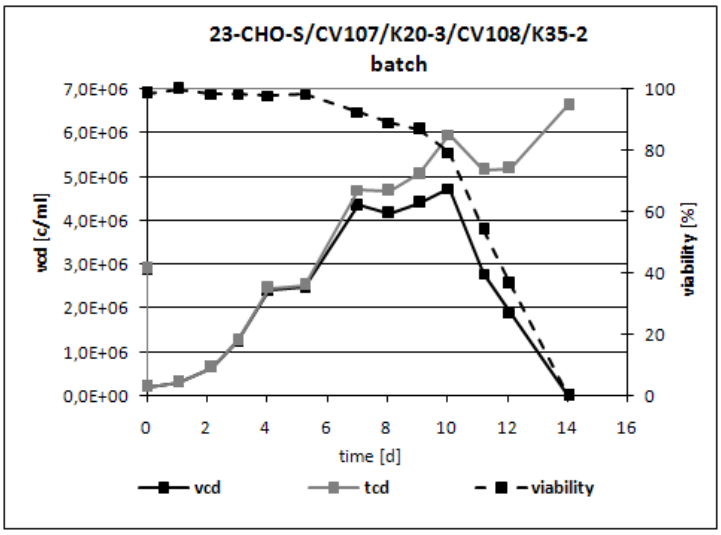

c)

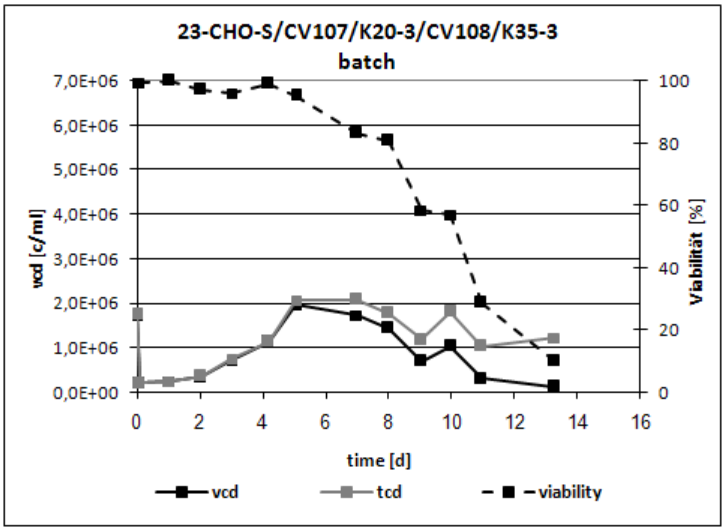

Part of Fig. 3-41 **Growth profiles of cell lines 23-CHO-S/CV017/K20-3/CV108/K35-1, -K35-2, -K35-3, -K99-1, -K99-2 and -K154-1.** Spinner cultivation in batch mode, inoculation density 0.3 x 10^6 cells/ml, inoculation volume 50 ml. Vcd – viable cell density, tcd – total cell density.

d)

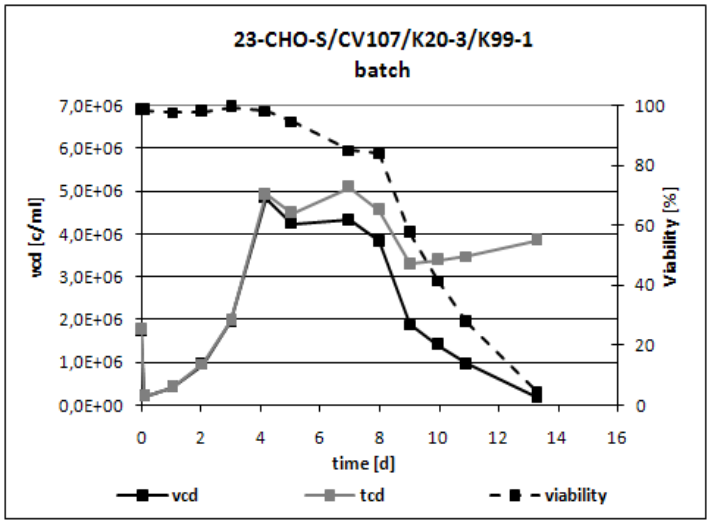

e)

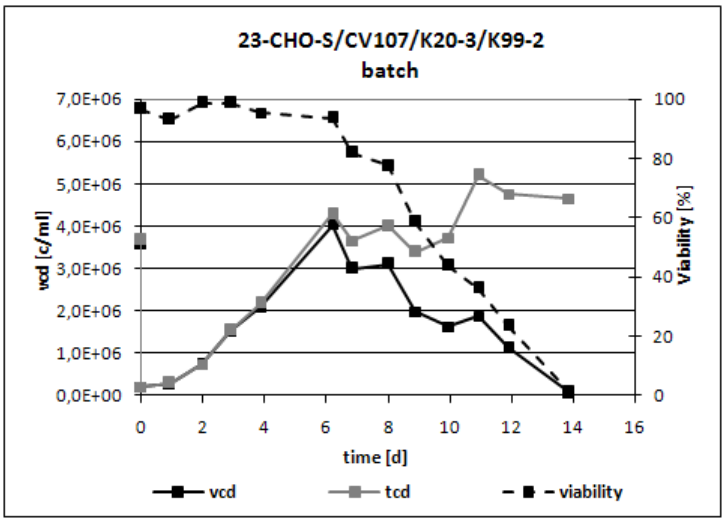

f)

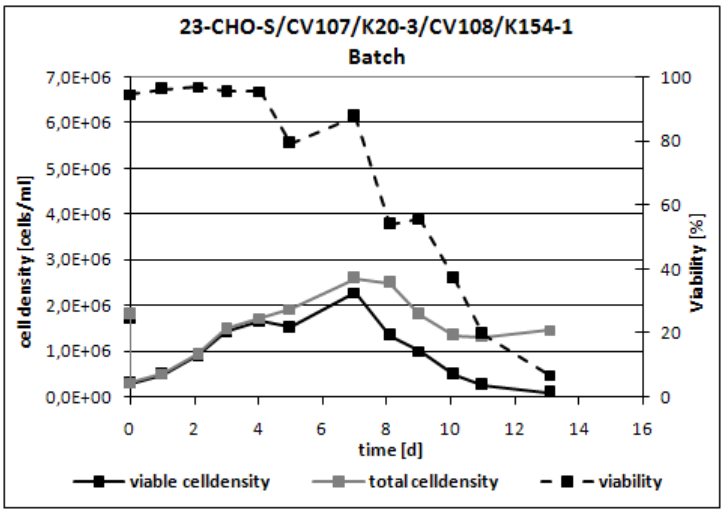

Figure 3-41 **Growth profiles of cell lines 23-CHO-S/CV017/K20-3/CV108/K35-1 (a), -K35-2 (b), -K35-3 (c), -K99-1 (d), -K99-2 (e) and -K154-1 (f).** Spinner cultivation in batch mode, inoculation density 0.3 x 10^6 cells/ml, inoculation volume 50 ml. Vcd – viable cell density, tcd – total cell density.

a)

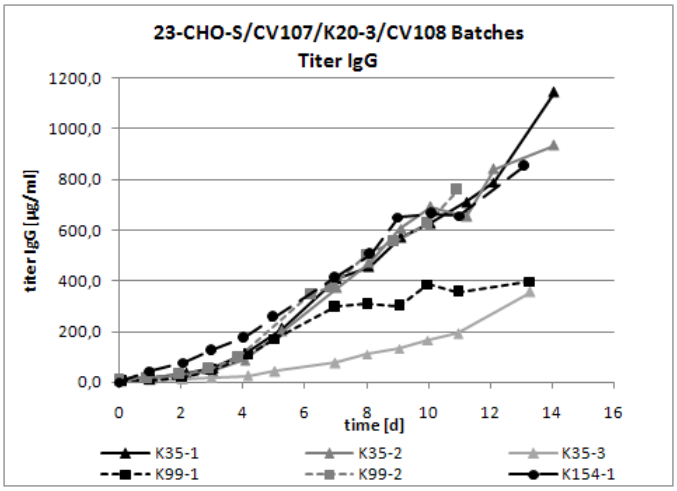

b)

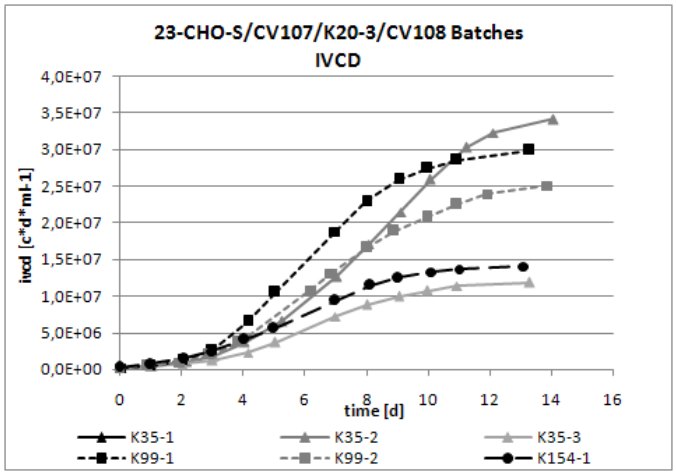

Figure 3-42 **Accumulation of product titer (A) and viable cells (B) during the above batch fermentation of cell lines 23-CHO-S/CV017/K20-3/CV108/K35-1, -K35-2, -K35-3, -K99-1, -K99-2 and –K154-1.** Product titer was determined by hIgG specific ELISA.

Taken all these results together, K35-1 and K35-2 can be regarded as suitable for a production process. Clone 154-1 is promising regarding its specific productivity but needs further improvement to achieve higher cell densities. From clones K35-1 and K35-2, a PSB and RMCB was laid down. Both cell banks were compared in terms of productivity to the respective cell line that had not undergone cryo-preservation (Figure 3-43). Productivity dropped with repeated cryopreservation, whereas the tendency was not as pronounced for K35-2 (31 pg/c/d to 19 pg/c/d) as for clone K35-1 (37pg/c/d to 20pg/c/d). However, both clones still exhibit a productivity twice as high as that of clone 20-3.

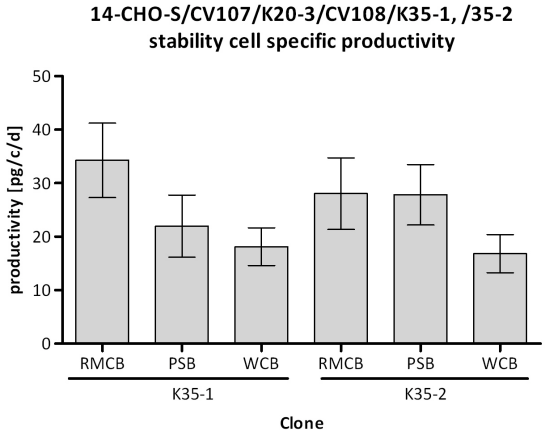

Figure 3-43 **Test for stability of cell specific productivity of cell lines 23-CHO-S/CV107/K20-3/CV108/K35-1 and /K35-2 after cryopreservation.** Productivity was calculated from IgG titers determined via hIgG specific ELISA from supernatants of three days 6-well cultivations. Data represent mean ± SD of productivity from the daily intervals.

3.3.3.2 Comparison of ATROSAB expressing cell lines 23-CHO-S/CV107/K20-3 and 23-CHO-S/CV107/K20-3/CV108/K35-2

Success of re-transfection was determined by comparison of cell lines 23-CHO-S/CV107/K20-3 and 23-CHO-S/CV107/K20-3/CV108/K35-2 with respect to growth behavior, product titer and product quality. The experiments in this section (3.3.3.2) were performed by Timo Liebig (Celonic AG, Basel Switzerland). 200 ml fed batches were performed in shake flasks in a blend of two commercial media, CDM4PerMab and CM1027, at 150 rpm, 37°C and 5 % CO_2. Cultures were inoculated at a cell density of 0.3 x 10^6 c/ml, samples were taken every other day. Cells were fed a feed medium developed by Celonic AG (Celonic Feed Medium 2-6, CFM2-6) every other day following the scheme listed below (Table 3-1).

Table 3-1 **Feed regime** during fed batches of cell lines 23-CHO-S/CV107/K20-3 and 23-CHO-S/CV107/K20-3/CV108/K35-2. Feed: CFM2-6).

Day	Feed volume [% inoculation volume]	Feedvolume [ml]
1	5	10
3	10	20
5	15	30
7	20	40
9	10	20
11	10	20
13	10	20
15	0	0

Growth of clones was similar with the re-transfected clone reaching 1.6 fold higher IVCD, due to prolonged cultivation time (Figure 3-44, Figure 3-45, Table 3-7). The titer of ATROSAB was determined by Protein A HPLC. Clone K35-2 exhibited a 2.7 fold increased product titer compared to K20-3 (1.6 g/l and 0.6 g/l, resp.).

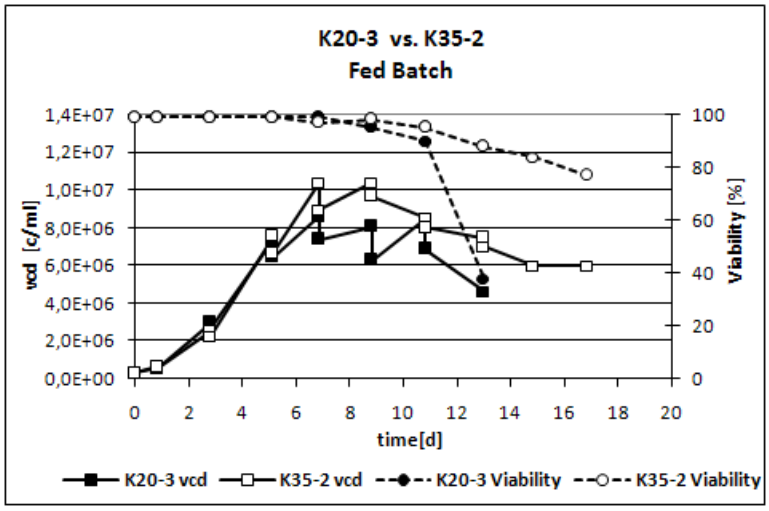

Figure 3-44 **Fed Batch of cell lines 23-CHO-S/CV107/K20-3 and 23-CHO-S/CV107/K20-3/CV108/K35-2** in 200 ml shake flasks, cultivated at 150 rpm, 37 °C and 5 % CO_2. Inoculation density 0.3 x 10^6 c/ml.

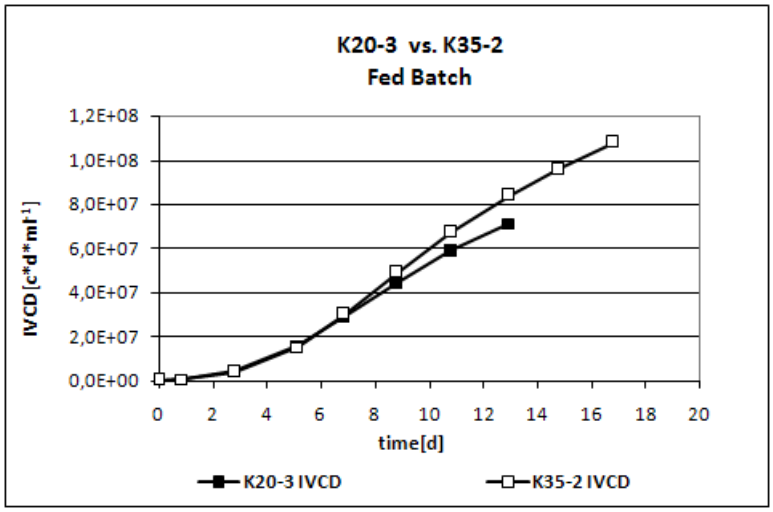

Figure 3-45 **Integrated viable cell density** calculated from viable cell densities of fed batches from cell lines 23-CHO-S/CV107/K20-3 and 23-CHO-S/CV107/K20-3/CV108/K35-2.

Protein from clone K35-2 was purified up to UF/DF stage from a fed batch performed under conditions representing the current GMP manufacturing process (termed V406-1). The material was then compared to K20-3 reference material obtained from such a GMP process (termed CE-110207). Analysis via HP-SEC revealed no major differences in these preparations (Figure 3-46). The reference contained 99.8 % fully assembled antibody and

0.2 % aggregates, whereas the purified material from K35-2 contained 99.7 % intact antibody and 0.3 % aggregates.

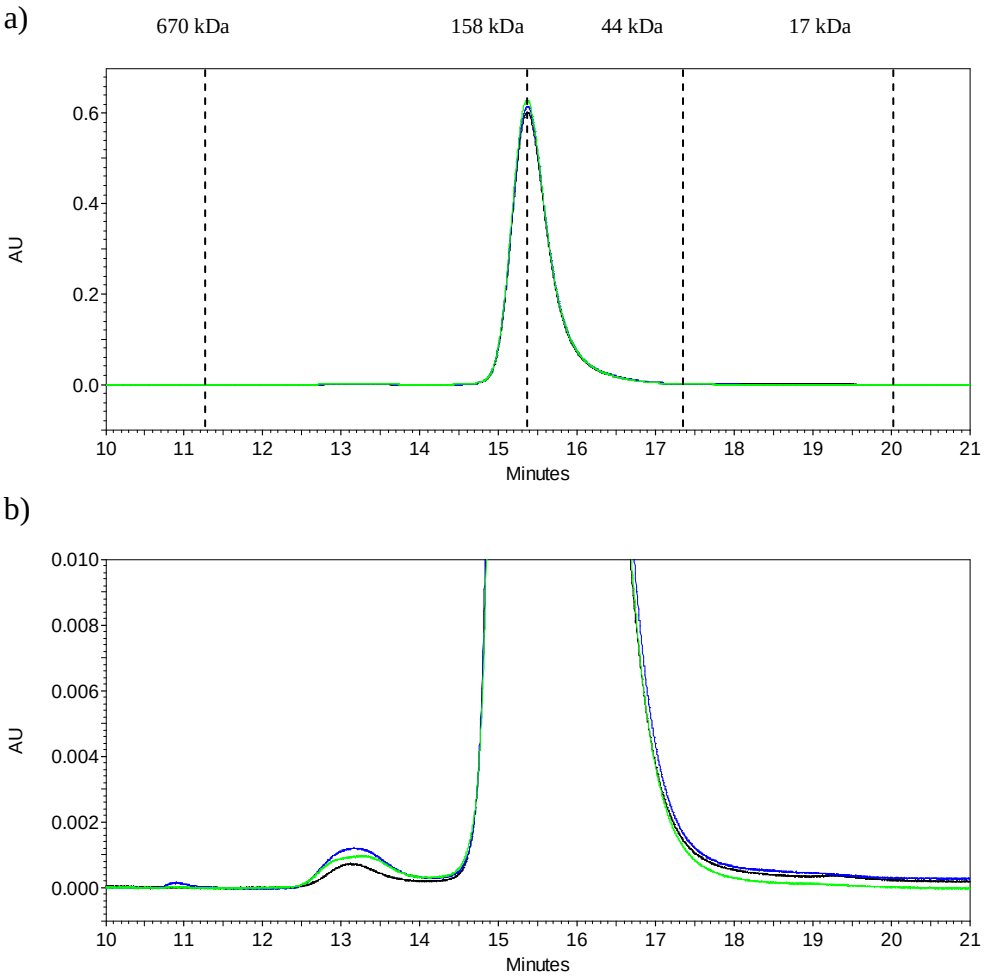

Figure 3-46 **HP-SEC of ATROSAB produced by K20-3 and K35-2** on a TSK gel G3000SWXG column with b) being a detail of a). The position of the protein standard is indicated by dotted lines in a). Black line: K20-3 reference (CE-110207), green line: K20-3 from experiment V406, blue line: K35-2 from experiment V406, AU – Absorption unit

In order to detect charge variants, isoelectric focusing was performed. A different banding pattern could be observed for K35-2, with significant shift towards isoforms with more positive charge (Figure 3-47, Table 3-2). The K20-3 reference showed a main band and less pronounced isoforms. The individual lanes were analyzed by photodensitometry, results are given in Table 2.

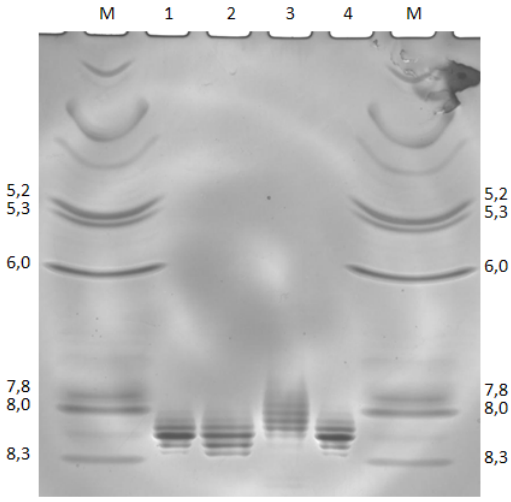

Figure 3-47 **Isoelectric focusing of ATROSAB from preparations of cultures performed either with K20-3 or K35-2.** Lane 1 – K20-3 from experiment V406, lane 2 – K35-2 from experiment V406, lane 3 – other sample, lane 4 – K20-3 reference (CE-110207). NuPAGE IEF Gel pH 3-10, Coomassie stained.

Table 3-2 **Analysis of IEF via photodensitometry**. Percentage of coomassie stained isoforms of ATROSAB. Percentages may not add to 100 % due to rounding or additional, hardly visible isoforms in the gel, respectively.

	K20-3 reference	K35-2 preparation
Isoform 1	1.9 %	1.4 %
Isoform 2	14.2 %	13.4 %
Isoform 3 (main product)	55.6 %	38.4 %
Isoform 4	18.2 %	32.8 %
Isoform 5	9.4 %	14.1 %

Cation exchange chromatography (CEX), performed with both preparations, confirmed this finding (Figure 3-48). The K20-3 reference as well as the material from K35-2 eluted with a main peak at ~ 3′54″ and at least four different isoforms eluted at 3′24″, 3′42″, 4′12″ and 4′33″. Yet, distribution of the total amount of protein was again different for the two preparations with positively charged isoforms being more prominent in the K35-2 preparation.

a)

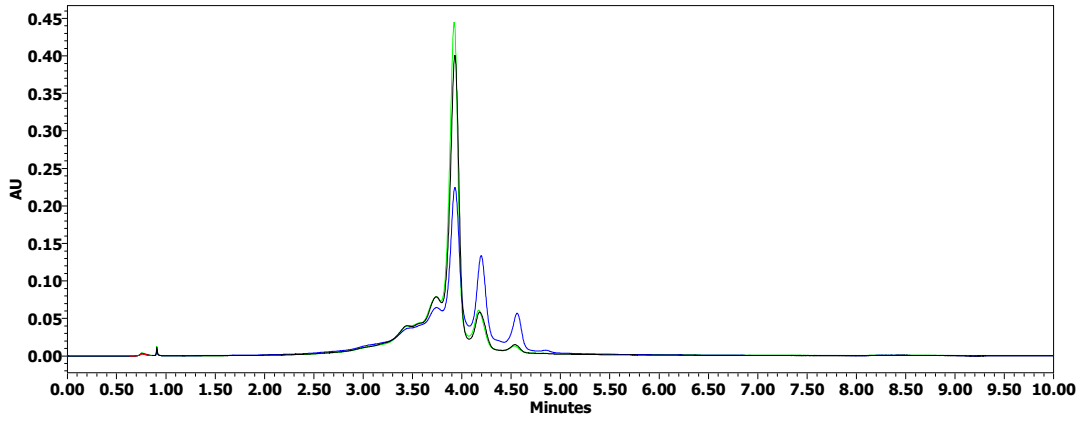

b)

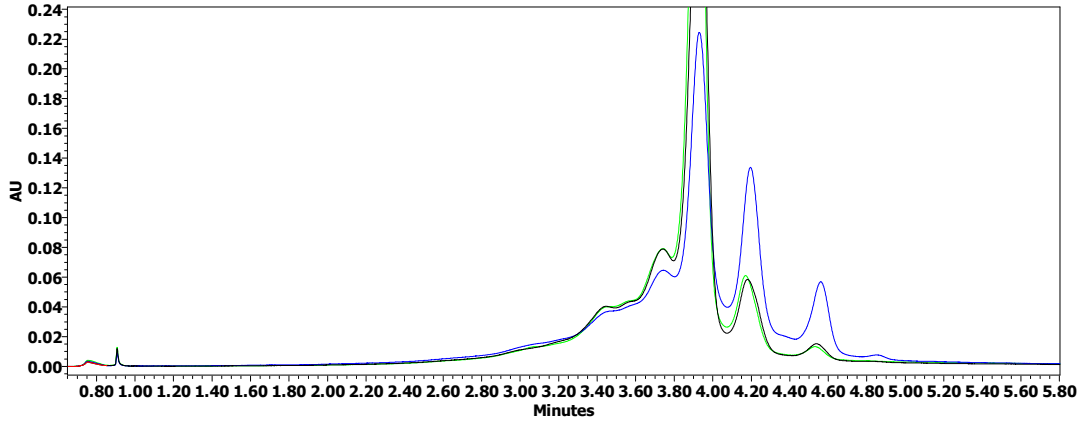

Figure 3-48 **Cation exchange chromatography (CEX) of ATROSAB** from different preparations on a TSKgel CM-STAT 7µm column (carboxymethyl group). Black line: K20-3 reference (CE-110207), green line: K20-3 from experiment V406, blue line: K35-2 from experiment V406. b) is a detail of a).

The potency of ATROSAB preparations from both clones was determined by means of the ability to rescue Kym-1 cells from TNF-mediated cytotoxicity (Figure 3-49). A reduced potency of only 66 % was found for ATROSAB produced by K35-2 compared to the K20-3 reference material ($EC_{50\ K20\text{-}3}$ 525 nM, $EC_{50\ K35\text{-}2}$ 792 nM).

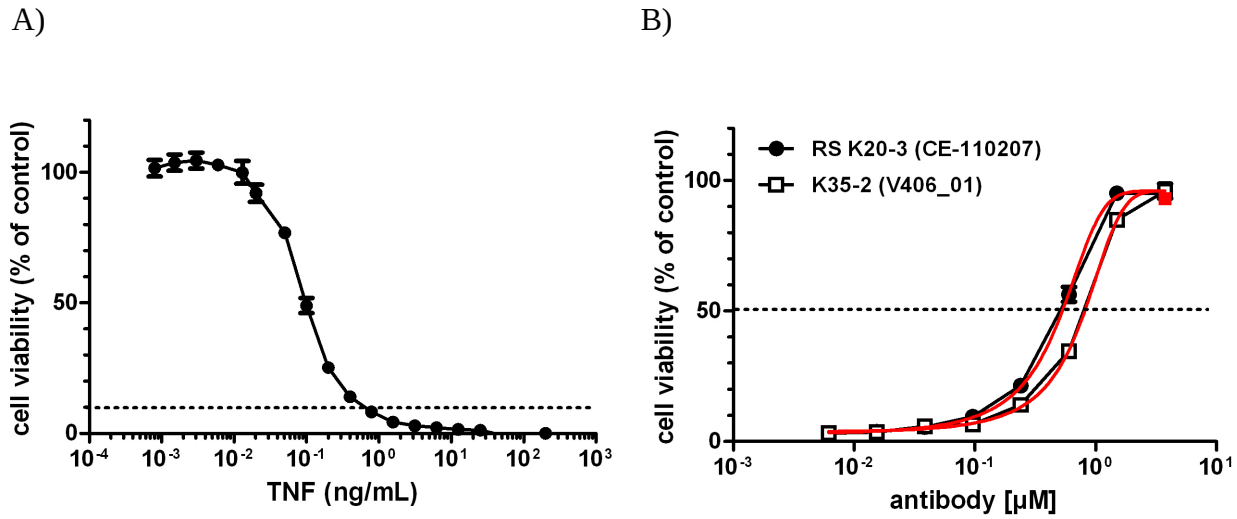

Figure 3-49 **Inhibition of TNFα mediated cytotoxicity by pre-incubation with ATROSAB** produced either from K20-3 (■) or K35-2 (•). Viability of Kym-1 cells pre-incubated with indicated concentrations of ATROSAB and 0.7 ng/ml TNF (LD_{90}) was assessed by incubation with a tetrazolium dye (n=2). Data in B) were fitted by non-linear regression assuming a log (agonist) vs. response reaction (4 parameter fit, red line).

3.4 Establishment of a an assay for the ex-vivo proof of ATROSAB action in clinical blood samples

For the upcoming clinical trials, an assay was established for the ex-vivo proof of ATROSAB activity in whole blood samples from probands. Active ATROSAB should be able to reduce the release of pro-inflammatory cytokines IL-6 and IL-8, induced artificially by incubation with an appropriate stimulus. ATROSAB was compared to Remicade in these experiments. Remicade (Infliximab) is a chimeric antibody directed against TNF (Centocor Inc, Malvern PA US). It was approved by the FDA in 1998 for Crohn´s disease.

In contrast to ATROSAB, which specifically targets TNFR1, Remicade neutralizes TNF. In a first approach, the immune reaction was induced with varying concentrations of lipopolysaccharide (LPS, 0,01-10 µg/ml). Next to IL-6 and IL-8, the release of TNF was measured to verify the different mechanisms of action of ATROSAB and Remicade. As expected, Remicade efficiently neutralized all TNF, while TNF levels for ATROSAB were comparable to those of the control. However, the levels of IL-6 and IL-8 were on control levels for both, Remicade and ATROSAB (Figure 3-50). This is most probably due to the large amounts of IL-6 and IL-8 that are induced by LPS/TLR-4 signaling, by-passing TNF/TNFR1 signaling. This way, IL-6 and IL-8 release that is induced by TNF/TNFR1 signaling cannot be discriminated from the cytokine levels induced by TLR-4 signaling.

Consequently, LPS is not an appropriate stimulus to specifically activate the TNF/TNFR signaling pathway.

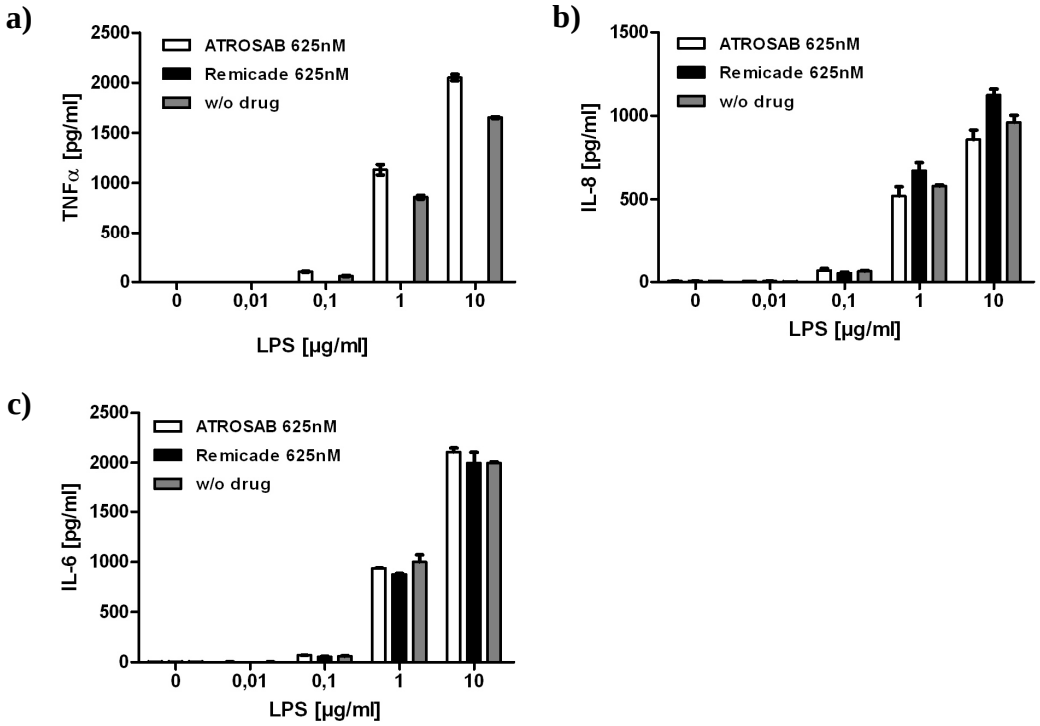

Figure 3-50 **Inhibition of LPS-induced cytokine release by ATROSAB ( ) and Remicade (■) in human whole blood.** a) TNFα levels after stimulation with LPS in combination with ATROSAB or Remicade. b) Inhibition of LPS-induced IL-6 release from human whole blood incubated either with ATROSAB or Remicade, resp. c) Inhibition of LPS-induced IL-6 release from human whole blood incubated either with ATROSAB or Remicade, resp.

In a second approach, blood samples were directly incubated with varying concentrations of TNF (4-16 ng/ml). Here again, measurement of TNF levels showed the potent TNF neutralizing activity of Remicade, while TNF levels remained stable when incubated with ATROSAB. But in contrast to LPS stimulation, a reduction of IL-6 and IL-8 release could be observed along with increasing concentrations of Atrosab and Remicade, respectively (Figure 3-51). The effect was more pronounced with Remicade for both cytokines. When the grip experiment was reproduced with more concentrations steps for ATROSAB and Remicade (Figure 3-52), a minor, not significant release of IL-8 was observed for ATROSAB at concentrations between 10 and 100 nM in absence of TNF. At the same concentrations, this effect could be also observed when ATROSAB was incubated with TNF (increase of 20 pg/ml IL-8 compared to the value of the next lower ATROSAB concentration). For the proof of ATROSAB action, whole blood samples from participants of the clinical trial will be

incubated with 8 ng/ml TNFα. IL-6 and IL-8 release will be measured and compared to results from samples taken before drug administration.

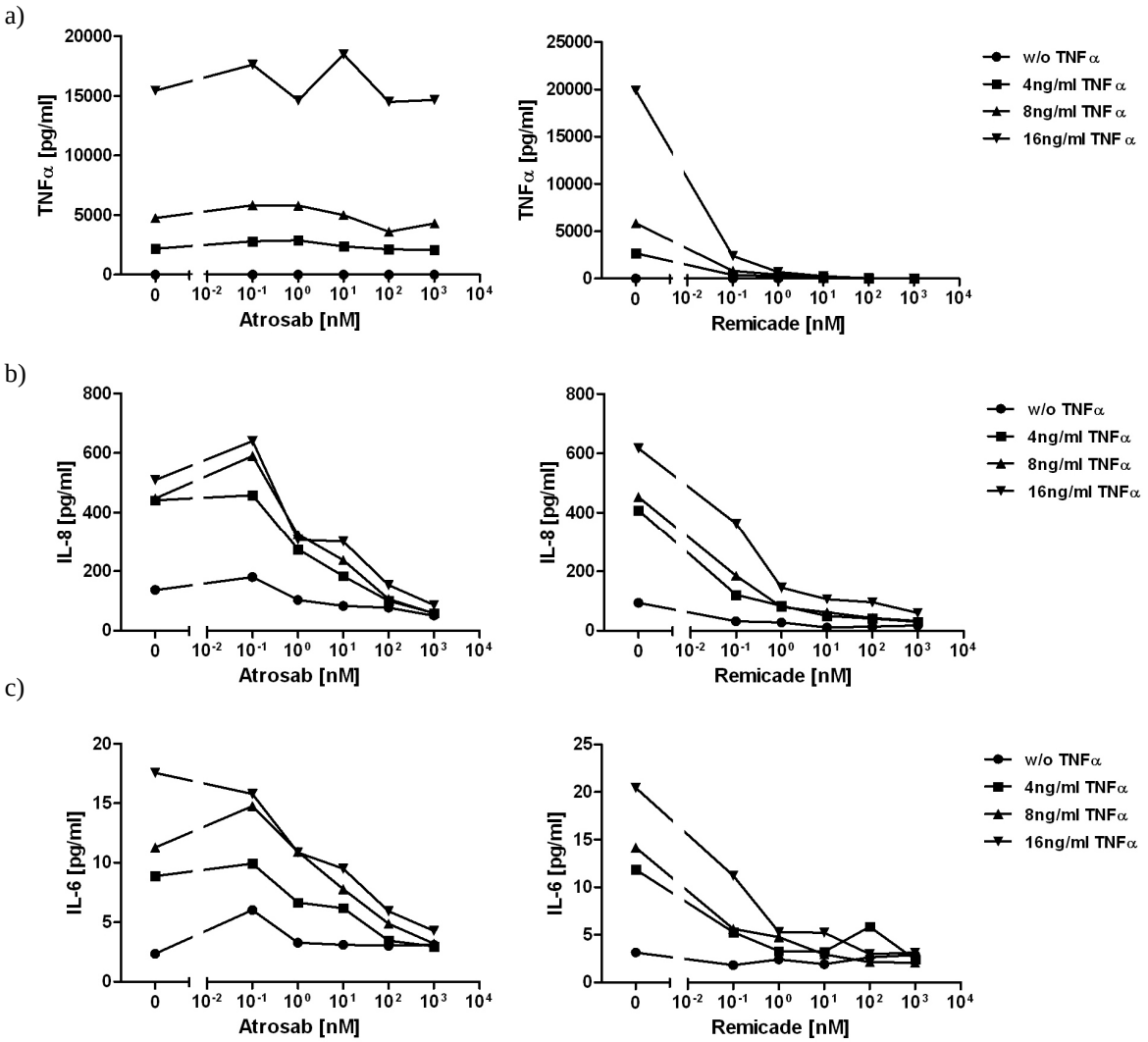

Figure 3-51 **Inhibition of TNF-induced cytokine release by ATROSAB and Remicade in human whole blood.** a) TNFα levels after stimulation with TNF(• w/o, ■ 4 ng/ml, ▲ 8 ng/ml, ▼ 16 ng/ml) in combination with ATROSAB or Remicade. b) Inhibition of TNF-induced IL-8 release from human whole blood incubated either with ATROSAB or Remicade, resp. c) Inhibition of TNF-induced IL-6 release from human whole blood incubated either with ATROSAB or Remicade, resp. (all n=1)

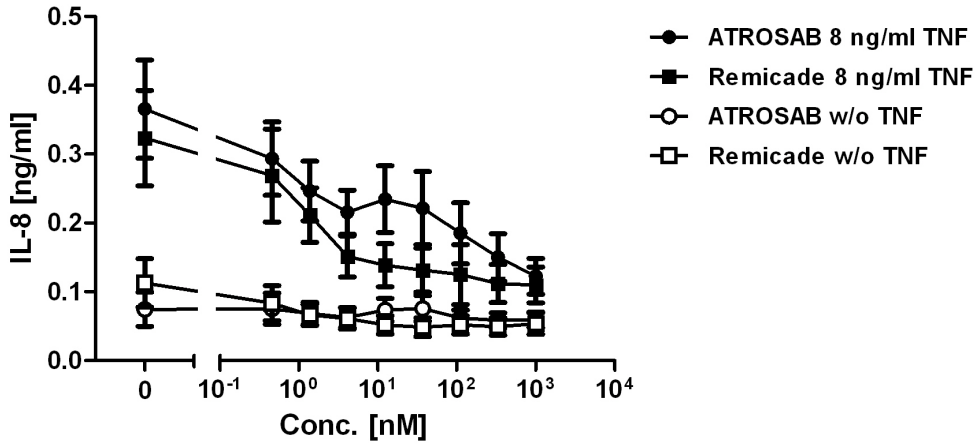

Figure 3-52 **Inhibition of TNF-induced cytokine release by ATROSAB and Remicade in human whole blood.** IL-8 levels determined by ELISA from incubation of human whole blood either with ATROSAB or Remicade in the presence and absence of 8 ng/ml TNF, resp. (● ATROSAB + 8 ng/ml TNF, ■ Remicade + 8 ng/ml TNF, ○ ATROSAB w/o TNF, □ Remicade w/o TNF) n=3.

3.5 Tables

	AV036 Batch	AV036 Fed Batch	AV037 Batch	AV037 Fed Batch	AV038 Batch	AV038 Fed Batch
max. vcd >80% [c/ml]	7.44E+06	6.81E+06	7.20E+06	1.02E+07	9.94E+06	9.96E+06
duration >80% [d]	9	9	9	10	8	9
PDT exponential growth phase [h]	36	41	37	55	26	28
IVCD at >80% viability [c*d*ml^{-1}]	3.07E+07	3.29E+07	3.51E+07	4.96E+07	3.19E+07	3.92E+07
IVCD total [c*d*ml^{-1}]	5.61E+07	5.19E+07	5.99E+07	7.92E+07	4.76E+07	6.47E+07
product titer >80% viability [µg/ml]	74	67	180	329	16	22
product max titer [µg/ml]	113	178	295	724	16	28

Table 3-3 **Cultivation characteristics** of batches and fed batches of cell lines 14-CHO-S/CV063/25.004/AV036/C4-1, /AV037/A1-1, /AV038/B1-1. vcd – viable cell density, PDT – population doubling time, IVCD – integrated viable cell density.

	K20-3	K20-7	K20-10	K20-11
max. vcd >80% [c/ml]	8.0E+06	9.3E+06	2.4E+06	1.5E+06
duration >80% [d]	9	7	5	7
PDT exponential growth phase [h]	58	31	34	80
IVCD at >80% viability [c*d*ml^{-1}]	2.6E+07	3.7E+07	5.2E+06	6.9E+06
IVCD total [c*d*ml^{-1}]	5.7E+07	5.7E+07	1.3E+06	1.1E+06
product titer >80% viability [µg/ml]	253	276	70	45
product max titer [µg/ml]	350	322	170	85

Table 3-4 **Cultivation characteristics** of batches from cell lines 23-CHO-S/CV107/K20-3, /K20-7, K20-10 and K20-11. vcd – viable cell density, PDT – population doubling time, IVCD – integrated viable cell density.

	K20-3 PSB	K20-3 WCB	K20-7 PSB	K20-7 WCB
max. vcd >80% [c/ml]	4.9E+06	4.4E+06	7.5E+06	2.9E+06
duration >80% [d]	8	5	7	5
PDT exponential growth phase [h]	29	31	35	42
IVCD at >80% viability [c*d*ml^{-1}]	2.2E+07	8.5E+06	2.3E+07	7.4E+06
IVCD total [c*d*ml^{-1}]	3.7E+07	1.7E+07	3.8E+07	1.4E+07
product titer >80% viability [µg/ml]	107	41	171	74
product max titer [µg/ml]	234	134	462	336

Table 3-5 **Cultivation characteristics** of batches from cell lines 23-CHO-S/CV107/K20-3 and /K20-7 at various stages of cell banking. vcd – viable cell density, PDT – population doubling time, IVCD – integrated viable cell density. For comparison with batches from respective cell lines without cryopreservation see table 3-4.

	K35-1	K35-2	K35-3	K99-1	K99-2	K154-1
max. vcd >80% [c/ml]	3,5E+06	4,7E+06	2,0E+06	4,8E+06	4,0E+06	2,3E+06
duration >80% [d]	8	9	8	8	7	7
PDT exponential growth phase [h]	38	29	45	21	40	59
IVCD at >80% viability [c*d*ml^{-1}]	1.4E+07	2.2E+07	8.8E+06	2.3E+07	1.3E+07	9.4E+06
IVCD total [c*d*ml^{-1}]	2.5E+07	3.4E+07	1.2E+07	3.0E+07	2.5E+07	1.4E+07
product titer >80% viability [µg/ml]	456	606	111	308	376	413
product max titer [µg/ml]	1143	936	356	398	760	853

Table 3-6 **Cultivation characteristics** of cell lines 23-CHO-S/CV107/K20-3/CV108/K35-1, /K35-2, /K53-3, /K99-1, /K99-2, /K154-1 in batch mode. vcd – viable cell density, PDT – population doubling time, IVCD – integrated viable cell density.

	K20-3 PSB	K35-2 WCB
max. vcd >80% [c/ml]	8.6E+06	10.4E+06
duration >80% [d]	11	15
PDT exponential growth phase [h]	44.6	34.6
IVCD at >80% viability [c*d*ml^{-1}]	5.9E+07	9.6E+06
product titer >80% viability [µg/ml]	600	1900

Table 3-7 **Cultivation characteristics of cell lines 23-CHO-S/CV107/K20-3 and 23-CHO-S/CV107/K20-3/CV108/K35-2 in fed batch mode.** Vcd – viable cell density, PDT – population doubling time, IVCD – integrated viable cell density.

	scFv-HSA	ATROSAB
Molecular mass	90 kDa	150 kDa
Thermal stability (DLS) - melting point	60 °C	78 °C
EC_{50} TNFR1-Fc binding (ELISA)	4.6 nM	0.29 nM
EC_{50} TNFR1-binding on MEF (FACS)	8.6 nM	0.19 nM
K_d (QCM)	29 nM	0.35 nM
IC_{50} TNF-induced IL-6 release (HeLa)	266 nM	41 nM
IC_{50} TNF-induced IL-8 release (HT1080)	339 nM	53 nM
Terminal serum half-life	1.2 d	8.3 d
AUC (0-7d)	522 µg/ml*h	1013 µg/ml*h

Table 3-8 **Summary of biochemical and bioactivity data for scFv-HSA and ATROSAB.** DLS – dynamic light scattering, QCM – quartz crystal microbalance.

4 DISCUSSION

A promising new molecular entity (NME) has been discovered in 1990, when mice were immunized with human TNF receptor 1 (TNFR1) and a hybridoma was generated that expressed an antibody specifically binding to TNFR1 (mouse monoclonal IgG2a, termed H398) [214]. In 2008, a humanized variant, termed IZI-06.1, was developed by CDR grafting that retained the binding specificity of H398 [123]. This made the antibody applicable for prospective use as a therapeutic in human diseases like rheumatoid arthritis, psoriasis or Crohn's disease. Regarding the emerging capability to individually combine and design fragments of monoclonal antibodies, structure variants different from the full length IgG were taken into account for the design of the future therapeutic. Three structure variants were designed and cloned by the Institute of Cell Biology and Immunology at the University of Stuttgart, a scFv-HSA, a Fab-HSA and an IgG1 with silenced ADCC/CDC function [11]. The present thesis describes part of Chemistry, Manufacturing and Control (CMC) for these three constructs with special emphasis on the IgG and the scFv-HSA. With these, variables like molecular mass (92 kDa and 115 kDa versus 150 kDa, respectively), composition (fusion of antibody fragments to HSA vs. a nearly natural structure) and valency (monovalent vs. bivalent) could be compared, that may have an impact on producibility, biochemical and functional properties.

4.1 Generation research cell lines for the three structure variants

In order to cover the question of producibility and to provide enough protein for initial biochemical and functional testing, research cell lines were developed using the CEMAX system for site directed integration of the GOI [77]. With theoretically the same copy number being integrated into the same genomic locus (random integrated copies are per definition not functional) the comparability for the different integrated constructs is much higher than with random integration. Therefore, differences in productivity, growth and viability can be ascribed to the specific protein being expressed.

A set of clones was generated for each construct. During cell line generation it was not possible to select clones in 96-well plates with a seeding density that would ensure for a single cell derived cell line. Instead, cells were spread into 150 mm culture dishes and cultivated until visible clones could be transferred to 24-well plates. So most probably, clone pools were transferred. This should not make a great difference in fact, since the integration

site of the GOI is identical. However, when comparing the specific productivity of the individual cell lines generated for the respective construct, there are obvious differences. Clone A5/1 for Fab-HSA for example expressed no protein or below the limit of detection of the employed ELISA. An explanation could be a combination of a DNA repair mechanism for (meganuclease induced) DNA double strand breaks, non homologous end-joining, and random integration of the transfected plasmid, which has already been reported for this expression system [77]. The recipient site for homologous recombination comprises next to the reporter gene cassette for the selection of the host cell line an incomplete, i.e. promoterless, *neo* resistance gene cassette. When the reporter gene is excised by *I-SceI* cleavage, fusion of DNA strands without homologous recombination might result in completion of a functional *neo* resistance gene cassette which subsequently confers resistance to Geneticin without correct integration of the GOI. When in turn the transfected plasmid integrates into an intron of an endogenously expressed gene, the GOI as well as the *zeo* resistance gene might be also expressed, although the gene cassette originally did not comprise a promoter and was intended to only be functional after correct integration of the designated genomic locus via homologous recombination. Interestingly, also survival of the transferred clones was different for each construct. While only 22 % and 32 % of the clones expressing Fab-HSA and IgG survived, resp., almost all clones (85 %) expressing scFv-HSA could be successfully expanded. Productivity of the respective best producing clones was comparable for IgG and scFv-HSA, whereas Fab-HSA exhibited an 8 to 10 fold reduced productivity. Product titers of 12 – 31 mg/l for scFv-HSA and 5 mg/l for Fab-HSA after three days of cultivation are in line with or even superior to titers achieved for a variety of other HSA fusion proteins for example in HEK293 cells ($scFv_2$-HSA, taFv-HSA, scDb-HSA, 5-13 mg/l, [159]) or in *pichia pastoris* (scFv-HSA, 7.5-9 mg/l, [204]). Still, when the respective best producing clones for scFv-HSA and Fab-HSA are compared, the latter is obiously expressed less efficiently. This is perhaps due to the increased size of the Fab-HSA and the requirement of the $VHCH_1$-HSA to correctly assemble with the separately expressed light chain via disulfide bonds, an effect that has also been observed in *E. coli* expression [203]. Low protein expression and poor survival might also be a result of trapped misfolded proteins that are not exported from the cell but rather subjected to mechanisms like the unfolded protein response (UPR). Cells that cannot cope with the high load of misfolded protein will undergo apoptosis [114, 83]. Specific productivity and product titer were more homogeneous for the clones expressing the scFv-HSA than that for clones expressing IgG or

Fab-HSA. Mean population doubling times were comparable for cell lines of all three structure variants. Average cell densities were lower for the cell lines expressing the IgG, those expressing the HSA fusion proteins reached similar maximum cell densities. HSA is widely used as an additive in cell culture and was shown to have a protective effect due to its antioxidant capacity, reduction of hydrodynamic stress and carrier function for a variety of endogenous and exogenous ligands important for cell physiology [69]. Cell lines expressing HSA fusion proteins could benefit from that, explaining the higher maximum cell densities. Although not explicitly shown yet for HSA fusion proteins, the growth promoting effect of HSA on hamster cells was already reported in 1978 [165].

In general, results from the specific productivity tests were confirmed by the data obtained from research scale spinner cultivations. In batch cultivation, the cell line expressing the full length IgG performed on the average between scFv-HSA on the one side and Fab-HSA on the other side. Cultivation duration at a high viability of over 80 % was comparable to that of scFv-HSA, the culture producing Fab-HSA fell below that threshold one day earlier. Similarly, population doubling times and integrated viable cell densities were comparable for IgG and scFv-HSA. Cell line 14-CHO-S/CV063/25.004/AV038/B1-1 (Fab-HSA) in turn achieved a higher maximum cell density and exhibited a lower population doubling time, but integrated viable cell density was lower. Culture viability dropped rapidly after achieving the peak maximum cell density. The highest product titer was achieved for scFv-HSA (295 mg/l batch, 724 mg/l fed batch), the worst for the Fab fusion protein (16 mg/l batch, 28 mg/l fed batch), but all significantly exceed the reported titers for HSA fusion proteins mentioned above. The differences between the constructs were expected from the results of the cell specific productivity test, although the difference in producibility between the IgG and the scFv-HSA are even more emphasized in the batch experiments. The three cell lines also responded differently to the applied feeding strategy. Whereas cell line 14-CHO-S/CV063/25.004/AV036/C4-1 (IgG) did not respond in terms of the parameters investigated, performance of the other both cell lines could be enhanced. For the Fab-HSA expressing cell line, product titer could be increased up to 27 %, the cultivation period extended for one day and integrated viable cell density could be increased up to 26 %. Cell line 14-CHO-S/CV063/25.004/AV037/A1-1 (scFv-HSA), tough, benefited most from feeding. Peak viable cell density was increased by 29 %, duration of cultivation was prolonged by one day, integrated viable cell density was increased by 24 % and, most importantly, product titer could be enhanced by 45 %. As the applied feeding strategy is

unspecific and will have to be replaced by a protocol more specifically addressing the requirements of the individual construct, it is very likely to further enhance cell line performance, also for the full length antibody. A great variety of feed media and strategies exist and especially protocols for the development of defined processes for monoclonal antibody production are available [118].

Analysis of product quality and integrity of in-process samples by Western Blotting revealed distinct, protein specific staining for scFv-HSA throughout the culture. No degradations were detectable, despite in the samples of the last two days of fed batch cultivation, which can be ascribed to the then low viability and protease activity [219, 142]. In contrast, in the samples of the full length IgG and the Fab-HSA, additional protein fractions of lower molecular weight were detectable (~ 50 kDa and 25 KDa). They very likely resemble free light chains and Fab fragments, remaining from incomplete protein assembly. While Ig heavy chains are not sectreted unless assembled with the light chain [35, 155], light chains can be secreted as monomers and dimers [207]. Therefore, light chain expression is a rate limiting step in antibody folding and a low ratio of HC:LC has been reported to be favourable for optimal assembly and high expression yields [193]. However, precise balance of the HC:LC ratio is difficult to achieve and several approaches have been made in vector construction (mono- and bicistronic, arrangements of cistrons) to address this problem with in part oppositional results [56, 92]. Therefore overexpression of light chains cannot be excluded by one specific vector arrangement. Yet, the amount of fragments was not as high in the samples containing the IgG as in that of the Fab-HSA fusion protein (in relation to the amount of fully assembled protein migrating at the correct molecular mass). The scFv-HSA in turn obviously benefits from its single chain design, since all its components are connected by glycin-serine linker and are therefore not dependent on correct formation of disulfide bonds. However, purification of the antibody via Fc specific Protein A chromatography will clear the final preparations from these fragments. For Fab-HSA, which is purified by taking advantage of HSA binding to Cibacron™ Blue F3G-A, this cannot be expected, since HSA unspecifically binds a great variety of substances. Purification of the IgG was the most straightforward, that of both HSA fusion proteins revealed some issues in terms of purity. This is not surprising since Protein A chromatography is highly specific for binding the fragment crystallizable (Fc) of antibodies and purities of >90 % are reported after a single purification step [63]. The cibacron blue dye instead binds a great variety of unrelated proteins due to its structural similarities with

naturally occurring biochemical reactants and co-factors [210]. As already mentioned above, components of the medium or host cell proteins may be co-purified and have to be removed by additional purification steps. Purification via Protein L, which is specific for human kappa light chains and could have complemented one another with cibacron blue chromatography, was not successful. This might be due to sterical hindrance caused by the fusion to HSA, since purification of a single chain variable fragment was possible, though. However, in order to comply with regulatory requirements for protein purity, more chromatography steps will have to be applied for purification of the IgG also. But in contrast to the fusion proteins, expert experience and established protocols exist for the purification of monoclonal antibodies [136, 105]. A complying purification strategy for both fusion proteins will have to be developed and approved anew. Accordingly, the IgG protein preparation was the purest compared to scFv-HSA and Fab-HSA. Remarkably, two distinct protein fractions of similar molecular weight were specifically detected in Western Blot. Heterogeneity is known for monoclonal antibodies and is often due to changes in protein charge [220, 79]. However, these differences are hardly detectable by SDS-PAGE. Degradations are routinely detected with this technique. But on the other hand, the small difference in molecular weight does not indicate degradation. However, HP-SEC analysis of protein produced under defined conditions did not reproduce this finding. When comparing both fusion proteins, the scFv-HSA preparation showed some remaining impurities, but mainly a defined protein portion that could be specifically detected by an antibody directed against HSA. In the Fab-HSA preparation in turn, two protein fractions of lower molecular weight than the fully assembled protein dominated. Since they were detected in Western Blot by the HSA specific antibody too, these portions have to be regarded as degradates. A possible reason might be cleavage of the glycine-serine linker. Depending on the context of the molecule, different linker molecules are more or less susceptible to degradation by proteases [6] and a different linker might improve stability.

From the data presented here, scFv-HSA and IgG can be regarded as applicable for the development of a prospective therapeutic. The cell line expressing scFv-HSA could be cultivated without obvious limitations in cell density or viability, the recombinant fusion protein could be produced at comparatively high levels and the cell line was respondent to further enhancement by feeding. The protein itself could be purified to satisfactory purity applying a single chromatography method. Productivity of the cell line expressing the IgG

was comparable to that of the scFv-HSA expressing cell line, but exhibited some issues in cell growth. The cell line was also not as readily respondent to feeding as the scFv-HSA cell line. Purification results in turn were superior to that of the scFv-HSA. The third variant, Fab-HSA, had several issues. The cell line did not produce well and showed an unfavourable growth profile in batch and fed batch cultivation, although being responsive to feeding. Additionally, the protein could not be purified as readily as the scFv-HSA. Therefore it was initially regarded as not suitable for further development.

4.2 Impact of composition, size and valency on effective huTNFR1 antagonism

In order to investigate the influence of variables like composition, size and valency on the bio-functional properties of a TNFR1 blocker in more detail, a monovalent fusion protein was compared to the bivalent, full length antibody (termed ATROSAB). Due to problems encountered with Fab-HSA (low productivity, ineffective purification), the scFv-HSA fusion protein was focused on. Albumin fusion proteins are currently investigated as an alternative to antibodies and antibody fragments since they have features from which some applications may benefit. For example they lack the Fcγ part of the full length antibody and are therefore not able to induce ADCC or CDC. Respective mutations can be introduced into the Fc-part of full length antibodies, but effective silencing has to be demonstrated. They are also of lower molecular mass compared to the antibody (here: $MW_{scFv\text{-}HSA}$ 92 kDa vs. $MW_{ATROSAB}$ 150 kDa), what may facilitate tissue penetration and higher accumulation of the molecule at the target site. Additionally, HSA is taken up by inflamed tissue and metabolized for an enhanced energy supply [211]. For example, fusion to HSA has been shown for two therapeutics to increase tissue accumulation due to increased extravasation, uptake and metabolic consumption of albumin by synovial cells [225, 143]. Yet, during inflammation, an effect known as enhanced permeability and retention (EPR) might also allow for accumulation of larger molecules like plasma proteins and immunoglobulins at the affected site [133, 171]. The lower molecular mass also affects plasma half-life of the fusion protein compared to the antibody. With 8.3 days, ATROSAB exhibited a half-life routinely observed for recombinant hIgGs. For Etanercept a half life of 4.0 days was reported [78], for Infliximab 9.5 days [51]. The fusion protein exhibited a shorter half life of 1.2 days, which is still better than observed for scFv (5.3-10.5 h for radiolabelled ^{123}I-scFv [21, 128]) and is comparable to data achieved for other antibody fragments fused to HSA. For a scFv-HSA directed against carcinoembryonic antigen (CEA) a half life of 15 h was reported [132], for an ErbB2/3

bispecific scFv-HSA-scFv 16.2 h – 22.6 h were reported [150]. The strategy of prolonging half life by fusion to HSA has already been described [122] and the results presented here confirm also data from previous studies directly comparing the influence of HSA fusion to antibody fragments on plasma half life [159].

Thermal stability, when determined by dynamic light scattering, was found to be highest for ATROSAB. With a melting point at 78 °C, it is as stable as an antibody specially engineered for better thermal stability with 76 °C [34]. The scFv-HSA fusion protein exhibited a metling point of approximately 60°C, whereas the scFv, after a more gradual degradation, showed a melting point at ~55°C. For a variety of scFv targeting EGFR or TNF, melting points between 54°C and 78°C have been reported [28]. Interestingly, the scFv-HSA is more stable than its respective antibody fragment scFv-IZI06.1, it obviously benefits from fusion to HSA, which has been observed for other HSA fusion proteins also [125]. However, like ATROSAB, scFv-HSA is highly stable under physiological conditions (human serum, 37°C). A similar high serum stability (5 days in human serum at 37°C) was also observed for an ErbB2/ErbB3 specific scFv-HSA-scFv [150].

Both derivatives were found to have retained TNFR1 specificity. TNFR1 expressing mouse embryonic fibroblasts specifically bound ATROSAB in flow cytometry analysis as well as the fusion protein, whereas TNFR2 expressing cells did not. However, TNFR1 affinity of scFv-HSA was reduced 16 – 63 fold compared to ATROSAB when determined by ELISA, flow cytometry and quarz crystal microbalance (QCBM). These results are also mirrored by the reduced capability of the albumin fusion protein to inhibit TNF-induced IL-6 and IL-8 release from HeLa and HT1080 cells, respectively. IC50 values were found to be 6 to 7 fold increased compared to ATROSAB. Recent data support a model for TNFR1 signaling that depends on ligand mediated stabilization of the receptors in an ON conformation and on formation of a network of receptors complexes [134]. The antagonistic activity of ATROSAB is proposed to be based on the combination of TNF binding inhibition as well as on keeping receptors in an OFF conformation (Richter et al, submitted). In principle, the same mode of action can be assumed for the monovalent fusion protein since it shares its eptiope with ATROSAB. However, it is only capable of monovalent binding, i. e. neutralizing one receptor per molecule, whereas the antibody is able to neutralize two receptors per molecule (higher avidity). The affinity values for the fusion protein comply with data found for monovalent interaction of ATROSAB with low concentrations of surface immobilized hu TNFR1-Fc (Richter et. al, submitted). This indicates that the reduced activity of scFv-HSA is exclusively

due to its monovalency. Taken together, the HSA fusion protein is functional with respect to TNFR1 specificity and its ability to inhibit TNF-mediated release of pro-inflammatory cytokines. Yet, further studies, especially in experimental models for inflammatory and neurodegenerative diseases, are required to determine the biofunctionality of the monovalent fusion protein scFv-HSA in comparison to ATROSAB, in order to proof it a valid alternative to the full length antibody.

The data presented in this study together with the results from initial functional tests at the Institute of Cell Biology and Immunology at the University of Stuttgart [232], suggest to focus on the full length antibody for the development of a prospective therapeutic, since it exhibits the higher affinity towards human TNFR1 and is more stable than the monovalent fusion protein.

4.3 Regulatory compliant cell line generation for ATROSAB

For the generation of regulatory compliant cell lines certain demands on traceability and safety have to be met [65, 66]. This includes the record of all used material and certificates thereof that demonstrate the absence of adventitious agents, documentation of cell line history and appropriate tests that assure that “the final product be uniform, consistent from lot-to-lot and free from adventitious agents” [65]. These tests may be different for the individual host cell line, the class of therapeutic to be produced and its intended application. But in general, they comprise tests for identity, morphology, split ratio, product quality and quantity as well as lot-to-lot consistency. Testing for cell line and product safety include tests for sterility, i.e. freedom from bacteria, mycoplasma, fungi and viruses. In addition to that, a cell banking system has to be established to ensure the supply of cells at a preferably low population doubling level (simplified: low passage number). As a consequence, all used material was recorded and either free from animal components or certified to be negative for adventitious agents (demonstrated by documentation of no-risk origin or specific testing). For every established cell bank the absence of mycoplasma was tested. One issue when dealing with adventitious agents is to prevent the propagation of Bovine Spongiform Encephalopathy (BSE). A main source of the responsible agent is fetal calf serum [14], which is why it was omitted during all steps of cell line development.

A CHO-K1 derived cell line growing under serum free conditions was chosen as host cell line, since Chinese hamster ovary cells are well established for the production of monoclonal antibodies [94]. They ensure for good post-translational modification of the product (e. g. glycosylation), can be cultivated under serum-free conditions and are easily maintained in a variety of cultivation systems, which facilitates scale-up for future production processes. In addition to that, much effort has been put successfully into process optimization of CHO cultivation [62, 226, 184]. The expression vector was designed in a bi-cistronic fashion in order to ensure for a favourable transcription efficiency of heavy and light chain due to the identical integration locus. An intron was inserted between promoter and coding sequence since it has been shown that splicing is involved in efficient transport from the nucleus to the cytoplasm [85]. The gene for the antibody heavy chain was put 5' to that of the light chain because the transcript is twice as large as that of the light chain and is expected to be processed more slowly. Since separate promoters were used for each gene, availability of sufficient light chains should be guaranteed. Plasmid DNA was transfected either supercoiled or linearized. Linearization has been shown to facilitate integration into the host cell genome, which should result in a higher copy number and subsequent higher productivity [212]. When the respective clone pools were compared in specific productivity, only a marginal difference could be observed, though. The use of amplified expression systems such as the *dhfr* system was not considered, since it has been reported that these high copy numbers result in chromosomal rearrangements and along with that in clonal variability [49]. This can lead to transgene silencing and considerable loss in productivity. Instead, a medium increase in copy number was achieved by simply re-transfecting the first cell line.

4.3.1 Limiting Dilution

A major bottleneck in the development of this cell line was limiting dilution. In order to comply with the requirement of uniformity, the cell line had to be single cell derived. Three major techniques exist for single cell cloning, which are limiting dilution, semi-solid cloning and FACS sorting. FACS and semi-solid cloning both require the integration of an additional (fluorescent) reporter gene for identification of high producers, while in limiting dilution product titer is easily assessed by ELISA from 96-well supernatants. In limiting dilution, it is a common approach to seed cells into 96-well plates at an average number of 1 or 0.3 cells per well. The number of wells with actually only one single cell can be described by the Poisson distribution. For the former seeding density the probability that any grown clone is a true

clone is 0.58 and for the latter 0.86. To overcome the remaining uncertainty, single cells were verified after seeding by microscopy. From these clones unexpectedly few survived limiting dilution. Cell culture medium composition was found to considerably contribute to the success of limited dilution cloning. While the presence of fetal calf serum (FCS) delivered stable results, hardly any clones grew under serum free conditions, instead, single cells seemed to run into limitations. The specific requirements of singled cells are not fully understood yet and cell culture companies provide a great variety of additives promising higher cloning efficiencies like Sigma-AFC (X-CELL® CHO Cloning Medium) or Life Technologies (AOF Cloning Medium) that are expensive and not always applicable. In this study, a variety of approaches were tested to improve single cell cloning and none succeeded. Therefore, the low cloning efficiency was compensated by omission of the antibiotic during limited dilution cloning and a high number of inoculated wells on the one hand and the intermediate step of generating mini-pools on the other hand. Very recently, a simple approach was reported, adding 1.5 g/l recombinant albumin to the cloning medium [235]. Although it was not possible to test this during cell line development for ATROSAB, later tests with the CHO host cell line resulted in significant higher cloning efficiencies of about 15 % (calculated for true single cells verified by microscopy).

4.3.2 Evaluation of cell line performance

In total, four promising cell lines for the high-level production of ATROSAB have been established. Two of them (23-CHO-S/CV107/K20-3 and /K20-7) by one-time transfection with ATROSAB expression vector pCV107. The others (23-CHO-S/CV107/K20-3/CV108/K35-1 and /K35-2) were generated by re-transfection of clone K20-3 with basically the same vector despite from a different resistance gene. While the single transfected cell line 23-CHO-S/CV107/K20-3 reached a specific productivity of 10 pg/c/d, already the clone pools of the re-transfection averaged 13 pg/c/d. The re-transfected single cell derived cell line 23-CHO-S/CV107/K20-3/CV108/K35-1 actually reached 34 pg/c/d, which equals a three fold increase in productivity. Along with this, product titer could be increased 2.7 fold in batch cultivation which yielded at the maximum 1.6 g/l after 14 days of cultivation. Growth behavior was different for the one-time and the re-transfected cell line, respectively. Whereas the originate cultures of the former reached peak maximum viable cell densities and an integral of viable cells typically observed with host-cell line 23-CHO-S, the latter showed a significant reduced growth. This might be due to the high load

of recombinant protein being expressed, which can lead to saturation of the cellular folding machinery so that cells are occupied with mechanisms like the unfolded protein response [10]. In fed batch cultivation, cell lines for the expression of recombinant proteins nowadays can reach specific productivities of up to 50 pg/c/d and product titer of 1-5 g/l [226]. This is mainly achieved by efficient process design and development of customized feeding strategies [36, 227, 62, 118]. Also several chemically defined feeds are available on the market. Three to eight fold increase in product titer have been reported [118]. With suitable feeding strategies being applied, the cell lines generated here very well compete with other production cell lines on the market and provide a promising basis for the establishment of a regulatory compliant, industrial production process.

4.3.3 Growth and expression stability

From cell lines 23-CHO-S/CV107/K20-3 and /K20-7 as well as for 23-CHO-S/CV107/K20-3/CV108/K35-1 and /K35-2, a two tired cell bank was established consisting of a primary seed bank (PSB) and a working cell bank (WCB). The PSBs of all cell lines were tested negative for mycoplasma and positive for sterility. The different stages of cryo-preservation were investigated in terms of protein expression and growth behavior. As already mentioned above, the originate cell line 23-CHO-S/CV107/K20-3 performed similar to the host cell line 23-CHO-S, but also to the respective IgG expressing research cell line 14-CHO-S/CV063/25.004/AV036/C4-1 in terms of growth parameters. While in the originate cell cultures typical values were reached for peak viable cell density, IVCD and culture longevity, a significant downshift in cell growth could be observed with the respective MCB and WCB. This effect was reproduced with cell line 23-CHO-S/CV107/K20-7. Peak maximum cell densities of the WCB did not exceed 5×10^6 c/ml. However, cell specific productivity did not drop but even rose. The separate test for cell specific productivity confirmed that PSB and WCB conserved the productivity determined for both clones in earlier CSP tests. When a vial from the respective WCB was later thawed for batch/fed batch experiments, the batch control again achieved cell densities observed for the originate cultures but additionally maintained the original productivity. In contrast, cell line 23-CHO-S/CV107/K20-3/CV108/K35-1, which was generated from the same WCB of clone K20-3, showed a continuously reduced growth. When originate cultures, PSB and WCB of the re-transfected cell lines were tested for cell specific productivity and compared to each other, a decrease in productivity could be observed (1.9 fold for K35-1 and 1.7 fold for

K35-2). Yet, growth behavior remained stable. Although cultivation conditions were sought to be identical, minor changes might already account for varying results. In addition, all cultivations were performed without regulation of pH and dO_2. A comparison in a more controlled environment may provide more coherent results. However, cell line stability is a major prerequisite for a regulatory compliant cell line. To thoroughly determine cell line stability, the time period for testing has to be broadened. According to ICH guideline, topic Q5D, stability of growth behavior and expression has to be determined at least at two time points. One at a comparatively low passage number and one beyond the defined life span of the planned production duration. This life span will be determined not before the development of the final production process has been completed.

4.3.4 Biochemical and functional comparison of ATROSAB produced by K20-3 and K35-2

In order to evaluate a possible impact of re-transfection on the quality of the expressed product, cultures of clones K20-3 and K35-2 were compared with respect to product titer, protein integrity and functionality. HP-SEC analysis revealed no major differences; the portion of aggregates was comparably low for both preparations. Yet, screening for charge variants by IEF and CEX uncovered a significant shift towards positively charged isoforms in the preparation of clone K35-2. The occurrence of charge variants in preparations of monoclonal antibodies is a known phenomenon [79]. Modifications like C-terminal lysine clipping, deamidation or oxidation can result in a change of the proteins charge. The shift towards positively charged isoforms that eluate later on weak CEX might be a sign of oxidation of methionine (Met) to sulfoxide [48]. Oxidation has been mainly reported as a consequence of long-term storage, exposure to light, after incubation in the presence of oxidants or at elevated temperatures. Interestingly, ATROSAB produced by clone K35-2 also showed a 1.5 fold reduced ability to rescue TNFR1 expressing Kym-1 cells from TNF-mediated cytotoxicity. This partial loss of function could be a consequence of the heterogeneity observed in CEX. To clear this up, preparative CEX will have to be performed and the main isoforms will have to be compared for their functionality in a potency assay.

4.3.5 Establishment of a test for assessing biological functionality of ATROSAB

In order to determine the ability of ATROSAB to suppress inflammation in humans, an in vitro test was established which measures the release of pro-inflammatory cytokine IL-8 upon

immunogenic stimulation. In a first approach, whole blood was challenged with lipopolysaccharide (LPS). LPS is a component of the outer membrane of gram-negative bacteria and known to cause the release of pro-inflammatory cytokine TNF via the Toll-like receptor 4 pathway [84]. Upon stimulation with LPS, binding of released TNF to TNFR1 will be blocked by ATROSAB, resulting in a reduced release of IL-8. Yet, this could be observed neither for ATROSAB nor for Remicade, which was included as a control. LPS induces a global immune response in which the reduction of IL-8 and IL-6 release due to TNFR1 signaling blockade cannot be distinguished from the IL-8 and IL-6 levels generated through other pathways [59]. Stimulant LPS was therefore exchanged by the more downstream signal TNF. Different concentrations of TNF were tested with success and an appropriate concentration was determined at which the effect of ATROSAB was well detectable. Comparison of ATROSAB with Remicade (Infliximab) showed that both drugs were able to suppress TNF-induced IL-6 and IL-8 release to control levels or even below. Measurement of TNF levels underlined the different modes of action of both drugs. While ATROSAB did not influence TNF levels, Remicade decreased TNF in the blood below the endogenous level. This effect was the most obvious at the effective concentrations. Along with this, also IL-8 was slightly suppressed below control levels. This stresses a major drawback of TNF-neutralizing therapeutics that are currently approved for the treatment of inflammatory diseases like rheumatoid arthritis or Crohn´s disease and for which Remicade is an example. They all efficiently neutralize TNF, but a certain level is still necessary to maintain a functional immune response. It is known that treatment with this class of drugs bears the risk of opportunistic infections, re-activation of tuberculosis, leukemia or new-onset psoriasis [54, 223]. However, incubation of whole blood with ATROSAB at concentrations between 10 and 100 nM revealed a minor, not significant increase in IL-8 release. This confirms data obtained from HT1080 cells that have been stably transfected with hTNFR1 and were incubated with the same range of ATROSAB concentrations. But in contrast to these experiments, this peak could be also observed in whole blood samples stimulated with 8 ng/ml TNF. The peak did not vanish at higher levels of IL-8 but rather added to the respective IL-8 concentration in the blood. A possible explanation might be founded in TNFR1 receptor stoichiometry. TNFR1 stoichiometry and its mechanism of activation in TNF signaling is not fully understood yet and a subject of current research (Richter et al, submitted)[29, 134].

In conclusion, the results of this study provide insight into the development of a promising new drug candidate on the cusp of drug discovery to industrial manufacturing. The impact of protein structure was investigated for the specific therapeutic question of TNFR1 selective antagonism. The results led to the establishment of a cell line that on the one hand expresses a protein applicable for effective and selective blockade of TNFR1 and on the other hand is able to compete well with other cell lines on the market that are intended for the use in an industrial and regulated environment.

5 REFERENCES

[1] (FDA), F.D.A. 2002. Adalimumab product approval information - licensing action 12/31/02. *Pharmacology Reviews*. (2002).

[2] (FDA), F.D.A. 2012. Drugs at FDA. Center for Drug Evaluation and Research Office of Communications Division of Online Communications.

[3] Abès R, T.J. 2010. Impact of Glycosylation on Effector Functions of Therapeutic IgG. *Pharmaceuticals*. 3, (2010), 146–57.

[4] Adler MJ, D.D. 2012. Therapeutic antibodies against cancer. *Hematol Oncol Clin North Am*. 26, (Jun. 2012), 447–81.

[5] Aggarwal, B. 2003. Signalling pathways of the TNF superfamily: a double-edged sword. *Nat Rev Immunol*. 3, (Sep. 2003), 745–56.

[6] Alfthan K, T.T. Takkinen K Sizmann D Söderlund H 1995. Properties of a single-chain antibody containing different linker peptides. *Protein Eng.* 8, (Jul. 1995), 725–31.

[7] Alt FW, S.R. Kellems RE Bertino JR 1978. Selective multiplication of dihydrofolate reductase genes in methotrexate-resistant variants of cultured murine cells. *J Biol Chem*. 10, (Mar. 1978), 1357–70.

[8] An Z, S.W. Forrest G Moore R Cukan M Haytko P Huang L Vitelli S Zhao JZ Lu P Hua J Gibson CR Harvey BR Montgomery D Zaller D Wang F 2009. IgG2m4, an engineered antibody isotype with reduced Fc function. *MAbs*. 1, (2009), 572–9.

[9] Andersen JT, E.C. Pehrson R Tolmachev V Daba MB Abrahmsén L 2011. Extending half-life by indirect targeting of the neonatal Fc receptor (FcRn) using a minimal albumin binding domain. *J Biol Chem*. 286, (2011), 5234–41.

[10] Anirikh Chakrabarti, J.D.V. Aaron W. Chen 2011. A Review of the Mammalian Unfolded Protein Response. *Biotechnol Bioeng.* 108, (Dec. 2011), 2777–2793.

[11] Armour KL, W.L. Clark MR Hadley AG 1999. Recombinant human IgG molecules lacking Fcgamma receptor I binding and monocyte triggering activities. *Eur J Immunol.* 29, (Aug. 1999), 2613–24.

[12] Arnett HA, T.J. Mason J Marino M Suzuki K Matsushima GK 2001. TNF alpha promotes proliferation of oligodendrocyte progenitors and remyelination. *Nat Neurosci.* 4, (Nov. 2001), 1116–22.

[13] Arnold JN, D.R. Wormald MR Sim RB Rudd PM 2007. The impact of glycosylation on the biological function and structure of human immunoglobulins. *Annu Rev Immunol.* 25, (2007), 21–50.

[14] Asher, D. 1999. Bovine sera used in the manufacture of biologicals: current concerns and policies of the U.S. Food and Drug Administration regarding the transmissible spongiform encephalopathies. *Dev Biol Stand.* 99, (1999), 41–4.

[15] Baert F, V.S.B.I.R.G. De Vos M Louis E 2007. Immunogenicity of infliximab: how to handle the problem? *Acta Gastroenterol Belg*. 70, (2007), 163–70.

[16] Barbosa MD, J.J. Vielmetter J Chu S Smith DD 2006. Clinical link between MHC class II haplotype and interferon-beta (IFN-beta) immunogenicity. *Clin Immunol*. 118, (Jan. 2006), 42–50.

[17] Bartsch JW, J.H. Wildeboer D Koller G Naus S Rittger A Moss ML Minai Y 2010. Tumor necrosis factor-alpha (TNF-alpha) regulates shedding of TNF-alpha receptor 1 by the metalloprotease-disintegrin ADAM8: evidence for a protease-regulated feedback loop in neuroprotection. *J Neurosci.* 30, (Sep. 2010), 12210–8.

[18] Bebbington CR, Y.G. Renner G Thomson S King D Abrams D 1992. High-level expression of a recombinant antibody from myeloma cells using a glutamine

synthetase gene as an amplifiable selectable marker. *Biotechnology (N Y)*. 10, (1992), 169–75.

[19] Becker E, K.H. Florin L Pfizenmaier K 2008. An XBP-1 dependent bottle-neck in production of IgG subtype antibodies in chemically defined serum-free Chinese hamster ovary (CHO) fed-batch processes. *J Biotechnol*. 135, (Jun. 2008), 217–23.

[20] Beers MM, B.M. van 2012. Minimizing immunogenicity of biopharmaceuticals by controlling critical quality attributes of proteins. *Biotechnol J*. 2, (Oct. 2012).

[21] Begent RH, R.L. Verhaar MJ Chester KA Casey JL Green AJ Napier MP Hope-Stone LD Cushen N Keep PA Johnson CJ Hawkins RE Hilson AJ 1996. Clinical evidence of efficient tumor targeting based on single-chain Fv antibody selected from a combinatorial library. *Nat Med.* 2, (Sep. 1996), 979–84.

[22] Benton T, B.C. Chen T McEntee M Fox B King D Crombie R Thomas TC 2002. The use of UCOE vectors in combination with a preadapted serum free, suspension cell line allows for rapid production of large quantities of protein. *Cytotechnology*. 38, (Jan. 2002), 43–6.

[23] Beutler B, C.A. 1986. Cachectin and tumour necrosis factor as two sides of the same biological coin. *Nature*. 320, (Apr. 1986), 584–8.

[24] Bhatnagar BS, P.M. Bogner RH 2007. Protein stability during freezing: separation of stresses and mechanisms of protein stabilization. *Pharm Dev Technol*. 12, (2007), 505–23.

[25] Black RA, C.D. Rauch CT Kozlosky CJ Peschon JJ Slack JL Wolfson MF Castner BJ Stocking KL Reddy P Srinivasan S Nelson N Boiani N Schooley KA Gerhart M Davis R Fitzner JN Johnson RS Paxton RJ March CJ 1997. A metalloproteinase disintegrin that releases tumour-necrosis factor-alpha from cells. *Nature*. 385, (1997), 729–33.

[26] Blick SK, C.M. 2007. Certolizumab pegol: in Crohn's disease. *BioDrugs*. 21, (2007), 195–201.

[27] Bongartz T, M.V. Sutton AJ Sweeting MJ Buchan I Matteson EL 2006. Anti-TNF antibody therapy in rheumatoid arthritis and the risk of serious infections and malignancies: systematic review and meta-analysis of rare harmful effects in randomized controlled trials. *JAMA*. 295, (May. 2006), 2275–85.

[28] Borras L, U.D. Gunde T Tietz J Bauer U Hulmann-Cottier V Grimshaw JP 2010. Generic approach for the generation of stable humanized single-chain Fv fragments from rabbit monoclonal antibodies. *J Biol Chem*. 285, (Mar. 2010), 9054–66.

[29] Boschert V, S.P. Krippner-Heidenreich A Branschädel M Tepperink J Aird A 2010. Single chain TNF derivatives with individually mutated receptor binding sites reveal differential stoichiometry of ligand receptor complex formation for TNFR1 and TNFR2. *Cell Signal*. 22, (Jul. 2010), 1088–96.

[30] Boshart M, S.W. Weber F Jahn G Dorsch-Häsler K Fleckenstein B 1985. A very strong enhancer is located upstream of an immediate early gene of human cytomegalovirus. *Cell*. 41, (Jun. 1985), 521–30.

[31] Boulianne GL, H.N. and MJ, S. 1984. Production of functional chimaeric mouse/human antibody. *Na*. 312, (Dec. 1984), 643–646.

[32] Boven K, C.N. Stryker S Knight J Thomas A van Regenmortel M Kemeny DM Power D Rossert J 2005. The increased incidence of pure red cell aplasia with an Eprex formulation in uncoated rubber stopper syringes. *Kidney Int*. 67, (Jun. 2005), 2346–53.

[33] Bradley, J. 2008. TNF-mediated inflammatory disease. *J Pathol*. 214, (2008), 149–60.

[34] Buchanan A, B.V. Clementel V Woods R Harn N Bowen MA Mo W Popovic B Bishop SM Dall'acqua W Minter R Jermutus L 2013. Engineering a therapeutic IgG molecule to address cysteinylation, aggregation and enhance thermal stability and expression. *MAbs*. 5, (2013), 255–62.

[35] Burrows P, K.J. LeJeune M 1979. Evidence that murine pre-B cells synthesise mu heavy chains but no light chains. *Nature*. 280, (Aug. 1979), 838–40.
[36] Butler M, M.-A.A. 2012. Recent advances in technology supporting biopharmaceutical production from mammalian cells. *Appl Microbiol Biotechnol*. 96, (Nov. 2012), 885–94.
[37] Carlage T, H.W. Hincapie M Zang L Lyubarskaya Y Madden H Mhatre R 2009. Proteomic profiling of a high-producing Chinese hamster ovary cell culture. *Anal Chem*. 81, (Sep. 2009), 7357–62.
[38] Carswell EA, W.B. Old LJ Kassel RL Green S Fiore N 1975. An endotoxin-induced serum factor that causes necrosis of tumors. *Proc Natl Acad Sci U S A.* 72, (Sep. 1975), 3666–70.
[39] Chamuleau ME, H.P. van de Loosdrecht AA 2010. Monoclonal antibody therapy in haematological malignancies. *Curr Clin Pharmacol*. 5, (Aug. 2010), 148–59.
[40] Chan AC, C.P. 2010. Therapeutic antibodies for autoimmunity and inflammation. *Nature Immunology*. 10, (May. 2010), 301–16.
[41] Chan, F. 2000. The pre-ligand binding assembly domain: a potential target of inhibition of tumour necrosis factor receptor function. *Ann Rheum Dis*. 59, (2000), i50–i53.
[42] Chapman BS, H.N. Thayer RM Vincent KA 1991. Effect of intron A from human cytomegalovirus (Towne) immediate-early gene on heterologous expression in mammalian cells. *Nucleic Acids Res.* 19, (Jul. 1991), 3979–86.
[43] Chaudhury C, A.C. Mehnaz S Robinson JM Hayton WL Pearl DK Roopenian DC 2003. The major histocompatibility complex-related Fc receptor for IgG (FcRn) binds albumin and prolongs its lifespan. *J Exp Med*. 197, (2003), 315–22.
[44] Chiang GG, S.W. 2005. Bcl-x(L) mediates increased production of humanized monoclonal antibodies in Chinese hamster ovary cells. *Biotechnol Bioeng*. 91, (Sep. 2005), 779–92.
[45] Chong WP, H.Y. Reddy SG Yusufi FN Lee DY Wong NS Heng CK Yap MG 2010. Metabolomics-driven approach for the improvement of Chinese hamster ovary cell growth: overexpression of malate dehydrogenase II. *J Biotechnol*. 147, (May. 2010), 116–21.
[46] Choy, E. 2012. Understanding the dynamics: pathways involved in the pathogenesis of rheumatoid arthritis. *Rheumatology (Oxford)*. 51, (Jul. 2012), 3–11.
[47] Chrousos, G. 1995. The hypothalamic-pituitary-adrenal axis and immune-mediated inflammation. *N Engl J Med*. 332, (May. 1995), 1351–62.
[48] Chumsae C, L.H. Gaza-Bulseco G Sun J 2007. Comparison of methionine oxidation in thermal stability and chemically stressed samples of a fully human monoclonal antibody. *J Chromatogr B Analyt Technol Biomed Life Sci.* 850, (May. 2007), 285–94.
[49] Chusainow J, Y.M. Yang YS Yeo JH Toh PC Asvadi P Wong NS 2009. A study of monoclonal antibody-producing CHO cell lines: what makes a stable high producer? *Biotechnol Bioeng.* 102, (Mar. 2009), 1182–96.
[50] Cleland JL, S.S. Powell MF 1993. The development of stable protein formulations: a close look at protein aggregation, deamidation, and oxidation. *Crit Rev Ther Drug Carrier Syst*. 10, (1993), 307–77.
[51] Cornillie F, R.P. Shealy D D'Haens G Geboes K Van Assche G Ceuppens J Wagner C Schaible T Plevy SE Targan SR 2001. Infliximab induces potent anti-inflammatory and local immunomodulatory activity but no systemic immune suppression in patients with Crohn's disease. *Aliment Pharmacol Ther.* 15, (Apr. 2001), 463–73.

[52] Cost GJ, G.P. Freyvert Y Vafiadis A Santiago Y Miller JC Rebar E Collingwood TN Snowden A 2010. BAK and BAX deletion using zinc-finger nucleases yields apoptosis-resistant CHO cells. *Biotechnol Bioeng*. 105, (2010), 330–40.

[53] Cromwell ME, J.F. Hilario E 2006. Protein aggregation and bioprocessing. *AAPS J*. 8, (Sep. 2006), 572–9.

[54] Culver EL, T.S. 2010. How to manage the infectious risk under anti-TNF in inflammatory bowel disease. *Curr Drug Targets*. 11, (2010), 198–218.

[55] Dall'Acqua WF, W.H. Kiener PA 2006. Properties of human IgG1s engineered for enhanced binding to the neonatal Fc receptor (FcRn). *J Biol Chem*. 281, (Aug. 2006), 23514–24.

[56] Davies SL, J.D. O'Callaghan PM McLeod J Pybus LP Sung YH Rance J Wilkinson SJ Racher AJ Young RJ 2011. Impact of gene vector design on the control of recombinant monoclonal antibody production by Chinese hamster ovary cells. *Biotechnol Prog.* 27, (2011), 1689–99.

[57] Desai NP, G.W. Trieu V Hwang LY Wu R Soon-Shiong P 2008. Improved effectiveness of nanoparticle albumin-bound (nab) paclitaxel versus polysorbate-based docetaxel in multiple xenografts as a function of HER2 and SPARC status. *Anticancer Drugs*. 19, (Oct. 2008), 899–909.

[58] Dietmair S, T.N. Nielsen LK 2012. Mammalian cells as biopharmaceutical production hosts in the age of omics. *Biotechnol J*. 7, (Jan. 2012), 75–89.

[59] Eggesbø JB, K.P. Hjermann I Høstmark AT 1996. LPS induced release of IL-1 beta, IL-6, IL-8 and TNF-alpha in EDTA or heparin anticoagulated whole blood from persons with high or low levels of serum HDL. *Cytokine*. 8, (1996), 152–60.

[60] Evans, T. 2002. Review article: albumin as a drug–biological effects of albumin unrelated to oncotic pressure. *Aliment Pharmacol Ther.* 16, Suppl. 5, (Dec. 2002), 6–11.

[61] Ewert S, P.A. Honegger A 2004. Stability improvement of antibodies for extracellular and intracellular applications: CDR grafting to stable frameworks and structure-based framework engineering. *Methods*. 34, (2004), 184–99.

[62] Li F, A.A. Vijayasankaran N Shen AY Kiss R 2010. Cell culture processes for monoclonal antibody production. *MAbs*. 2, (2010), 466–79.

[63] Fahrner RL, B.G. Knudsen HL Basey CD Galan W Feuerhelm D Vanderlaan M 2001. Industrial purification of pharmaceutical antibodies: development, operation, and validation of chromatography processes. *Biotechnol Genet Eng Rev.* 18, (2001), 301–27.

[64] Faustman D, D.M. 2010. TNF receptor 2 pathway: drug target for autoimmune diseases. *Nat Rev Drug Discov.* 9, (Jun. 2010), 482–93.

[65] FDA 1993. Points to Consider in the Characterization of Cell Lines Used to Produce Biologicals. *DOCKET NO. 84N-01541*. Memorandum, (1993), 1–42.

[66] FDA 1997. Points to Consider in the Manufacture and Testing of Monoclonal Antibody Products for Human. *Docket No. 94D-0259*. Memorandum, (1997), 1–50.

[67] Florin L, K.H. Pegel A Becker E Hausser A Olayioye MA 2009. Heterologous expression of the lipid transfer protein CERT increases therapeutic protein productivity of mammalian cells. *J Biotechnol.* 141, (Apr. 2009), 84–90.

[68] Fontaine V, E.U. Mohand-Said S Hanoteau N Fuchs C Pfizenmaier K 2002. Neurodegenerative and neuroprotective effects of tumor Necrosis factor (TNF) in retinal ischemia: opposite roles of TNF receptor 1 and TNF receptor 2. *J Neurosci*. 22, (Apr. 2002), RC216.

[69] Francis, G.L. 2010. Albumin and mammalian cell culture: implications for biotechnology applications. *Cytotechnology*. 62, (Jan. 2010), 1–16.

[70] Gannes GC, D.J. de Ghoreishi M Pope J Russell A Bell D Adams S Shojania K Martinka M 2007. Psoriasis and pustular dermatitis triggered by TNF-alpha inhibitors in patients with rheumatologic conditions. *Arch Dermatol*. 143, (2007), 223–31.

[71] Gardam MA, V.D. Keystone EC Menzies R Manners S Skamene E Long R 2003. Anti-tumour necrosis factor agents and tuberculosis risk: mechanisms of action and clinical management. *Lancet Infect Dis*. 3, (Mar. 2003), 148–55.

[72] Genentech 2013. Rituxan MEDICATION GUIDE. (2013).

[73] Geyer CR, S.S. McCafferty J Dübel S Bradbury AR 2012. Recombinant antibodies and in vitro selection technologies. *Methods Mol Biol*. 901, (2012), 11–32.

[74] Girod PA, M.N. Nguyen DQ Calabrese D Puttini S Grandjean M Martinet D Regamey A Saugy D Beckmann JS Bucher P 2007. Genome-wide prediction of matrix attachment regions that increase gene expression in mammalian cells. *Nat Methods*. 4, (Sep. 2007), 747–53.

[75] Grell M, S.P. Douni E Wajant H Löhden M Clauss M Maxeiner B Georgopoulos S Lesslauer W Kollias G Pfizenmaier K 1995. The transmembrane form of tumor necrosis factor is the prime activating ligand of the 80 kDa tumor necrosis factor receptor. *Cell*. 83, (Dec. 1995), 793–802.

[76] Grell M, S.P. Wajant H Zimmermann G 1998. The type 1 receptor (CD120a) is the high-affinity receptor for soluble tumor necrosis factor. *Proc. Natl. Acad. Sci. USA*. 95, (Jan. 1998), 570–75.

[77] Greulich, B. 2012. *Development of the CEMAX system for cell line development based on site-specific integration of expression cassettes*. Logos Verlag Berlin.

[78] Lee H, P.C. Kimko HC Rogge M Wang D Nestorov I 2003. Population pharmacokinetic and pharmacodynamic modeling of etanercept using logistic regression analysis. *Clin Pharmacol Ther*. 73, (Apr. 2003), 348–65.

[79] Liu H, S.J. Gaza-Bulseco G Faldu D Chumsae C 2008. Heterogeneity of monoclonal antibodies. *J Pharm Sci*. 97, (Jul. 2008), 2426–47.

[80] Hamilton SR, G.T. Davidson RC Sethuraman N Nett JH Jiang Y Rios S Bobrowicz P Stadheim TA Li H Choi BK Hopkins D Wischnewski H Roser J Mitchell T Strawbridge RR Hoopes J Wildt S 2006. Humanization of yeast to produce complex terminally sialylated glycoproteins. *Science*. 313, (Aug. 2006), 1441–3.

[81] Hermeling S, J.W. Crommelin DJ Schellekens H 2004. Structure-immunogenicity relationships of therapeutic proteins. *Pharm Res*. 21, (Jun. 2004), 897–903.

[82] Hermeling S, J.W. Crommelin DJ Schellekens H 2004. Structure-immunogenicity relationships of therapeutic proteins. *Pharm Res*. 21, (Jun. 2004), 897–903.

[83] Hetz, C. 2012. The unfolded protein response: controlling cell fate decisions under ER stress and beyond. *Nat Rev Mol Cell Biol*. 13, (Jan. 2012), 89–102.

[84] Heumann D, R.T. 2002. Initial responses to endotoxins and Gram-negative bacteria. *Clin Chim Acta*. 323, (Sep. 2002), 59–72.

[85] Le Hir H, M.M. Nott A 2003. How introns influence and enhance eukaryotic gene expression. *Trends Biochem Sci*. 28, (Apr. 2003), 215–20.

[86] Hoet RM, L.R. Cohen EH Kent RB Rookey K Schoonbroodt S Hogan S Rem L Frans N Daukandt M Pieters H van Hegelsom R Neer NC Nastri HG Rondon IJ Leeds JA Hufton SE Huang L Kashin I Devlin M Kuang G Steukers M Viswanathan M Nixon AE Sexton DJ Hoogenboom HR 2005. Generation of high-affinity human antibodies by combining donor-derived and synthetic complementarity-determining-region diversity. *Nature Biotechnology*. 23, (Mar. 2005), 344–8.

[87] Holliger P, H.P. 2005. Engineered antibody fragments and the rise of single domains. *Nat Biotechnol*. 23, (Sep. 2005), 1126–36.

[88] Hopp J, K.R. Hornig N Zettlitz KA Schwarz A Fuss N Müller D 2010. The effects of affinity and valency of an albumin-binding domain (ABD) on the half-life of a single-chain diabody-ABD fusion protein. *Protein Eng Des Sel*. 23, (Nov. 2010), 827–34.

[89] Horton HM, Z.E. Bernett MJ Pong E Peipp M Karki S Chu SY Richards JO Vostiar I Joyce PF Repp R Desjarlais JR 2008. Potent in vitro and in vivo activity of an Fc-engineered anti-CD19 monoclonal antibody against lymphoma and leukemia. *Cancer Res.* 68, (Oct. 2008), 8049–57.

[90] Huang, C. 2009. Receptor-Fc fusion therapeutics, traps, and MIMETIBODY technology. *Curr Opin Biotechnol.* 20, (Dec. 2009), 692–9.

[91] Huang YM, R.T. Hu W Rustandi E Chang K Yusuf-Makagiansar H 2010. Maximizing productivity of CHO cell-based fed-batch culture using chemically defined media conditions and typical manufacturing equipment. *Biotechnol Prog*. 26, (2010), 1400–10.

[92] Li J, J.T. Menzel C Meier D Zhang C Dübel S 2007. A comparative study of different vector designs for the mammalian expression of recombinant IgG antibodies. *J Immunol Methods.* 318, (Jan. 2007), 113–24.

[93] Jahn EM, S.C. 2009. How to systematically evaluate immunogenicity of therapeutic proteins - regulatory considerations. *N Biotechnol*. 25, (Jun. 2009), 280–6.

[94] Jayapal KP, Y.M. Wlaschin KF Hu WS 2007. Recombinant prottein therapeutics from CHO-cells - 20 years and counting. *Chem Eng Prog*. 103, (2007), 40–7.

[95] Jazayeri JA, C.G. 2008. Fc-based cytokines : prospects for engineering superior therapeutics. *BioDrugs*. 22, (2008), 11–26.

[96] Jefferis, R. 2012. Isotype and glycoform selection for antibody therapeutics. *Arch Biochem Biophys.* 526, (Oct. 2012), 159–66.

[97] Jones LS, M.C. Kaufmann A 2005. Silicone oil induced aggregation of proteins. *J Pharm Sci*. 94, (Apr. 2005), 918–27.

[98] Jones PT, W.G. Dear PH Foote J Neuberger MS 1986. Replacing the complementarity-determining regions in a human antibody with those from a mouse. *Nature*. 321, (1986), 522–525.

[99] Joubert MK, J.V. Hokom M Eakin C Zhou L Deshpande M Baker MP Goletz TJ Kerwin BA Chirmule N Narhi LO 2012. Highly aggregated antibody therapeutics can enhance the in vitro innate and late-stage T-cell immune responses. *J Biol Chem*. 287, (Jul. 2012), 25266–79.

[100] Kameyama Y, K.M. Kawabe Y Ito A 2010. An accumulative site-specific gene integration system using Cre recombinase-mediated cassette exchange. *Biotechnol Bioeng*. 105, (Apr. 2010), 1106–14.

[101] Kaneko Y, A.H. Sato R 2010. Changes in the quality of antibodies produced by Chinese hamster ovary cells during the death phase of cell culture. *J Biosci Bioeng*. 109, (Mar. 2010), 281–9.

[102] Kaneko Y, R.J. Nimmerjahn F 2006. Anti-inflammatory activity of immunoglobulin G resulting from Fc sialylation. *Science*. 313, (Aug. 2006), 670–3.

[103] Kannicht C, S.H. Ramström M Kohla G Tiemeyer M Casademunt E Walter O 2012. Characterisation of the post-translational modifications of a novel, human cell line-derived recombinant human factor VIII. *Thromb Res*. S0049-3848, (Oct. 2012), 743–8.

[104] Kashmiri SV, S.J. De Pascalis R Gonzales NR 2005. SDR grafting - a new approach to antibody humanization. *Methods*. 36, (2005), 25–34.

[105] Kelley, B. 2007. Very large scale monoclonal antibody purification: the case for conventional unit operations. *Biotechnol Prog.* 23, (2007), 995–1008.

[106] Kennard ML, M.J. Goosney DL Monteith D Zhang L Moffat M Fischer D 2009. The generation of stable, high MAb expressing CHO cell lines based on the artificial

chromosome expression (ACE) technology. *Biotechnol Bioeng*. 104, (Oct. 2009), 540–53.

[107] Lee KH, B.J. Sburlati A Renner WA 1996. Deregulated expression of cloned transcription factor E2F-1 in Chinese hamster ovary cells shifts protein patterns and activates growth in protein-free medium. *Biotechnol Bioeng*. 50, (May. 1996), 273–9.

[108] Kiese S, M.H. Papppenberger A Friess W 2008. Shaken, not stirred: mechanical stress testing of an IgG1 antibody. *J Pharm Sci*. 97, (Oct. 2008), 4347–66.

[109] Kim JD, Y.J. Yoon Y Hwang HY Park JS Yu S Lee J Baek K 2005. Efficient selection of stable chinese hamster ovary (CHO) cell lines for expression of recombinant proteins by using human interferon beta SAR element. *Biotechnol Prog*. 21, (2005), 933–7.

[110] Kim MS, L.G. 2008. Use of Flp-mediated cassette exchange in the development of a CHO cell line stably producing erythropoietin. *J Microbiol Biotechnol*. 18, (Jul. 2008), 1342–51.

[111] Kim MS, L.G. Kim NS Sung YH 2001. Biphasic culture strategy based on hyperosmotic pressure for improved humanized antibody production in Chinese hamster ovary cell culture. *In Vitro Cell Dev Biol Anim*. 38, (Jun. 2001), 314–9.

[112] Kim MS, L.G. Kim WH 2008. Characterization of site-specific recombination mediated by Cre recombinase during the development of erythropoietin producing CHO cell lines. *Biotechnology and Bioprocess Engineering*. 13, (2008), 418–423.

[113] Kim NS, L.G. Overexpression of bcl-2 inhibits sodium butyrate-induced apoptosis in Chinese hamster ovary cells resulting in enhanced humanized antibody production. *Biotechnol Bioeng*. 71, 184–93.

[114] Kim R, M.S. Emi M Tanabe K 2006. Role of the unfolded protein response in cell death. *Apoptosis*. 11, (Jan. 2006), 5–13.

[115] Kim YG, L.G. Kim JY 2009. Effect of XIAP overexpression on sodium butyrate-induced apoptosis in recombinant Chinese hamster ovary cells producing erythropoietin. *J Biotechnol*. 144, (Dec. 2009), 299–303.

[116] Kimball JA, Norman DJ Shield CF Schroeder TJ Lisi P Garovoy M O'Connell JB Stuart F McDiarmid SV and W, W. 1995. The OKT3 antibody response study: A multicentre study of human antimouse antibody (HAMA) production following OKT3 use in solid organ transplantation. *Transplant. Immunol.* 3, (1995), 212.

[117] Kleinbongard P, S.R. Heusch G 2010. TNFalpha in atherosclerosis, myocardial ischemia/reperfusion and heart failure. *Pharmacol Ther*. 127, (Sep. 2010), 295–314.

[118] Kochanowski N, M.L. Siriez G Roosens S 2011. Medium and feed optimization for fed-batch production of a monoclonal antibody in CHO cells. *BMC Proc.* 5 (Suppl. 8), (Nov. 2011), 75.

[119] Köhler G, M.C. 1975. Continuous cultures of fused cells secreting antibody of predefined specificity. *Nature*. 256, (1975), 495–497.

[120] Komatsu M, W.N. Kobayashi D Saito K Furuya D Yagihashi A Araake H Tsuji N Sakamaki S Niitsu Y 2001. Tumor necrosis factor-alpha in serum of patients with inflammatory bowel disease as measured by a highly sensitive immuno-PCR. *Clin Chem*. 47, (2001), 1297–301.

[121] Kontermann, R. 2004. Intrabodies as therapeutic agents. *Methods*. 34, (2004), 163–170.

[122] Kontermann, R. 2009. Strategies to extend plasma half-lives of recombinant antibodies. *BioDrugs*. 23, (2009), 93–109.

[123] Kontermann RE, P.K. Münkel S Neumeyer J Müller D Branschädel M Scheurich P 2008. A humanized tumor necrosis factor receptor 1 (TNFR1)-specific antagonistic

antibody for selective inhibition of tumor necrosis factor (TNF) action. *J Immunother*. 31, (Apr. 2008), 225–34.

[124] Kontermann RE, P.K. Scheurich P 2009. Antagonists of TNF action: clinical experience and new developments. *Expert Opin. Drug Discov.* 4, (2009), 279–92.

[125] Kratz F, U.C. Warnecke A Scheuermann K Stockmar C Schwab J Lazar P Drückes P Esser N Drevs J Rognan D Bissantz C Hinderling C Folkers G Fichtner I 2002. Probing the cysteine-34 position of endogenous serum albumin with thiol-binding doxorubicin derivatives. Improved efficacy of an acid-sensitive doxorubicin derivative with specific albumin-binding properties compared to that of the parent compound. *J Med Chem.* 45, (Dec. 2002), 5523–33.

[126] Krönke M, P.K. Hensel G Schlüter C Scheurich P Schütze S 1988. Tumor necrosis factor and lymphotoxin gene expression in human tumor cell lines. *Cancer Res.* 48, (Oct. 1988), 5417–21.

[127] Kumar S, S.S. Mitchell MA Rup B 2012. Relationship between potential aggregation-prone regions and HLA-DR-binding T-cell immune epitopes: implications for rational design of novel and follow-on therapeutic antibodies. *J Pharm Sci*. 101, (Aug. 2012), 2686–701.

[128] Larson SM, C.A. El-Shirbiny AM Divgi CR Sgouros G Finn RD Tschmelitsch J Picon A Whitlow M Schlom J Zhang J 1997. Single chain antigen binding protein (sFv CC49): first human studies in colorectal carcinoma metastatic to liver. *Cancer*. 80, (Dec. 1997), 2458–68.

[129] Lazar GA, D.B. Dang W Karki S Vafa O Peng JS Hyun L Chan C Chung HS Eivazi A Yoder SC Vielmetter J Carmichael DF Hayes RJ 2006. Engineered antibody Fc variants with enhanced effector function. *Proc Natl Acad Sci U S A.* 103, (Mar. 2006), 4005–10.

[130] Legler DF, B.C. Micheau O Doucey MA Tschopp J 2003. Recruitment of TNF receptor 1 to lipid rafts is essential for TNFalpha-mediated NF-kappaB activation. *Immunity*. 18, (May. 2003), 655–64.

[131] Lencer WI, B.R. 2005. A passionate kiss, then run: exocytosis and recycling of IgG by FcRn. *Trends Cell Biol*. 15, (Jan. 2005), 5–9.

[132] Leung, K. 2008. 111In-1,4,7,10-Tetraazacyclododecane-N,N',N",N"-tetraacetic acid-T84.66 scFv-human serum albumin 111In-DOTA-T84.66 scFv-HSA. *Molecular Imaging and Contrast Agent Database (MICAD)*. (2008).

[133] Levick, J. 1981. Permeability of rheumatoid and normal human synovium to specific plasma proteins. *Arthritis Rheum.* 24, (Dec. 1981), 1550–60.

[134] Lewis AK, S.J. Valley CC 2012. TNFR1 Signaling Is Associated with Backbone Conformational Changes of Receptor Dimers Consistent with Overactivation in the R92Q TRAPS Mutant. *Biochemistry*. 51, (2012), 6545–6555.

[135] Van Liedekerke BM, D.L.A. Nelis HJ Kint JA Vanneste FW 1991. Quality control of albumin solutions by size-exclusion high-performance liquid chromatography, isoelectric focusing, and two-dimensional immunoelectrophoresis. *J Pharm Sci.* 80, (Jan. 1991), 11–6.

[136] Liu, R.B. Hui F Junfen Ma Charles Winter 2010. Recovery and purification process development for monoclonal antibody production. *MAbs.* 2, (2010), 480–99.

[137] Llewelyn MB, R.S. Hawkins RE 1992. Discovery of antibodies. *BMJ*. 305, (Nov. 1992), 1269–72.

[138] Lobito AA, K.F. Gabriel TL Medema JP 2011. Disease causing mutations in the TNF and TNFR superfamilies: Focus on molecular mechanisms driving disease. *Trends Mol Med.* 17, (Sep. 2011), 494–505.

[139] Locksley RM, L.M. Killeen N 2001. The TNF and TNF Receptor Superfamilies: Integrating Mammalian Biology. *Cell*. 104, (2001), 487–501.
[140] Loetscher H, L.W. Gentz R Zulauf M Lustig A Tabuchi H Schlaeger EJ Brockhaus M Gallati H Manneberg M 1991. Recombinant 55-kDa tumor necrosis factor (TNF) receptor. Stoichiometry of binding to TNF alpha and TNF beta and inhibition of TNF activity. *J Biol Chem*. 266, (Sep. 1991), 18324–9.
[141] Lonberg N, et al Taylor LD Harding FA Trounstine M Higgins KM Schramm SR Kuo CC Mashayekh R Wymore K McCabe JG 1994. Antigen-specific human antibodies from mice comprising four distinct genetic modifications. *Nature*. 368, (Apr. 1994), 856–9.
[142] M, S.R. al-Rubeai 1998. Apoptosis in cell culture. *Curr Opin Biotechnol*. 9, (Apr. 1998), 152–6.
[143] Liu M, Y.X. Huang Y Hu L Liu G Hu X Liu D 2012. Selective delivery of interleukine-1 receptor antagonist to inflamed joint by albumin fusion. *BMC Biotechnol*. 12, (Sep. 2012), 68.
[144] Maeda E, K.K. Kita S Kinoshita M Urakami K Hayakawa T 2012. Analysis of nonhuman N-glycans as the minor constituents in recombinant monoclonal antibody pharmaceuticals. *Anal Chem*. 84, (Mar. 2012), 2373–9.
[145] Maloney DG, Grillo-López AJ White CA Bodkin D Schilder RJ Neidhart JA Janakiraman N Foon KA Liles TM Dallaire BK Wey K Royston I Davis T and R, L. 1997. IDEC-C2B8 (Rituximab) anti-CD20 monoclonal antibody therapy in patients with relapsed low-grade non-Hodgkin's lymphoma. *Blood*. 90, (1997), 2188–2195.
[146] Männel DN, M.S. Moore RN 1980. Macrophages as a source of tumoricidal activity (tumor-necrotizing factor). *Infect Immun*. 30, (Nov. 1980), 523–30.
[147] Marchetti L, E.U. Klein M Schlett K Pfizenmaier K 2004. Tumor necrosis factor (TNF)-mediated neuroprotection against glutamate-induced excitotoxicity is enhanced by N-methyl-D-aspartate receptor activation. Essential role of a TNF receptor 2-mediated phosphatidylinositol 3-kinase-dependent NF-kappa B pathway. *J Biol Chem*. 279, (Jul. 2004), 32869–81.
[148] Mazur X, B.J. Fussenegger M Renner WA 1998. Higher productivity of growth-arrested Chinese hamster ovary cells expressing the cyclin-dependent kinase inhibitor p27. *Biotechnol Prog*. 14, (1998), 705–13.
[149] McCafferty J, C.D. Griffiths AD Winter G 1990. Phage antibodies: filamentous phage displaying antibody variable domains. *Nature*. 348, (1990), 552–554.
[150] McDonagh CF, N.U. Huhalov A Harms BD Adams S Paragas V Oyama S Zhang B Luus L Overland R Nguyen S Gu J Kohli N Wallace M Feldhaus MJ Kudla AJ Schoeberl B 2012. Antitumor activity of a novel bispecific antibody that targets the ErbB2/ErbB3 oncogenic unit and inhibits heregulin-induced activation of ErbB3. *Mol Cancer Ther. 2012*. 11, (Mar. 2012), 582–93.
[151] Micheau O, T.J. 2003. Induction of TNF receptor I-mediated apoptosis via two sequential signaling complexes. *Cell*. 114, (Jul. 2003), 181–90.
[152] Monden Y, S.K. Kubota T Inoue T Tsutsumi T Kawano S Ide T Tsutsui H 2007. Tumor necrosis factor-alpha is toxic via receptor 1 and protective via receptor 2 in a murine model of myocardial infarction. *Am J Physiol Heart Circ Physiol*. 293, (Jul. 2007), 743–53.
[153] Moore GL, L.G. Chen H Karki S 2010. Engineered Fc variant antibodies with enhanced ability to recruit complement and mediate effector functions. *MAbs*. 2, (2010), 181–9.

[154] Morrison SL, O.V. Johnson MJ Herzenberg LA 1984. Chimeric human antibody molecules: mouse antigen-binding domains with human constant region domains. *Proc Natl Acad Sci USA*. 81, (1984), 6851–6855.
[155] Morrison SL, S.M. 1975. Heavy chain-producing variants of a mouse myeloma cell line. *J Immunol.* 114, (1975), 655–9.
[156] Lao MS, T.D. 1997. Effects of ammonium and lactate on growth and metabolism of a recombinant Chinese hamster ovary cell culture. *Biotechnol Prog*. 13, (1997), 688–91.
[157] Mukherjee R, I.H. Adhikary L Khedkar A 2010. Probing deamidation in therapeutic immunoglobulin gamma (IgG1) by 'bottom-up' mass spectrometry with electron transfer dissociation. *Rapid Commun Mass Spectrom.* 24, (Apr. 2010), 879–84.
[158] Müller D, G.J. Katinger H 2008. MicroRNAs as targets for engineering of CHO cell factories. *Trends Biotechnol*. 26, (Jul. 2008), 359–65.
[159] Müller D, K.R. Karle A Meissburger B Höfig I Stork R 2007. Improved pharmacokinetics of recombinant bispecific antibody molecules by fusion to human serum albumin. *J Biol Chem*. 282, (Apr. 2007), 12650–60.
[160] Muppidi JR, S.R. Tschopp J 2004. Life and death decisions: secondary complexes and lipid rafts in TNF receptor family signal transduction. *Immunity. 2004 Oct;21(4):461-5.* 21, (Oct. 2004), 461–5.
[161] Myszka, D. 1997. Kinetic analysis of macromolecular interactions using surface plasmon resonance biosensors. *Curr Opin Biotechnol.* 8, (1997), 50–7.
[162] Myszka DG, M.T. 1998. CLAMP: a biosensor kinetic data analysis program. *Trends Biochem Sci*. 23, (Apr. 1998), 149–50.
[163] Natsume A, N.R. In M Takamura H Nakagawa T Shimizu Y Kitajima K Wakitani M Ohta S Satoh M Shitara K 2008. Engineered antibodies of IgG1/IgG3 mixed isotype with enhanced cytotoxic activities. *Cancer Research*. 68, (May. 2008), 3863–72.
[164] Neut Kolfschoten M, P.P. van der Schuurman J Losen M Bleeker WK Martínez-Martínez P Vermeulen E den Bleker TH Wiegman L Vink T Aarden LA De Baets MH van de Winkel JG Aalberse RC 2007. Anti-inflammatory activity of human IgG4 antibodies by dynamic Fab arm exchange. *Science*. 317, (Sep. 2007), 1554–7.
[165] Nilausen, K. 1978. Role of fatty acids in growth-promoting effect of serum albumin on hamster cells in vitro. *J Cell Physiol.* 96, (Jul. 1978), 1–14.
[166] Norman, D. 1988. An overview of the use of the monoclonal antibody OKT3 in renal transplantation. *Transplant Proc.* 20, (Dec. 1988), 1248–52.
[167] Nothaft H, S.C. 2010. Protein glycosylation in bacteria: sweeter than ever. *Nat Rev Microbiol.* 8, (Nov. 2010), 765–78.
[168] Ohya T, O.H. Hayashi T Kiyama E Nishii H Miki H Kobayashi K Honda K Omasa T 2008. Improved production of recombinant human antithrombin III in Chinese hamster ovary cells by ATF4 overexpression. *Biotechnol Bioeng*. 100, (Jun. 2008), 317–24.
[169] Omasa T, O.H. Cao Y Park JY Takagi Y Kimura S Yano H Honda K Asakawa S Shimizu N 2009. Bacterial artificial chromosome library for genome-wide analysis of Chinese hamster ovary cells. *Biotechnol Bioeng*. 104, (Dec. 2009), 986–94.
[170] Padler-Karavani V, V.A. 2011. Potential Impact of the Non-Human Sialic Acid N-Glycolylneuraminic Acid on Transplant Rejection Risk. *Xenotransplantation.* 18, (2011), 1–5.
[171] Palframan R, N.A. Airey M Moore A Vugler A 2009. Use of biofluorescence imaging to compare the distribution of certolizumab pegol, adalimumab, and infliximab in the inflamed paws of mice with collagen-induced arthritis. *J Immunol Methods.* 348, (Aug. 2009), 36–41.

[172] Panichi V, P.R. Migliori M De Pietro S Taccola D Andreini B Metelli MR Giovannini L 2000. The link of biocompatibility to cytokine production. *Kidney Int Suppl*. 76, (Aug. 2000), 96–103.
[173] Pendley C, W.C. Schantz A 2003. Immunogenicity of therapeutic monoclonal antibodies. *Curr Opin Mol Ther*. 5, (Apr. 2003), 172–9.
[174] Peng A, B.-I.S. Gaitonde P Kosloski MP Miclea RD Varma P 2009. Effect of route of administration of human recombinant factor VIII on its immunogenicity in Hemophilia A mice. *J Pharm Sci*. 98, (Dec. 2009), 4480–4.
[175] Peng RW, F.M. 2009. Molecular engineering of exocytic vesicle traffic enhances the productivity of Chinese hamster ovary cells. *Biotechnol Bioeng*. 102, (Mar. 2009), 1170–81.
[176] Peng RW, F.M. Abellan E 2011. Differential effect of exocytic SNAREs on the production of recombinant proteins in mammalian cells. *Biotechnol Bioeng*. 108, (Mar. 2011), 611–20.
[177] Perini P, G.P. Facchinetti A Bulian P Massaro AR Pascalis DD Bertolotto A Biasi G 2001. Interferon-beta (INF-beta) antibodies in interferon-beta1a- and interferon-beta1b-treated multiple sclerosis patients. Prevalence, kinetics, cross-reactivity, and factors enhancing interferon-beta immunogenicity in vivo. *Eur Cytokine Netw*. 12, (Mar. 2001), 56–61.
[178] Plückthun A, P.P. 1997. New protein engineering approaches to multivalent and bispecific antibody fragments. *Immunotechnology*. 3, (Jun. 1997), 83–105.
[179] Praditpornsilpa K, E.-O.S. Kupatawintu P Mongkonsritagoon W Supasyndh O Jootar S Intarakumthornchai T Pongskul C Prasithsirikul W Achavanuntakul B Ruangkarnchanasetr P Laohavinij S 2009. The association of anti-r-HuEpo-associated pure red cell aplasia with HLA-DRB1*09-DQB1*0309. *Nephrol Dial Transplant*. 24, (May. 2009), 1545–9.
[180] Presta, L. 2006. Engineering of therapeutic antibodies to minimize immunogenicity and optimize function. *Adv Drug Deliv Rev*. 58, (2006), 640–656.
[181] Quinlan GJ, E.T. Martin GS 2005. Albumin: biochemical properties and therapeutic potential. *Hepatology*. 41, (Jun. 2005), 1211–9.
[182] Ramos-Casals M, K.M. Brito-Zerón P Soto MJ Cuadrado MJ 2008. Autoimmune diseases induced by TNF-targeted therapies. *Best Pract Res Clin Rheumatol*. 22, (Oct. 2008), 847–61.
[183] Regenmortel MHV, B.F. van Boven K 2005. Immunogenicity of Biopharmaceuticals: An Example from Erythropoietin. *BioPharm International*. 18, (Aug. 2005), 36–52.
[184] Rita Costa A, O.R. Elisa Rodrigues M Henriques M Azeredo J 2010. Guidelines to cell engineering for monoclonal antibody production. *Eur J Pharm Biopharm.* 74, (2010), 127–38.
[185] Robak T, S.H. Gladalska A 1998. The tumour necrosis factor family of receptors/ligands in the serum of patients with rheumatoid arthritis. *Eur Cytokine Netw*. 9, (Jun. 1998), 145–54.
[186] Roche M, B.E. Rondeau P Singh NR Tarnus E 2008. The antioxidant properties of serum albumin. *FEBS Lett.* 582, (Jun. 2008), 1783–7.
[187] Rommer PS, Z.U. Patejdl R 2012. Monoclonal antibodies in the treatment of neuroimmunological diseases. *Curr Pharm Des*. 18, (2012), 4498–507.
[188] Ron D, W.P. 2007. Signal integration in the endoplasmic reticulum unfolded protein response. *Nat Rev Mol Cell Biol*. 8, (Jul. 2007), 519–29.
[189] Running Deer J, A.D. 2004. High-level expression of proteins in mammalian cells using transcription regulatory sequences from the Chinese hamster EF-1alpha gene. *Biotechnol Prog*. 20, (2004), 880–9.

[190] Rup, B. 2003. Immunogenicity and immune tolerance coagulation Factors VIII and IX. *Dev Biol*. 112, (2003), 55–9.
[191] Salfeld, J. 2007. Isotype selection in antibody engineering. *Nature Biotechnology*. 25, (2007), 1369–1372.
[192] Schellekens, H. 2008. How to predict and prevent the immunogenicity of therapeutic proteins. *Biotechnol Annu Rev*. 14, (2008), 191–202.
[193] Schlatter S, J.D. Stansfield SH Dinnis DM Racher AJ Birch JR 2005. On the optimal ratio of heavy to light chain genes for efficient recombinant antibody production by CHO cells. *Biotechnol Prog.* 21, (2005), 122–33.
[194] Schneider-Brachert W, S.S. Tchikov V Neumeyer J Jakob M Winoto-Morbach S Held-Feindt J Heinrich M Merkel O Ehrenschwender M Adam D Mentlein R Kabelitz D 2004. Compartmentalization of TNF receptor 1 signaling: internalized TNF receptosomes as death signaling vesicles. *Immunity*. 21, (Sep. 2004), 415–28.
[195] Schnitzer, J. 1992. gp60 is an albumin-binding glycoprotein expressed by continuous endothelium involved in albumin transcytosis. *Am J Physiol*. 262, (Jan. 1992), 246–54.
[196] Schnitzer JE, O.P. 1994. Albondin-mediated capillary permeability to albumin. Differential role of receptors in endothelial transcytosis and endocytosis of native and modified albumins. *J Biol Chem*. 269, (1994), 6072–82.
[197] Seamons A, G.J. Sutton J Bai D Baird E Bonn N Kafsack BF Shabanowitz J Hunt DF Beeson C 2003. Competition between two MHC binding registers in a single peptide processed from myelin basic protein influences tolerance and susceptibility to autoimmunity. *J Exp Med*. 197, (May. 2003), 1391–7.
[198] Shibata H, T.Y. Yoshioka Y Ohkawa A Abe Y Nomura T Mukai Y Nakagawa S Taniai M Ohta T Mayumi T Kamada H Tsunoda S 2008. The therapeutic effect of TNFR1-selective antagonistic mutant TNF-alpha in murine hepatitis models. *Cytokine*. 44, (Nov. 2008), 229–33.
[199] Shibata H, T.Y. Yoshioka Y Ohkawa A Minowa K Mukai Y Abe Y Taniai M Nomura T Kayamuro H Nabeshi H Sugita T Imai S Nagano K Yoshikawa T Fujita T Nakagawa S Yamamoto A Ohta T Hayakawa T Mayumi T Vandenabeele P Aggarwal BB Nakamura T Yamagata Y Tsunoda S Kamada H 2008. Creation and X-ray structure analysis of the tumor necrosis factor receptor-1-selective mutant of a tumor necrosis factor-alpha antagonist. *J Biol Chem*. 283, (Jan. 2008), 998–1007.
[200] Shields RL, P.L. Namenuk AK Hong K Meng YG Rae J Briggs J Xie D Lai J Stadlen A Li B Fox JA 2001. High resolution mapping of the binding site on human IgG1 for Fc gamma RI, Fc gamma RII, Fc gamma RIII, and FcRn and design of IgG1 variants with improved binding to the Fc gamma R. *J Biol Chem.* 276, (Mar. 2001), 6591–604.
[201] Shinkawa T, S.K. Nakamura K Yamane N Shoji-Hosaka E Kanda Y Sakurada M Uchida K Anazawa H Satoh M Yamasaki M Hanai N 2003. The absence of fucose but not the presence of galactose or bisecting N-acetylglucosamine of human IgG1 complex-type oligosaccharides shows the critical role of enhancing antibody-dependent cellular cytotoxicity. *J Biol Chem.* 278, (Jan. 2003), 3466–73.
[202] Silva G, P.F. Poirot L Galetto R Smith J Montoya G Duchateau P 2011. Meganucleases and other tools for targeted genome engineering: perspectives and challenges for gene therapy. *Curr Gene Ther*. 11, (2011), 11–27.
[203] Skerra A, I.P.& A.P. 1991. The Functional Expression of Antibody Fv Fragments in Ischhuchia coli: Improved Vectors and a Generally Applicable Purification Technique. *Nature Biotechnology*. 9, (1991), 273–278.
[204] Smith BJ, S.A. Popplewell A Athwal D Chapman AP Heywood S West SM Carrington B Nesbitt A Lawson AD Antoniw P Eddelston A 2001. Prolonged in vivo

residence times of antibody fragments associated with albumin. *Bioconjug Chem.* 12, (2001), 750–6.

[205] Smith, G. 1985. Filamentous fusion phage: novel expression vectors that display cloned antigens on the virion surface. *Science*. 228, (Jun. 1985), 1315–7.

[206] Smith RA, B.C. 1987. The Active Form of Tumor Necrosis Factor Is a Trimer. *JBC*. 262, (May. 1987), 6951–6954.

[207] Sonenshein GE, G.M. Siekevitz M Siebert GR 1978. Control of immunoglobulin secretion in the murine plasmacytoma line MOPC 315. *J Exp Med.* 148, (Jul. 1978), 301–12.

[208] Sparwasser T, W.H. Koch ES Vabulas RM Heeg K Lipford GB Ellwart JW 1998. Bacterial DNA and immunostimulatory CpG oligonucleotides trigger maturation and activation of murine dendritic cells. *Eur J Immunol*. 28, (Jun. 1998), 2045–54.

[209] Steed PM, D.B. Tansey MG Zalevsky J Zhukovsky EA Desjarlais JR Szymkowski DE Abbott C Carmichael D Chan C Cherry L Cheung P Chirino AJ Chung HH Doberstein SK Eivazi A Filikov AV Gao SX Hubert RS Hwang M Hyun L Kashi S Kim A Kim E Kung J Martinez SP Muchhal US Nguyen DH O'Brien C O'Keefe D Singer K Vafa O Vielmetter J Yoder SC 2003. Inactivation of TNF signaling by rationally designed dominant-negative TNF variants. *Science*. 301, (Sep. 2003), 1895–8.

[210] Steel LF, B.T. Trotter MG Nakajima PB Mattu TS Gonye G 2003. Efficient and specific removal of albumin from human serum samples. *Mol Cell Proteomics.* 2, (Apr. 2003), 262–70.

[211] Stehle G, H.D. Sinn H Wunder A Schrenk HH Stewart JC Hartung G Maier-Borst W 1997. Plasma protein (albumin) catabolism by the tumor itself–implications for tumor metabolism and the genesis of cachexia. *Crit Rev Oncol Hematol*. 26, (1997), 77–100.

[212] Stuchbury G, M.G. 2010. Optimizing the generation of stable neuronal cell lines via pre-transfection restriction enzyme digestion of plasmid DNA. *Cytotechnology.* 62, (Jul. 2010), 189–94.

[213] Sunley K, B.M. 2010. Strategies for the enhancement of recombinant protein production from mammalian cells by growth arrest. *Biotechnol Adv*. 28, (2010), 385–94.

[214] Thoma B, S.P. Grell M Pfizenmaier K 1990. Identification of a 60-kD tumor necrosis factor (TNF) receptor as the major signal transducing component in TNF responses. *J Exp Med*. 172, (Oct. 1990), 1019–23.

[215] Tiruppathi C, M.A. Song W Bergenfeldt M Sass P 1997. Gp60 activation mediates albumin transcytosis in endothelial cells by tyrosine kinase-dependent pathway. *J Biol Chem*. 272, (Oct. 1997), 25968–75.

[216] Turan S, B.J. Galla M Ernst E Qiao J Voelkel C Schiedlmeier B Zehe C 2011. Recombinase-mediated cassette exchange (RMCE): traditional concepts and current challenges. *J Mol Biol*. 407, (Mar. 2011), 193–221.

[217] Tyagi AK, C.J. Randolph TW Dong A Maloney KM Hitscherich C Jr 2009. IgG particle formation during filling pump operation: a case study of heterogeneous nucleation on stainless steel nanoparticles. *J Pharm Sci*. 98, (Jan. 2009), 94–104.

[218] Urlaub G, C.L. 1980. Isolation of Chinese hamster cell mutants deficient in dihydrofolate reductase activity. *Proc Natl Acad Sci U S A.* 77, (Jul. 1980), 4216–20.

[219] Vives J, G.F. Juanola S Cairó JJ 2003. Metabolic engineering of apoptosis in cultured animal cells: implications for the biotechnology industry. *Metab Eng.* 5, (Apr. 2003), 124–32.

[220] Vlasak J, I.R. 2008. Heterogeneity of monoclonal antibodies revealed by charge-sensitive methods. *Curr Pharm Biotechnol.* 9, (Dec. 2008), 468–61.

[221] Wang X, K.S. Das TK Singh SK 2009. Potential aggregation prone regions in biotherapeutics: A survey of commercial monoclonal antibodies. *MAbs*. 1, (2009), 254–67.
[222] Weyand CM, G.J. Hicok KC Conn DL 1992. The influence of HLA-DRB1 genes on disease severity in rheumatoid arthritis. *Ann Intern Med*. 117, (Nov. 1992), 801–6.
[223] Winthrop, K. 2006. Risk and prevention of tuberculosis and other serious opportunistic infections associated with the inhibition of tumor necrosis factor. *Nat Clin Pract Rheumatol.* 2, (Nov. 2006), 602–10.
[224] Wlaschin KF, H.W. 2007. Engineering cell metabolism for high-density cell culture via manipulation of sugar transport. *J Biotechnol*. 131, (Aug. 2007), 168–76.
[225] Wunder A, F.C. Müller-Ladner U Stelzer EH Funk J Neumann E Stehle G Pap T Sinn H Gay S 2003. Albumin-based drug delivery as novel therapeutic approach for rheumatoid arthritis. *J Immunol.* 170, (May. 2003), 4793–801.
[226] Wurm 2004. Production of recombinant protein therapeutics in cultivated mammalian cells. *Nat Biotechnol.* 22, (Nov. 2004), 1393–8.
[227] Wurm, F. 2004. Production of recombinant protein therapeutics in cultivated mammalian cells. *Nat Biotechnol*. 22, (Nov. 2004), 1393–8.
[228] Xanthoulea S, K.G. Pasparakis M Kousteni S Brakebusch C Wallach D Bauer J Lassmann H 2004. Tumor necrosis factor (TNF) receptor shedding controls thresholds of innate immune activation that balance opposing TNF functions in infectious and inflammatory diseases. *J Exp Med*. 200, (Aug. 2004), 367–76.
[229] Yamane-Ohnuki N, S.M. Kinoshita S Inoue-Urakubo M Kusunoki M Iida S Nakano R Wakitani M Niwa R Sakurada M Uchida K Shitara K 2004. Establishment of FUT8 knockout Chinese hamster ovary cells: an ideal host cell line for producing completely defucosylated antibodies with enhanced antibody-dependent cellular cytotoxicity. *Biotechnol Bioeng.* 87, (Sep. 2004), 614–22.
[230] Zahn-Zabal M, M.N. Kobr M Girod PA Imhof M Chatellard P de Jesus M Wurm F 2001. Development of stable cell lines for production or regulated expression using matrix attachment regions. *J Biotechnol*. 87, (Apr. 2001), 29–42.
[231] Zalevsky J, S.D. Secher T Ezhevsky SA Janot L Steed PM O'Brien C Eivazi A Kung J Nguyen DH Doberstein SK Erard F Ryffel B 2007. Dominant-negative inhibitors of soluble TNF attenuate experimental arthritis without suppressing innate immunity to infection. *J Immunol*. 179, (Aug. 2007), 1872–83.
[232] Zettlitz, K. 2010. *Engineered antibodies for the therapy of cancer and inflammatory diseases*. Fakultät Energie-, Verfahrens- und Biotechnik, Universität Stuttgart.
[233] Zettlitz KA, K.R. Lorenz V Landauer K Münkel S Herrmann A Scheurich P Pfizenmaier K 2010. ATROSAB, a humanized antagonistic anti-tumor necrosis factor receptor one-specific antibody. *MAbs*. 2, (2010), 639.
[234] Zhou M, S.A. Crawford Y Ng D Tung J Pynn AF Meier A Yuk IH Vijayasankaran N Leach K Joly J Snedecor B 2011. Decreasing lactate level and increasing antibody production in Chinese Hamster Ovary cells (CHO) by reducing the expression of lactate dehydrogenase and pyruvate dehydrogenase kinases. *J Biotechnol*. 153, (Apr. 2011), 27–34.
[235] Zhu J, M.T. Wooh JW Hou JJ Hughes BS Gray PP 2012. Recombinant human albumin supports single cell cloning of CHO cells in chemically defined media. *Biotechnol Prog.* 28, (2012), 887–91.

6 ACKNOWLEDGEMENTS

First of all I want to express my gratitude to Prof. Klaus Pfizenmaier and Prof. Roland Kontermann for giving me the opportunity to do my PhD at the University of Stuttgart. Thank you for your guidance and the willingness to accept me in your research group. Without your support this thesis would not have been written.

I do want to thank Dr. Andreas Herrmann for providing the subject as well as the opportunity to do my PhD in the laboratories of Celonic GmbH. Thank you for the guidance, it were the constructive meetings that gave my work new impulse. Thank you also for critically reviewing the manuscript and the useful comments.

Special thanks go to Silke Schindler for her active support in the development of the regulatory compliant cell line for ATROSAB. I hope the plethora of 96-well plates did not give you bad dreams. I also want to thank Timo Liebig from Celonic AG Basel for conducting the analytics comparing the both ATROSAB clones K20-3 and K35-2.

I am particulary grateful for the warm welcome and support in the Kontermann Lab for the three months of my stay there. Especially Fabian Richter made it easy to familiarize with the lab and techniques. But also Oliver Seifert, Nora Hornig, Vanessa Kermer, Felix Unverdorben, Sina Fellermeier, Aline Färber-Schwarz and Aline Plappert helped me in numerous ways, be it mouse tails or FACS analysis.

For the straightforward organizational support I do want to thank Prof. Peter Scheurich, Dr. Dafne Müller and Gabi Sawall.

Finally I want to thank my colleagues at Celonic GmbH, as there are: Ann-Florence Delhaes, Dr. Arndt-René Kelter, Beat Thalmann, Benedikt Greulich, Birgit Roski, Cornelia Schoeling, Dr. Hendrik Otto, Iris Landen, Dr. Karsten Böhse, Katharina Dahle, Kerstin Otto, Matthias Mann, Melanie Rüping and Susanne Kremer. Thank you for going with me through workaday life, the support in the lab routine and all the discussions and chin wagging, of course.

7 CURRICULUM VITAE

Verena Berger, née Lorenz

birth date: 27th July 1980
present address: Försterstraße 6
D-50823 Cologne
Germany
mobile: 0176-21629393
e-mail: verena.berger@baliopharm.com
berger.ve@t-online.de

Experience

April 2012 until present
Scientist
Baliopharm GmbH, Jülich, Germany

November 2005 – March 2012
PhD student, Scientist
Celonic GmbH, Jülich, Germany

Doctorate under supervision of Roland E. Kontermann at the **Institute of Cell Biology and Immunology at the University of Stuttgart**, group of Biomedical Engineering
Allmandring 31, D-70569 Stuttgart, Germany
PhD thesis title: "Cell Development and characterization of Mono- and Divalent Antibody Derivatives"

→ CHO-S cell line development for mono- and divalent antibody derivatives of a TNFR1 specific antagonist. Biochemical and – functional characterization of the product and generation of a fully regulatory compliant for the IgG1.

January 2005 – October 2005
PhD student at the **Institute for Environmental Medicine, department of Immunology and Allergology, University of Düsseldorf**
Auf´m Hennekamp 50, D-40225 Düsseldorf, Germany
Group of Prof. Dr. Gleichmann
Subject: Mechanisms of Nickel Tolerance

Education

October 2004	Diploma exam at the **University of Konstanz** Subjects: Immunology, Cell- and Developmental Biology Grade: excellent
February 2004 – October 2004	**University of Konstanz,** **Department of Biochemical Pharmacology** Diploma thesis under the supervision of PD Dr. Dr. Thomas Hartung Thesis title: "The synergism of CpG and MDP in inducing cytokine release from human immune cells" Grade: excellent
October 1999 – October 2004	Studies of **Biology at the University of Konstanz,** **Universitätsstraße 10, D-78464 Konstanz, Germany** Major subjects: Immunology, Neurobiology, Neurophysiology, Developmental Physiology
August 1990 – June 1999	**Gymnasium "Marie Curie", Dresden, Germany** Abitur (general qualification for university entrance) Grade: 1.6

Internships

Nov./Dec. 2004	**University of Konstanz**, Department of Biochemical Pharmacology, Group of PD Dr. Dr. T. Hartung Further work on the subject of the diploma
Feb. 2001 – Apr. 2001	**University of Konstanz**, Department of Developmental Physiology, Group of Prof. Dr. Malchow Investigations on the Ca^{2+} dependent motility of *D. discoideum*
Nov. 2000 – Jan. 2001 Jun. 2001 – Aug. 2001	**University of Konstanz**, Department of Limnology, Group of Dr. Groß Project work within the SFB "Bodenseelitoral"

Advanced Training Courses

Bio-Informatics, Bio-Mathematics, Course in breeding biology, Course in appropriate handling of small laboratory animals

Publications

Zettlitz KA, **Lorenz V**, Landauer K, Münkel S, Herrmann A, Scheurich P, Pfizenmaier K, Kontermann R. ATROSAB, a humanized antagonistic anti-tumor necrosis factor receptor one-specific antibody. mAbs 2. 2010;2(6):639–647.

Landauer K, Unutmaz C, Egli S, **Berger V**, Lais S, Liebig T, Steiner D, Maier J, Rostalski I, Forcellino F, Herrmann A: Process Development of ATROSAB, an anti TNFR1 Monoclonal Antibody: in Three Steps from Research to GMP. BMC Proceedings 2011, 5 (Suppl 8): P43

Greulich B, **Berger V**, Poppe M, Hepp N, Landauer K, Herrmann A. Cell line development using the SEFEX system. BMC Proceedings 2011, 5 (Suppl 8): P43